

GREEN SYSTHESIS OF CARBOXYMETHYL CELLULOSE

Natasha Bannerman

A Dissertation submitted to the Faculty of Science, University of the Witwatersrand, Johannesburg, in fulfilment of the requirements for the degree of Master of Science.

Johannesburg, 2018

EMBARGO

This Dissertation is embargoed at the request of SENMIN and is not be released for public scrutiny by the University until March 2021.

DECLARATION

I declare that this Dissertation is my own, unaided work. It is being submitted for the Degree of Masters of Science at the University of the Witwatersrand, Johannesburg. It has not been submitted before for any degree or examination at any other University.



(Signature of Candidate)

Signed on the 25th Day of May 2018 in Johannesburg

ABSTRACT

Contemporary production of Carboxymethyl Cellulose (CMC) is carried out almost exclusively by the solvent slurry process which utilises large quantities of solvents such as isopropyl alcohol, ethanol and methanol. This study has focused on reducing the environmental impact of the CMC production by evaluating water as an alternative solvent and microwave energy as an alternative heating source.

Due to poor reaction efficiency and product quality the historical dry/aqueous CMC manufacturing process was abandoned in the late 1950's. To address these shortcomings the reaction conditions were optimised and the best reaction products then compared to those produced by the conventional solvent slurry process. Current investigations into the use of microwave technology for the carboxymethylation of cellulose focus mainly on solvent based reactions. The application of microwave technology for the dry/aqueous reaction was evaluated by comparing reactions where microwave and conventional heating were used respectively.

X-ray diffraction (XRD) was used to evaluate the degree to which the cellulose was swelled during mercerisation, while the product quality and molecular characteristics of the CMC products were used to evaluate the results of the etherification reactions. By comparing the change in slope of the conformational plot, as determined by size exclusion chromatography with multi-angle light scattering (SEC-MALS), to the degree of thixotropy of the polymer solutions it was found that the slope could be used as a new and novel method for estimating the uniformity of the substituent distribution along the cellulose backbone. This is a parameter which has a significant impact on the solubility and rheology of the CMC.

This investigation concluded that water could be used as a viable alternative solvent for the industrial production of technical grade CMC's. Comparable reaction efficiencies of 74.8% to the solvent slurry process were achieved for the low DS products and the use of microwave heating was found to significantly reduce the reaction time.

ACKNOWLEDGEMENTS

I would like to thank the following people for their assistance with my research and dissertation

Zsuzsanna Foldvari for her assistance with the XRD study, for acting as a valuable sounding board for my theories and providing much needed support.

Daniel Radebe for his assistance with the running of the pilot plant and solvent reactions.

Dineo Nyathi for her assistance with the analysis of the CMC products and performing of the hysteresis loop analysis. Thanks as well to Lolita Gwiji for her valuable input on the hysteresis loop analysis.

Mojalefa Mofokeng for his assistance with performing of the GPC analysis.

Volker Eggert for taking the time to proof read and comment on my dissertation even though he bears no love of the subject matter.

Prof Dave Billings for his assistance in the interpretation of the XRD data.

Patrick Dicks for proof reading my novella and his always valuable insights.

Lastly my supervisor Prof Dean Brady for his assistance in finding the “impossible to find” article and his guidance through this process.

I would also like to thank AECI and the University of the Witwatersrand for allowing me the opportunity to complete my studies.

CONTENTS

Embargo	ii
Declaration	ii
Abstract	iii
Acknowledgements	iv
List of Figures	viii
List of Tables	xiii
1 Introduction	16
1.1 General Introduction	16
1.2 Cellulose	17
1.2.1 The Supra-molecular Structure of Cellulose	18
1.2.2 The Morphology of Cellulose	20
1.2.3 Swelling of Cellulose	22
1.2.4 The Chemistry	23
1.2.5 Cellulose Mercerisation	25
1.2.6 The Etherification Reaction	26
1.2.7 Degree of Substitution	28
1.2.8 Distribution of Substitution	28
1.2.9 Methods of Manufacture	29
1.3 Application of Green Chemistry to CMC Synthesis	34
1.4 Molecular Characterisation of CMC	37
1.4.1 Size Exclusion Chromatography (SEC)	37
1.4.2 Detectors	39
1.4.3 Molecular Weight and Molecular Weight Distributions	45
1.4.4 Molecular Size and Conformation	48
1.5 Objectives	53
2 Materials and Methods	54
2.1 Materials	54
2.2 Experimental Procedures	54
2.2.1 Preparation of Powdered Cellulose	54
2.2.2 Preparation of CMC by the Solvent Slurry Process	54

2.2.3	Preparation of CMC by the Dry Aqueous Process	54
2.2.4	Microwave Reactions	56
2.3	Analysis Methods	57
2.3.1	Purity	57
2.3.2	Degree of Substitution	57
2.3.3	Insoluble Content	58
2.3.4	Solution Viscosity	58
2.3.5	Calculation of Reaction Efficiency	59
2.3.6	SEC with Triple Detection	59
2.3.7	XRD Analysis	59
2.3.8	Hysteresis Loop Analysis	60
3	The Combined Influence of Sodium Hydroxide Concentration and Temperature on Fibre Swelling During Mercerisation	61
3.1	Background	61
3.2	Objective and Approach	65
3.3	Results and Discussion	67
3.4	Conclusion	71
4	The Influence of a Nitrogen Atmosphere on Fibre Swelling During Mercerisation	72
4.1	Background	72
4.2	Objective and Approach	73
4.3	Results and Discussion	73
4.4	Conclusions	78
5	The Influence of the form of etherification agent	79
5.1	Background	79
5.2	Objective and Approach	81
5.3	Results and Discussion	81
5.4	Conclusions	85
6	Effect of Temperature during MCA addition	87
6.1	Background	87
6.2	Objectives and Approach	89
6.3	Results and Discussion	89
6.4	Conclusions	94
7	Microwave reactions	96

7.1	Background	96
7.2	Objectives and Approach	99
7.3	Results and Discussion	100
7.4	Conclusions	102
8	The Application Of Green Chemistry to the Production of CMC	103
8.1	Background	103
8.2	Objectives and Approach	110
8.3	Results and Discussion	110
8.4	Conclusions	114
9	Determining the Distribution of substitution of CMC using SEC-MALS	
	Analysis: A Simplified Analysis for Application in Industry	115
9.1	Background	115
9.2	Objectives and Approach	120
9.3	Results and Discussion	121
9.4	Conclusions	131
10	Conclusions	133
11	Future Work	135
12	References	136
	Appendix A	150

LIST OF FIGURES

Figure 1-1 The molecular structure of cellulose adapted from Klemm, et al., (2001a)	17
Figure 1-2 Inter- and intramolecular hydrogen bonding pattern in cellulose.	18
Figure 1-3 The most probable patterns of the hydrogen bonds in cellulose I and II	19
Figure 1-4 Interconversion of cellulose polymorphs (O'Sullivan, 1997)	20
Figure 1-5 Super-molecular structure of cellulose (Egal, 2006).....	21
Figure 1-6 Reaction steps for the synthesis of CMC	23
Figure 1-7 Photos of the dry/aqueous reaction (left) and the solvent slurry reaction (right). The dry/aqueous reaction mass has no free liquid is present while for the solvent slurry reaction there is a clear solid liquid separation between the cellulose (bottom) and the solvent (top) when the agitator is stopped.....	24
Figure 1-8 Fibril rearrangement during mercerization (Okano & Sarko, 1985) ...	25
Figure 1-9 Possible side reactions which can occur during the production of CMC	27
Figure 1-10 Flow sheet for the German batch process for CMC manufacture....	30
Figure 1-11 The modern slurry process for the production of purified CMC (Stigsson, et al., 2004).....	34
Figure 1-12 Schematic representation of the relative hydrodynamic volumes of a linear and a branched polymer with the same molecular weight.	38
Figure 1-13 Separation of polymer molecules by hydrodynamic volume by SEC/GPC	39
Figure 1-14 Basic design of a differential viscometer consisting of, 4 capillary tubes (R1-R4) which are arranged in a balanced bridge configuration, a differential pressure transducer (DP), an inlet pressure transducer (IP) and a delay volume (Malvern Instruments Limited, 2015).....	41

Figure 1-15 Shown on the left is the optical bench for the Dawn Helios II (Wyatt Technology) multiangle light scattering photometer (Wyatt Technology, 2010). The diagram on the right is a schematic representation of how the multiangle light scattering measurement is made (Wyatt, 2013).	44
Figure 1-16 HPLC/SEC system with triple detector array	45
Figure 1-17 A monodisperse MWD indicating the typical positions of the molecular weight averages (Agilent Technologies, 2015).	47
Figure 1-18 Examples of differential MWD plots, showing the different distribution symmetry and shapes which can be obtained for CMC products	48
Figure 1-19 Examples of conformations which polymers can assume in solution	49
Figure 1-20 Graphic Representation of a Polymer Showing the Difference Between r = End-to-End distance and R = Mean Square Radius (Su, 2013).	49
Figure 1-21 Conformational plot showing the variation in the plot slope related to changes in polymer conformation in solution	51
Figure 3-1 Binary phase diagram of NaOH and water (Wang, 2008)	62
Figure 3-2 Representation of the organisation of an 9% aqueous NaOH solution (w/w)	63
Figure 3-3 Various forms and corresponding hydrodynamic diameters of alkali hydrates	64
Figure 3-4 Phase diagram of the various Na-cellulose forms.	65
Figure 3-5 XRD scan of raw unswelled cellulose	67
Figure 3-6 Stacked overlay of XRD scans for alkalised cellulose at a swelling temperature of 0°C for NaOH concentrations of 25%, 37%, 43% and 48%	67
Figure 3-7 Stacked overlay of XRD scans for alkalised cellulose at a swelling temperature of 5°C for NaOH concentrations of 25%, 37%, 43% and 48%	68

Figure 3-8 Stacked overlay of XRD scans for alkalised cellulose at a swelling temperature of 10°C for NaOH concentrations of 25%, 37%, 43% and 48%.....	69
Figure 3-9 Stacked overlay of XRD scans for alkalised cellulose at a swelling temperature of 20°C for NaOH concentrations of 25%, 37%, 43% and 48%.....	69
Figure 4-1 Stacked overlay of XRD scans for alkalised cellulose at a swelling temperature of 10°C and NaOH concentration of 25% with and without the presence of a nitrogen blanket during mercerisation.....	73
Figure 4-2 Temperature profile overlay for the mercerisation of cellulose with a starting swelling temperature of 10°C and NaOH concentration of 25%, with (-) and without (-) the presence of a nitrogen blanket during mercerisation.....	74
Figure 4-3 Differential MWD overlay of CMC products produced with (-) and without (-) the presence of a nitrogen blanket.....	76
Figure 4-4 Conformational plot overlay of CMC products produced with (-) and without (-) the presence of a nitrogen blanket.....	77
Figure 5-1 Differential MWD overlay for CMC _{SMCA} (-) and CMC _{MCA} (-).....	83
Figure 5-2 Conformational Plot Overlays for CMC _{SMCA} (-) and CMC _{MCA} (-)..	85
Figure 6-1 Overlay of temperature profiles for the NaOH addition and swelling period as well as the MCA addition and adsorption period for reactions CMC ₁₇ to CMC ₄₅ , showing the temperature variations for the MCA addition and adsorption period.	90
Figure 6-2 Differential MWD overlays for CMC ₁₇ (-), CMC ₂₀ (-), CMC ₂₅ (-), CMC ₂₈ (-), CMC ₃₂ (-), CMC ₃₈ (-) and CMC ₄₅ (-)	91
Figure 6-3 Cumulative MWD overlays for CMC ₁₇ (-), CMC ₂₀ (-), CMC ₂₅ (-), CMC ₂₈ (-), CMC ₃₂ (-), CMC ₃₈ (-) and CMC ₄₅ (-)	92
Figure 6-4 Conformational plot overlays for CMC ₁₇ (-), CMC ₂₀ (-), CMC ₂₅ (-), CMC ₂₈ (-), CMC ₃₂ (-), CMC ₃₈ (-) and CMC ₄₅ (-)	93
Figure 6-5 Plot of reaction efficiency versus maximum temperature during the MCA addition and adsorption period for the reactions CMC ₁₇ to CMC ₄₅	94

Figure 7-1 Illustration of the heating mechanisms for (a) conventional heating and (b) microwave heating (Nomanbhay & Ong, 2017)	97
Figure 8-1 Core Principles of Green Chemistry.....	103
Figure 8-2 EHS scores for Methanol, Ethanol and IPA adapted from Connolly (2015).....	105
Figure 8-3 System model used for the life-cycle assessment method (Capello, et al., 2007)	106
Figure 8-4 Combination of EHS and LCA method outcomes for the environmental assessment of 26 organic solvents (Capello, et al., 2007)	106
Figure 8-5 Plot Showing the Relative Reaction Efficiencies of the Optimised Dry/aqueous Process (-) relative to the Historical Dry/aqueous Process (-) and the Solvent Slurry Process	114
Figure 9-1 Distribution of substituents in CMC on different structural levels.....	115
Figure 9-2 Possible distribution of substituents at a monomer level (Adden, 2009)	116
Figure 9-3 Possible Distribution of Substituents at a Polymer Chain Level (Richardson & Gorton, 2003)	117
Figure 9-4 Rheogram of pseudoplastic CMC solution behaviour on the left and thixotropic behaviour on the right (deButts, et al., 1957)	119
Figure 9-5 Schematic representation of the intermolecular interactions which can occur between unsubstituted areas of the CMC (Liebert & Heinze, 2001)	120
Figure 9-6 Hysteresis loop response for CMC_{Aqu2} at solution concentrations of 1% (-), 2% (-) and 3% (-) solutions.	121
Figure 9-7 Hysteresis loops for CMC_{Aqu1} (-), CMC_{Aqu2} (-) and CMC_{Aqu3} (-) at a solution concentration of 1%.....	123
Figure 9-8 Hysteresis loops for CMC_{Aqu2} (-) and CMC_{Aqu3} (-) at a solution concentration of 3%.....	123

Figure 9-9 Conformational plot overlays for CMC_{Aqu1} (—), CMC_{Aqu2} (—) and CMC_{Aqu3} (—)	124
Figure 9-10 The change in conformation in solution relative to the change in chain aggregation resulting from unsubstituted segments of the CMC polymer. A. High degree of chain aggregation corresponding to a spherical conformation in solution. B. Reduced chain aggregation corresponding to non-expanded random coil conformation in solution C. Low chain aggregation corresponding to expanded random coil conformation in solution.....	126
Figure 9-11 Hysteresis loops for CMC_{Aqu2} (—) and $CMC_{Solvent}$ (—) at a solution concentration of 3%	127
Figure 9-12 Conformational plot overlays for CMC_{Aqu2} (—) and $CMC_{Solvent}$ (—)	128
Figure 9-13 Hysteresis loops for CMC_{WNB} (—) and CMC_{NNB} (—) at a solution concentration of 3%	129
Figure 9-14 Hysteresis loops for CMC_{SMCA} (—) and CMC_{MCA} (—) at a solution concentration of 1%	131
Figure A-1 Schematic representation of the pilot plant set-up used for the carboxymethylation reactions.....	150
Figure A-2 Average temperature profiles for the swelling and adsorption periods	154
Figure A-3 Raw SEC-MALS results for the MCA reactions with and without nitrogen blanket.....	156
Figure A-4 Raw SEC-MALS results for the MCA and SMCA reactions	157
Figure A-5 Raw SEC-MALS results for the for the reactions which were part of study investigating the impact of temperature during the MCA addition and adsorption periods	160

LIST OF TABLES

Table 1-1 CMC grade and typical applications (Stigsson, et al., 2001).....	16
Table 1-2 Schematic overview of CMC process development (Stigsson, et al., 2001)	33
Table 1-3 Relationship of conformational plot slope to the conformation. Adapted from Clasen & Kulicke, (2001)	51
Table 2-1 Outline of microwave heating reactions.....	56
Table 3-1 Composition and temperature range of NaOH – water hydrates. Adapted from Budtova & Navard (2016)	62
Table 4-1 Analytical characterisation results of carboxymethylation reactions performed with and without the presence of a nitrogen blanket.....	75
Table 4-2 SEC-MALS characterisation results of carboxymethylation reactions performed with and without the presence of a nitrogen blanket. <i>The Z-average data is used for the R_g and R_h.</i>	75
Table 5-1 Analytical characterisation results of carboxymethylation reactions performed with SMCA and MCA.	82
Table 5-2 SEC-MALS characterisation results of carboxymethylation reactions performed with SMCA and MCA as etherification reagents. <i>The Z-average data is used for the R_g and R_h.</i>	82
Table 6-1 Analytical characterisation results for reactions CMC ₁₇ to CMC ₄₅ performed with variations in temperature for the MCA addition and adsorption Period.	90
Table 6-2 SEC-MALS characterisation results for reactions CMC ₁₇ to CMC ₄₅ performed with variations in temperature for the MCA addition and adsorption period.	91
Table 7-1 Reaction conditions and DS values for the CMC reactions performed using conventional and microwave heating.....	101

Table 8-1 Comparative reaction efficiencies for solvent slurry and aqueous CMC production.....	111
Table 9-1 Summary of results for CMC_{Aq1} , CMC_{Aq2} and CMC_{Aq3}	125
Table 9-2 Summary of results for $CMC_{Solvent}$ and CMC_{Aq2}	128
Table 9-3 Summary of results for CMC_{WNB} and CMC_{NNB}	130
Table 9-4 Summary of results for CMC_{MCA} and CMC_{SMCA}	131
Table A-1 Batch temperatures for the MCA powder reactions with nitrogen.....	151
Table A-2 Batch temperatures for the SMCA powder reactions with nitrogen ..	152
Table A-3 Batch temperatures for the MCA powder reactions without nitrogen blanket.....	153
Table A-4 Results of the analytical characterisation for the MCA, SMCA and MCA without nitrogen blanket	155
Table A-5 Average temperatures for the reactions which were part of study investigating the impact of temperature during the MCA addition and adsorption periods.....	158
Table A-6 Analytical results for the reactions which were part of study investigating the impact of temperature during the MCA addition and adsorption periods	159
Table A-7 Characterisation results for the microwave reactions performed at 85 W	161
Table A-8 Characterisation results for the microwave reactions performed at 255 W.....	161
Table A-9 Characterisation results for the microwave reactions performed at 425 W.....	161
Table A-10 Characterisation results for the microwave reactions performed at 595 W.....	162

Table A-11 Raw hysteresis loop results for $CMC_{A_{qu2}}$ at 1% solution concentration	163
Table A-12 Raw hysteresis loop results for $CMC_{A_{qu2}}$ at 2% solution concentration	166
Table A-13 Raw hysteresis loop results for $CMC_{A_{qu2}}$ at 3% solution concentration	169

1 INTRODUCTION

1.1 General Introduction

Cellulose is the most abundant and widely encountered biopolymer on earth as it is the principal structural component of cell walls in plants (Perez & Mazeau, 2005). Cellulose contains numerous polar hydroxyl groups which can be chemically transformed to yield derivatives with a variety of different properties and uses. Of these derivatives carboxymethyl cellulose (CMC), is the most commercially important cellulose ether (Klemm, et al., 2001b; Thielking & Schimdt, 2012). It is used in a number of applications as a thickener, binding agent, emulsifier and stabiliser.

The results of a market study, published by Markets and Markets in August 2015, stated that the CMC market was expected to grow to an estimated \$1.46 Billion by 2020 from \$1.15 Billion in 2014. The report showed that the largest application of CMC was in the food and beverage sector where growth is driven by the ever increasing demand for processed, ready-to-eat and low-fat foods. Also contributing to the increased demand are pharmaceutical and cosmetic production together with growing oil drilling and exploration activities (MarketsandMarkets, 2015).

CMC is available in various levels of purity; products with an active content of 55 – 85% are considered to be “unpurified” and are commonly referred to as technical grades while, purity levels of 85 – 95% are termed “semi-purified” and those with a purity around 98% are termed “purified”, products with an active content greater than 99.5% are classed as “highly purified” or “extra purified” (Thielking & Schimdt, 2012). A summary of where these different grades find their application can be seen in Table 1 below.

Table 1-1 CMC grade and typical applications (Stigsson, et al., 2001)

Quality of CMC	Examples of Application Areas	Content of CMC (%)	Content of Salts (%)
Technical	Detergents, mining flotation	< 75	>25
Semi-purified	Oil and gas drilling muds	75 – 85	15 – 25
Purified	Paper coating, textile sizing and printing, ceramic glazing, oil drilling muds	> 98	< 2
Extra purified	Food, toothpaste, pharmaceuticals	> 99.5	< 0.5

Large-scale production of CMC is almost exclusively carried out by a one-step slurry process which incorporates the use of an alcohol, such as isopropanol, as a co-solvent (Heinze, 2005). Low pulp mass fractions utilised for the slurry process require the use of large quantities of alcohol (Thielking & Schimdt, 2012). The replacement of volatile solvents with environmentally benign alternatives is a key principal of green chemistry as such solvents account for most of the mass wasted in synthetic and industrial processes (Farran, et al., 2015). Although the environmental impact of the current process is mitigated somewhat by virtue of the fact that the solvent is recycled (Stigsson, et al., 2001); moving towards a completely solvent free process could significantly reduce the environmental impact of the CMC synthesis.

1.2 Cellulose

The primary starting material for CMC production is cellulose, which is a linear homopolymer consisting of anhydroglucose units (AGU) linked together by β -(1,4) glucosidic bonds (Klemm, et al., 2001a). The two ends of the cellulose chain differ chemically with one end having a reducing aldehyde group and, the other a non-reducing hydroxyl group (Almlof, 2010).

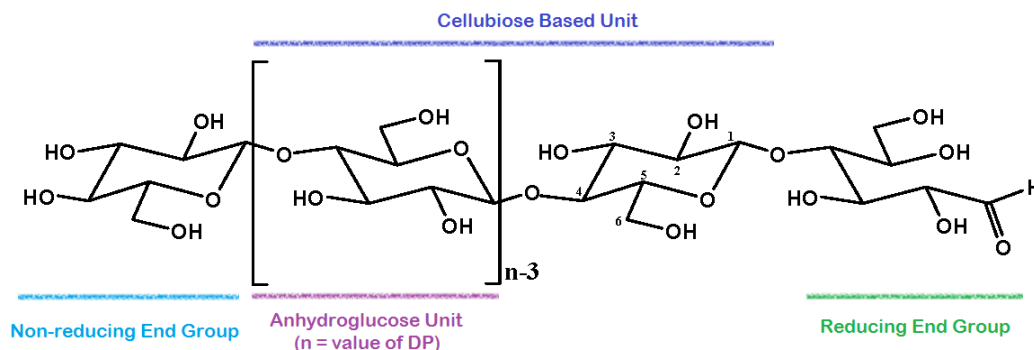


Figure 1-1 The molecular structure of cellulose adapted from Klemm, et al., (2001a)

There are three reactive hydroxyl groups per AGU; the primary hydroxyl on C-6 and the two secondary hydroxyls on C-2 and C-3 (Purves, 1963). These groups can take part in all the classical reactions of a hydroxyl group, such as etherification, esterification and oxidation reactions (Howsmon & Sisson, 1963; Feddersen & Thorp, 1993). The order of reactivity of the hydroxyl groups has been found to be dependent on the conditions in which the reaction is performed (Salmi, et al., 1994), however, the OH-3 is considered to be much less reactive than the OH-6 and OH-2 (Richardson & Gorton, 2003).

The polar hydroxyl groups participate in the formation of intra- and intermolecular hydrogen bonding which makes up the supramolecular structure of the cellulose fibre (Wang, 2008). The hydrogen bonding network consists of two intramolecular bonds, which exist between the C3 and the C5 oxygen as well as the C2 hydroxyl group and C6 oxygen of adjacent residues, while the predominant intermolecular bond is between the C6 and C3 oxygen of neighbouring chains (Gardner & Blackwell, 1974). This extensive hydrogen bonding network prevents the dissolution of cellulose in common organic solvents and water (Prusov, et al., 2014).

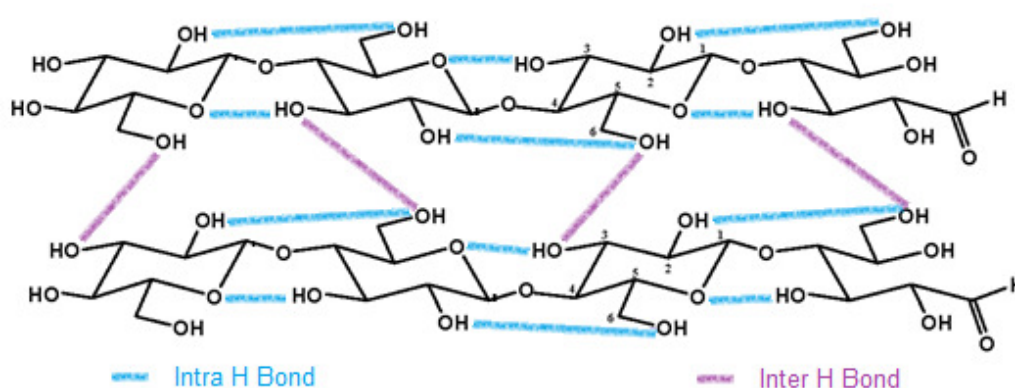


Figure 1-2 Inter- and intramolecular hydrogen bonding pattern in cellulose.

Adapted from Bergh (2011)

1.2.1 The Supra-molecular Structure of Cellulose

The intra- and intermolecular hydrogen bonding which occurs between the free hydroxyl groups gives rise to various ordered crystalline arrangements (Perez & Mazeau, 2005). Four principal polymorphs of cellulose have been identified and are named cellulose I, II, III and IV (Howsmon & Sisson, 1963).

The natural form of cellulose, and most abundant, is cellulose I or native cellulose. Atalla and Van der Hart (1984) showed that cellulose I comprises two distinct crystalline forms, cellulose I α and I β , and that these two phases can occur in variable proportions depending on the source of the cellulose. The cellulose produced by primitive organisms, such as bacteria and algae, have a higher proportion of the I α phase, whereas the cellulose from higher plants consists mostly of the I β phase. X-ray analysis has confirmed that both forms exhibit parallel chain arrangement (Zugenmaier, 2001).

Cellulose II can be obtained when cellulose I (native cellulose) is either mercerised or regenerated. Mercerisation is the swelling of native cellulose fibres in concentrated aqueous NaOH followed by washing and drying, while regeneration is the dissolution of cellulose in an appropriate solvent followed by re-precipitation (Kolpak, et al., 1978). The different ways of preparing cellulose II result in similar crystal and molecular structures, where the crystal structure consists of antiparallel chains with different conformations (Perez & Mazeau, 2005). The transition from cellulose I to cellulose II is not reversible as the higher density of hydrogen bonds present in the cellulose II makes it more stable compared to the metastable cellulose I (Kolpak & Blackwell, 1976).

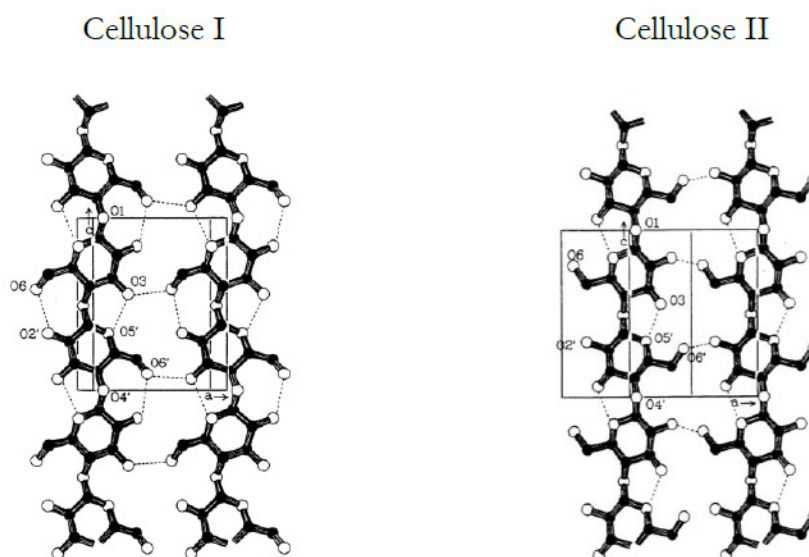


Figure 1-3 The most probable patterns of the hydrogen bonds in cellulose I and II
(Kroon-Batenburg, et al., 1986)

Cellulose III can be prepared from either cellulose I or cellulose II by treatment with liquid ammonia or certain amines, which results in cellulose III_I and cellulose III_{II} respectively. Treating cellulose III at high temperatures in glycerol transforms it into cellulose IV. Two types exist, cellulose IV_I and cellulose IV_{II} obtained from cellulose III_I and cellulose III_{II} respectively (Perez & Mazeau, 2005; O'Sullivan, 1997).

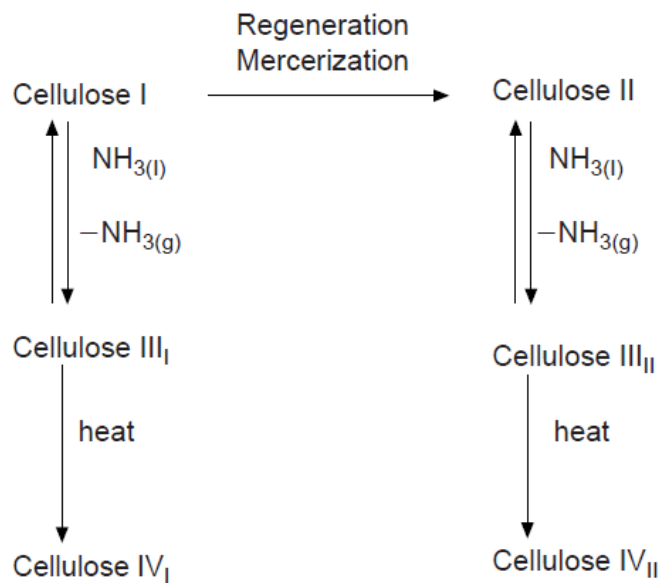


Figure 1-4 Interconversion of cellulose polymorphs (O'Sullivan, 1997)

1.2.2 The Morphology of Cellulose

Cellulose chains have a strong tendency to aggregate into highly ordered structures due to their chemical composition and spatial conformation (Klemm, et al., 2001a). The predominant factor responsible for the interchain cohesion is the intermolecular hydrogen bonds, this cohesion is favoured by the spatial regularity of the free hydroxyl groups and by the involvement of all three hydroxyl groups in the hydrogen-bond network (Klemm, et al., 2001a).

The order of the macromolecules in a cellulose fibre is not uniform and there are both disordered (amorphous) and highly ordered (crystalline) regions (Howsmon & Sisson, 1963). The Fringed Fibril model is the predominant model used to explain the occurrence of both crystalline and amorphous regions (Hearle, 1963) as well as allowing for both parallel and anti-parallel chain arrangements (Zugenmaier, 2008). It describes the fibrils as being crystalline portions of a continuous network of chain molecules rather than self-contained units embedded in a "cement" matrix (Hearle, 1958). This model is important for the understanding of heterogeneous cellulose reactions.

Cellulose morphology is a well organised architecture of fibrillar elements arranged in a hierarchy of fibrillar entities (Klemm, et al., 2001a). The most commonly accepted view is that cellulose chains aggregate to form micro-fibrils, which are the smallest morphological unit (Perez & Mazeau, 2005; Klemm, et al., 2001a) and have a diameter in the range of 2-20 nm depending on the origin of the cellulose (O'Sullivan, 1997). The micro-fibrils are packed together to form larger aggregates called macro-fibrils which have diameters in the range of 60-360 μm (Egal, 2006).

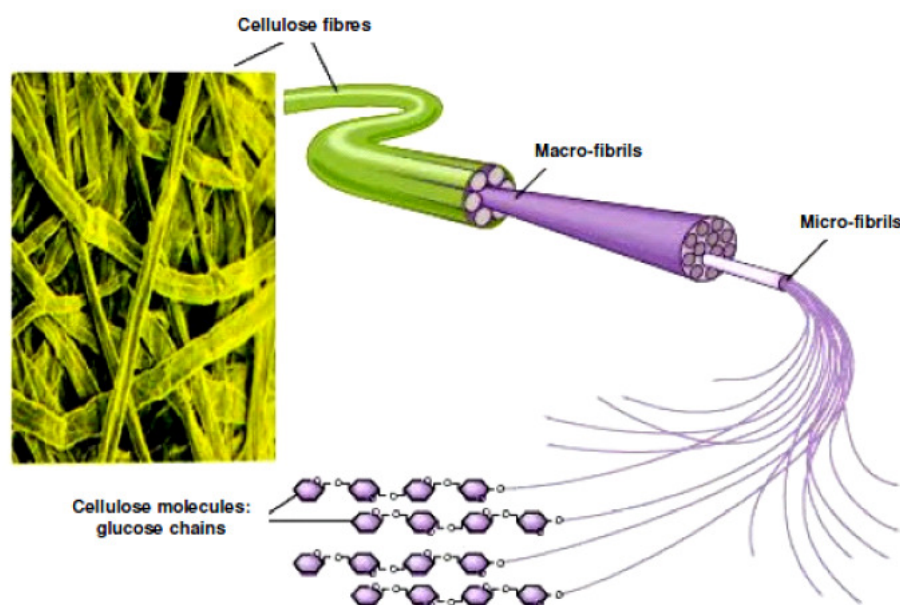


Figure 1-5 Super-molecular structure of cellulose (Egal, 2006)

Cellulose reactivity has been shown to be a function of the degree of cellulose crystallinity (Howsmon & Sisson, 1963), which varies significantly between different cellulose samples and depends on the origin and pre-treatment of the cellulose (Klemm, et al., 2001a).

The type of cellulose employed for the CMC manufacture largely depends on the final product characteristics and quality required. The most common sources of cellulose are cotton linters and dissolving pulps from hard or soft woods (Heinze, 2005).

1.2.3 Swelling of Cellulose

The swelling of cellulose is a prerequisite for subsequent controlled functionalization and without which the desired reactions would only occur on the surface layer of the cellulose (Klemm, et al., 2001a). During the process of swelling the gross structure of the cellulose is largely maintained, therefore it remains a two phase system, whereas during dissolution the system becomes a single phase and the original supra-molecular structure of the sample is destroyed. Both dissolution and swelling serve to enhance the accessibility of the cellulose hydroxyl groups for subsequent reactions (Klemm, et al., 2001a).

There are two principle types of swelling which occur; intercrystalline swelling, where the swelling reagent penetrates only the amorphous regions, and intracrystalline swelling where the swelling reagent penetrates the crystalline and amorphous regions (Howsmon & Sisson, 1963). In both cases the intermolecular cohesion between polymer chains is maintained but the intermolecular bonds are broken to varying extents (Klemm, et al., 2001a).

Intercrystalline and intracrystalline swelling are essentially similar processes that differ only in the degree to which the swelling occurs and, in fibres where the amorphous and crystalline regions are similar in terms of order, can be difficult to distinguish between (Howsmon & Sisson, 1963). The swelling within a given system is dependent upon temperature, concentration, specific interaction between the cellulose and the swelling agent (Howsmon & Sisson, 1963), as well as the origin of the fibre (Cuissinat & Navard, 2006).

Swelling of the cellulose can occur in both aqueous and nonaqueous media, the best example of intercrystalline swelling is the swelling of cellulose fibres in water (Howsmon & Sisson, 1963). In general organic liquids, like alcohols, swell cellulose less than water, the degree of swelling is affected by the solvent basicity, molar volume and the ability to form strong hydrogen bonds (Fidale, et al., 2008; Prusov, et al., 2014). Some protic as well as aprotic organic liquids show a significantly higher swelling power than water, such as formamide, dimethyl sulfoxide (DMSO), or ethanolamine (Klemm, et al., 2001a).

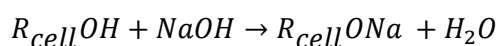
Swelling beyond the water-swollen condition can be achieved with certain aqueous solutions of acids, bases, or salts as well as, aqueous solutions of various organic compounds (Howsmon & Sisson, 1963). In general it appears that a high hydrogen-bond forming activity or polarity is connected with a high swelling power (Klemm, et al., 2001a). At high concentrations most strong acids and bases, as well as a few salts, produce both intercrystalline and intracrystalline swelling (Howsmon & Sisson, 1963).

1.2.4 The Chemistry

The preparation of carboxymethyl cellulose (CMC) can be said to have two distinct steps: mercerization, which is the preparation of alkali cellulose, and etherification, where the alkali cellulose reacts with an etherification reagent such as sodium monochloroacetate (SMCA) or monochloroacetic acid (MCA) (Klemm, et al., 2001b).

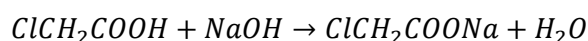
Due to the participation of the cellulose's free hydroxyl groups in both inter- and intramolecular hydrogen bonding, the cellulose first needs to be "activated" or swelled before it can be etherified, as detailed in the previous section. For the synthesis of CMC the cellulose is first treated with an aqueous NaOH solution at 20 to 40°C at a concentration of 18 to 32% to form alkali cellulose (Budtova & Navard, 2016). This process is referred to as mercerization. This opens up the cellulose's natural structure to obtain a sufficiently swollen material that is accessible to reaction with further reagents (Thielking & Schimdt, 2012). Unlike the untreated cellulose, the alkali cellulose (Na-cellulose) is highly reactive towards the etherification reagents (Ambjornsson, et al., 2013).

Mercerisation



Etherification

Step 1 - Neutralisation of the MCA



Step 2 – Reaction of SMCA with Cellulose

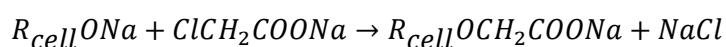


Figure 1-6 Reaction steps for the synthesis of CMC

Through this swelling process several properties of the end product are predetermined, as the degree and uniformity of swelling influences the eventual distribution of the substituents introduced in the subsequent etherification reaction (Thielking & Schimdt, 2012).

The Williamson etherification reaction is an exothermic process that is normally carried out at about 50 to 70°C over several hours (Davidson, 1980; Klemm, et al., 2001b), and can be performed in either an aqueous (dry) or aqueous-alcoholic medium (slurry) (Thielking & Schimdt, 2012). The full aqueous process is referred to as a dry process because no free liquid is visible during the reaction unlike the aqueous-alcoholic slurry process where the relatively small quantity of cellulose is suspended in the organic media, example shown in Figure 1-7 below.



Figure 1-7 Photos of the dry/aqueous reaction (left) and the solvent slurry reaction (right). The dry/aqueous reaction has no free liquid present while for the solvent slurry reaction there is a clear solid liquid separation between the cellulose (bottom) and the solvent (top) when the agitator is stopped.

The yield from this process varies between 65% and 85% in relation to the etherifying agent (Thielking & Schimdt, 2012) with up to 30% of the etherifying agent being consumed in a side reaction with aqueous NaOH, forming predominantly sodium glycolate by hydrolysis of the chloroacetate (Klemm, et al., 2001a).

1.2.5 Cellulose Mercerisation

The process of Mercerisation was patented in 1850 by its inventor, John Mercer, and involves the treatment of native cellulose with a concentrated aqueous NaOH solution (Budtova & Navard, 2016). Mercerisation is not fibre dissolution but rather a change in the morphology and crystalline structure of the cellulose fibre from native cellulose I to cellulose II. This transformation of the cellulose occurs via the intermediate crystalline species called alkali-cellulose or Na-cellulose. (Budtova & Navard, 2016).

In a series of articles published from 1984 to 1985, Okano and Sarko proposed a mechanism for the mercerisation process which identified the existence of unique Na-cellulose intermediate structures. During the first step of mercerisation the alkali solution penetrates the amorphous regions, which results in the swelling of the cellulose fibre and the formation of an anti-parallel Na-cellulose I, with very little initial effect on the crystalline regions. In the next stage the Na-cellulose I continues to adsorb more NaOH thereby converting to the Na-cellulose II structure in which all contacts between adjacent chains in the unit cell have been removed. In the final step the NaOH is washed out of the structure and the cellulose chains are converted to the cellulose II polymorphic form (Okano & Sarko, 1984; Okano & Sarko, 1985).

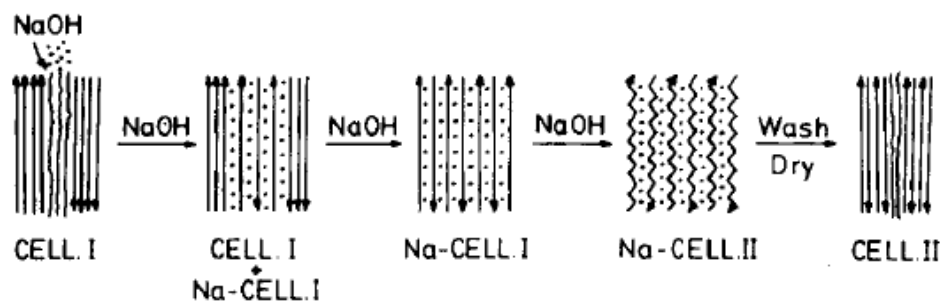


Figure 1-8 Fibril rearrangement during mercerization (Okano & Sarko, 1985)

For the carboxymethylation reaction it is the alkali-celluloses which are of the greatest interest. These intermediates are important because they have an enhanced chemical reactivity in comparison to the native cellulose (Sjostrom, 1993). Reagents are able to penetrate the swelled cellulose more easily and the substitution reaction with the hydroxyl groups is easier because the nucleophilic attraction between the O-H has been decreased (Almlof, 2010).

Five different crystalline forms of alkali-cellulose have been identified and these can be divided into two types based on their crystallographic fibre repeats. Na-cellulose I, III, and IV exhibit a repeat of 10.3 Å, while type Na-cellulose IIA and IIB have a repeat of 15.0 Å (Okano & Sarko, 1984). The type of alkali cellulose formed is dependent on the NaOH concentration, temperature and subsequent treatments. The most important forms of alkali cellulose are Na-cell I and Na-cell II.

The uptake of alkali metal hydroxides has been found to be an adsorption process rather than a purely chemical one (Almlof, 2010). Serkov (2000) proposed a two-step process where initially rapid swelling takes place for 1 -3 minutes driven by a mechanism of convective diffusion. The second stage occurs by molecular diffusion, driven by a difference in concentration between the outer solution and the adsorbed solution, over 1 to 1.5 hours (Serkov, 2000). It has been observed that cellulose contacted with NaOH dissolved in aliphatic alcohols such as isopropanol show a markedly reduced swelling in comparison with aqueous systems and proceed at a reduced rate (Klemm, et al., 2001a).

1.2.6 The Etherification Reaction

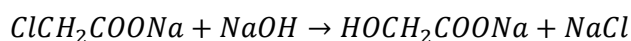
The etherification reaction proceeds via a nucleophilic substitution reaction known as the Williamson synthesis (Klemm, et al., 2001a). This synthesis consists of an S_N2 reaction of a sodium alkoxide, in this case the alkali cellulose, with an alkyl halide, the SMCA. If MCA is used as the etherification reagent then it must first be neutralised in-situ to form its sodium salt.

Although steps have been made towards a homogeneous reaction system at an academic level, on an industrial scale CMC is produced almost exclusively via a heterogeneous reaction system (Klemm, et al., 2001b) i.e. where the principal reactants remain in the solid state either as dry matter or suspended in a solvent medium (Richardson & Gorton, 2003). Generally heterogeneous systems have reduced reaction rates, lower degree of conversion and restricted accessibility of reaction sites, compared with homogeneous systems. For cellulose these parameters are controlled to a large extent by the supra-molecular structure and fibrillar architecture of the polymer (Klemm, et al., 2001a). This all points to why the swelling of the native cellulose is so important for its activation.

Although the most predominant side reaction which occurs during the carboxymethylation reaction is that of the SMCA with the aqueous NaOH to form sodium glycolate, side reactions can also occur with water if it is present in a large excess to form glycolic acid (Klemm, et al., 2001a).

These two side reactions need to be carefully controlled so that the etherification reaction can be promoted (Omiya, 1984). In the presence of a large excess of NaOH the SMCA is converted to sodium glycolate thereby reducing the availability of the expensive etherifying agent and reducing the efficiency of the substitution reaction.

Formation of Sodium Glycolate



Formation of Glycolic Acid

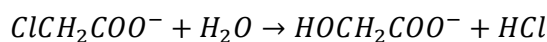


Figure 1-9 Possible side reactions which can occur during the production of CMC

If there is no NaOH available in the reaction system the SMCA reacts with water to form glycolic acid thereby making the reaction system acidic. The glycolic acid attacks the carboxyl groups of the CMC converting parts of the CMC into its free acid form and seriously reducing its solubility. Both these side reactions can be minimised by carefully controlling the NaOH to MCA ratio throughout the reaction (Omiya, 1984).

The pattern of the substitution of the AGU is governed by the reactivity of the hydroxyl groups, which varies depending on the substitution reaction and the conditions (Salmi, et al., 2011). Most studies have used the quantitative distribution of substituents between the three reactive hydroxyl groups as an indication of their relative reactivity, however there appears to be little consensus between the results (Nicholson, 1976; Baar, et al., 1994; Klemm, et al., 2001b; Salmi, et al., 2011).

The OH-2 hydroxyl group is the most acidic (Sjostrom, 1993), due to its proximity to the electron withdrawing anomeric centre, and is therefore the most reactive at low alkali concentrations (Nicholson, 1976; Salmi, et al., 1994; Richardson & Gorton, 2003). However, as the size of the substituent increases, steric factors become more important and the OH-6 would then be preferred (Nicholson, 1976; Sjostrom, 1993; Salmi, et al., 2011), higher alkali concentrations also favour the OH-6 group (Richardson & Gorton, 2003).

1.2.7 Degree of Substitution

The extent to which the cellulose hydroxyl groups react to form a derivative is termed the degree of substitution (DS) and corresponds to the average number of hydroxyl groups which have reacted per AGU (Klemm, et al., 2001a).

Therefore, if only one of the three hydroxyl groups has been carboxymethylated the DS will be 1.0 and the theoretical maximum obtainable DS is 3.0 (Davidson, 1980). The generally accepted threshold for CMC solubility in water is a DS of 0.4 (Feddersen & Thorp, 1993) and increasing the DS will increase the solubility (Sjostrom, 1993). A CMC with a DS of 0.6 will have good solubility but at a DS of 0.2 it will retain the fibrous character of the cellulose starting material and will not be soluble (Ambjornsson, et al., 2013). Most commercially available CMCs have a DS of less than 1.5, with the most common range being between 0.4 and 0.8 (Feddersen & Thorp, 1993).

1.2.8 Distribution of Substitution

The uniformity of the substituent distribution has a profound impact on the properties of the final CMC product (Feddersen & Thorp, 1993). Nicholson (1976) stated that a non-uniform cellulose derivatisation would result in a CMC with mixed solubility, where the substituted portions of the cellulose would be soluble while the unsubstituted regions wouldn't be, this results in large variations in the behaviour of plain water solutions of CMC. deButts, et al. (1957), reported that the uniformity of the substituent distribution along the polymer chain had a profound effect on the rheological properties of CMC solutions. Uniform substitution resulted in CMC solutions exhibiting pseudo plastic behaviour whereas non-uniformity produced thixotropic solutions, which arose because of the presence of a very small quantity of unsubstituted crystalline residues in the CMC (deButts, et al., 1957; Elliot & Ganz, 1974).

Other characteristics of CMC solutions affected are; the shear and temperature stability (Cheng, et al., 1998), the interaction with other solution components such as dissolved salts and solids (Francis, 1961; Feddersen & Thorp, 1993) and the solution behaviour in different solvents (Francis, 1961).

The heterogeneous nature of the carboxymethylation reaction raises questions regarding the uniformity of the substituent distribution along and between the polymer chains (Feddersen & Thorp, 1993) In a homogeneous reaction system, where all the hydroxyl groups remain equally accessible for substitution, a random distribution of substituents will result (Richardson & Gorton, 2003). If, however, all the hydroxyl groups do not have equal accessibility for substitution then a more heterogeneous distribution of substituents will result, this can occur if, for example, un-activated crystalline regions remain in the native cellulose (Adden, 2009). Further deviation from the random substituent distribution will occur if the reactivity of the hydroxyl groups changes as the reaction proceeds (Richardson & Gorton, 2003). Areas could become either more reactive, due to changes in polarity or improved solubility of the substituted polymer, or less so due to steric hindrance or electrostatic repulsion (Adden, 2009).

The determination of the distribution of substituents at both a monomer and polymer chain level is the focus of numerous research papers which is well summarised in a review conducted by Richardson & Gorton (2003).

1.2.9 Methods of Manufacture

The process for the synthesis of CMC was invented in 1918 but it was not until its application as an anti-redeposition agent in powder detergents was discovered in 1935 that commercial production began to gain momentum. In 1940 the German company Kalle and Co., a subsidiary of I.G. Farbenindustrie A.G., produced the first commercial technical grade CMC's which were sold under the trade name Tylose HBR (NIIR Board, 2003).

The original manufacturing process for CMC, which was limited to the production of technical grades (Stigsson, et al., 2001), involved steeping sheets of sulphite pulp in an 18% aqueous NaOH solution for several hours at 18 to 20°C (NIIR Board, 2003). The excess NaOH was then pressed from the alkali cellulose before being passed through toothed roll mills and horizontal disk shredders to produce a fine alkali cellulose crumb.

The alkali cellulose crumb was then charged to a jacketed kneader where it was reacted with dry SMCA at 35°C to 45°C for 2 to 4 hours. The reaction was completed in a tumbling drum at 50 to 70°C for up to 10 hours after which the product was passed through another mill to produce the final fine granular CMC (NIIR Board, 2003). The outline for this process is shown in Figure 1-10.

This original process was an entirely batch process which required the use of a considerable amount of heavy equipment and the two major steps of the reaction, namely mercerization and etherification, were carried out in separate reactors with a dry solids content of about 80 to 90% (Stigsson, et al., 2001).

This process was characterised by excessive times for mixing of the ingredients to obtain uniform distribution of the reactants, while completely water soluble products could only be obtained by using excessive quantities of expensive MCA or SMCA (Branan, 1953). The amounts of etherification reagents used exceeded, by a considerable degree, the amounts theoretically required. The quality and characteristics of the CMC e.g. the DS, solubility, viscosity and homogeneity varied considerably (Hodge, et al., 1953). The steeping and pressing procedures for the preparation of the alkali cellulose were also problematic because the alkali cellulose prepared in this way retained far more NaOH and water than is required for the economic preparation of the CMC (Grassie & Wallis, 1954).

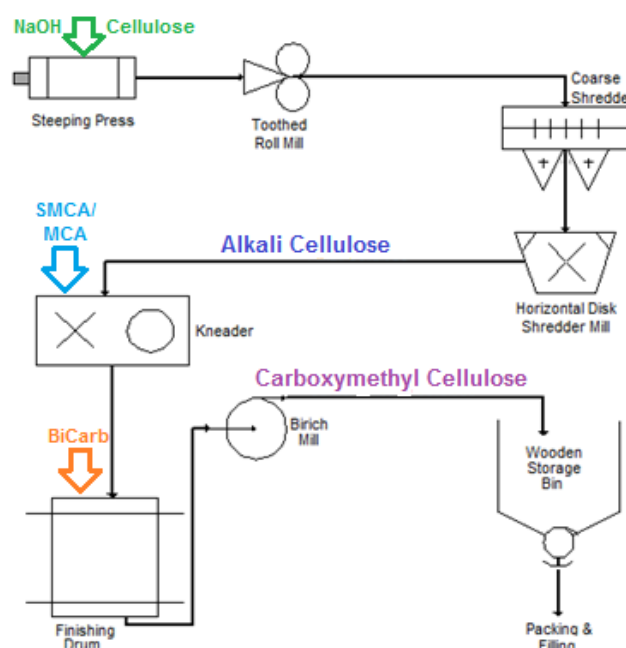


Figure 1-10 Flow sheet for the German batch process for CMC manufacture. Adapted from NIIR Board (2003)

In 1947 Wyandotte Chemicals Corp. developed a continuous process for the manufacture of CMC (NIIR Board, 2003). A bleached sulphite pulp powder was sprayed with a 35% NaOH solution as it entered a 6.1 m long rotating drum reactor, after a residence time of an hour in the feed zone of the reactor it moved into the central zone where it was sprayed with a 78% solution of MCA. The reaction mass temperature was maintained between 35 and 45°C for a further 2 hours before being discharged from the reactor into drums where it was allowed to age for 8 to 10 hours at 50 to 55°C. The drum contents were then fed into a primary mill followed by a flash dryer to produce the final dried product (NIIR Board, 2003).

The 1950's saw the emergence of alcohol based semi-dry processes, with a solids content of approximately 50%, which improved the CMC quality and decreased the consumption of chemicals (Stigsson, et al., 2001). Various dough-mixing and dry-mixing procedures were proposed over time to overcome the inherent shortcomings of the steeping process. However, these also failed to yield the desired uniformity because the small amounts of NaOH and water required for economic preparation of the CMC could not be uniformly distributed on the cellulose by dough-mixing or dry-mixing (Grassie & Wallis, 1954).

The concerns around the uniformity of mixing and distribution of reactants arose from the knowledge that uniform distribution of reactants during the etherification of the cellulose would produce a more uniform product thereby improving the solubility of the CMC even at relatively low DS (Paddison & Sommers, 1961; Grassie & Wallis, 1954). It was common to find that aqueous solutions of CMC, with DS ranging from 0.3 to 1.5, were hazy and contained undesirable amounts of insoluble matter, which was indicative of non-uniform substitution (Swinehart, 1950). For many commercial uses a CMC is unacceptable unless the aqueous solution has a haze rating of "Good" or better and contains little to no insoluble material. Even at its best the quality of the CMC obtainable with the dry/aqueous process was considered to be inferior (Cordrey, et al., 1963).

In order to obtain a uniform distribution of the ingredients a liquid medium is required, the most logical of which would be water. Although a certain amount of water is required in order to provide the initial swelling of the cellulose in the presence of the NaOH and to carry the etherifying agent into the cellulose fibre, if the quantity of water is increased above a certain limit the now soluble CMC produces a gummy, unworkable mass which prevents further reaction and mixing (Paddison & Sommers, 1961). This gummy mass cannot be readily re-dissolved in water, the drying of the material is complicated, and the removal of the salt by-products is rendered extremely difficult (Branan, 1954).

The reaction efficiency of the MCA is also strongly dependent on the total water content of the reaction. Ideally the water content should be between 5 and 15% however as the water content decreases it becomes increasingly difficult to ensure a homogeneous blend of the chemicals and therefore increases the risk of variations in the product quality (Stigsson, et al., 2001).

Hercules Powder Company introduced the slurry-process based on the patent by Klug and Tinsley (1950) in the 1960's. Using a solvent as the liquid media in which the reaction is conducted allows for more homogeneous mixing of the reactants and results in a more uniform reaction (Branan, 1953). Water-miscible alcohols also aid in the wetting of the cellulose thereby facilitating penetration of the aqueous caustic mixture and aiding activation of the cellulose (Paddison & Sommers, 1961). The use of a solvent media makes it possible to produce a water soluble CMC without employing excessive ratios of the reactants and with reasonable reaction efficiency (Branan, 1953). The slurry process therefore eliminates many of the disadvantages of the dry/aqueous process i.e. heavy mixing equipment is not required, reaction periods are substantially shorter and the quality of the product is improved (Cordrey, et al., 1963).

The one step slurry process utilises a fine powder cellulose, with an average particle size of 0.75 mm, this is a critical requirement for the quality of the end product (Stigsson, et al., 2001). The powdered cellulose is suspended in a water-alcohol mixture with a solids content of 10%, isopropanol is the most commonly used solvent.

The cellulose is then treated with a concentrated NaOH solution at 20-30°C, followed by the addition of dry MCA or SMCA. The etherification reaction is normally carried out between 50 and 80°C (Almlof, 2010). Depending on the required purity of the product the CMC is washed with an alcohol-water mixture, methanol or ethanol are more efficient for the washing of the CMC than isopropanol (Stigsson, et al., 2001). The excess alcohol is stripped from the product before the grinding and drying processes. The suspension and washing liquids are then recovered and reprocessed by either distillation or by membrane processes for reuse (Thielking & Schimdt, 2012).

During the 1970's and 1980's, CMC developed into one of the most versatile thickeners with a large number of industrial applications (Stigsson, et al., 2001). The introduction of vacuum technology and the replacement of aqueous MCA with MCA flakes significantly improved the reaction efficiency and allowed for the production of higher DS products (Stigsson, et al., 2001). The historical improvements to the CMC manufacturing process are summarised in Table 1-2.

Table 1-2 Schematic overview of CMC process development (Stigsson, et al., 2001)

Time Period	Production Method
1920 - 1940	Dry process (80-90% dry solids)
1950	Semi-dry process (~50% dry solids)
1960	Slurry process (~10% dry solids)
1970-1980	Vacuum operation in the semi-dry process
1990	Continuous optimisation of the processes

Since the 1990's the process has remained basically the same with improvements focussed mainly on the reduction of solvent losses and improvement of process economy (Stigsson, et al., 2001). A simplified process flow diagram for the contemporary industrial production of purified CMC is shown in Figure 1-11.

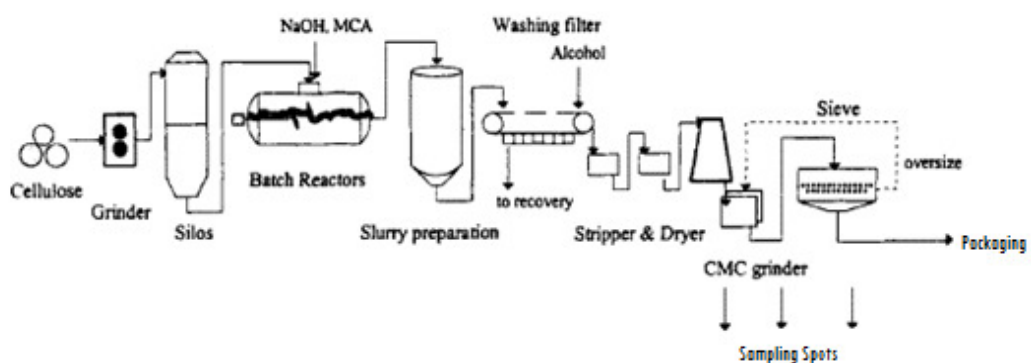


Figure 1-11 The modern slurry process for the production of purified CMC (Stigsson, et al., 2004)

Today commercial production of CMC's is almost exclusively carried out by means of the slurry process (Heinze, 2005).

Recent work on the dry/aqueous process has been limited with most authors addressing elements of the process but not the process as a whole. Heydarzadeh, et al. (2009) looked at optimising the NaOH and MCA solution concentrations while Cheprasova, et al. (2012) looking at the use of different solvents, including water, for the carboxymethylation of wood with microwave radiation. Most recently Alban Reyes, et al., 2017 investigated the alkalisation of dissolving cellulose pulps with highly concentrated NaOH solutions used in low stoichiometric excess in relation to the cellulose. It is therefore felt that the opportunity exists to optimise the dry/aqueous process further to make it a more acceptable, environmentally friendly alternative to the current slurry process for the production of technical grade CMC's on an industrial scale.

1.3 Application of Green Chemistry to CMC Synthesis

It is necessary to define the concept of green chemistry and the principles that govern it in order to understand where these could be applied to the synthesis of CMC. A definition of green chemistry was proposed by Paul Anastas and John Warner in 1998 as the design of chemical products and processes that reduce or eliminate the use or generation of hazardous substances. Green chemistry is commonly presented as a set of twelve principles which may be summarized as follows:

1. Prevention: Chemistry must avoid the production of toxic and hazardous waste rather than removing these wastes after they are formed.

2. Atom economy: In a synthesis, all components used should be incorporated to the maximum extent possible into a final product.
3. Less hazardous chemical syntheses: Wherever possible, chemical synthesis should be designed to use and generate substances with low toxicity and low environmental impact.
4. Designing safer chemicals: Chemical products should be designed to exhibit their desired function with a minimum level of toxicity.
5. Safer solvents and auxiliaries: Auxiliary substances (for example, solvents) should be avoided if possible and should be innocuous when used.
6. Design for energy efficiency: Energy requirements of chemical processes should be minimized to reduce their environmental impact, and if possible, processes should be performed at ambient temperature and pressure.
7. Use of renewable feedstocks: Raw materials or feedstock should be renewable.
8. Reduce derivatives: Whenever possible, unnecessary derivatization (for example, protection/deprotection) should be reduced or avoided.
9. Catalysis: It is best to employ catalytic reagents (as selective as possible) rather than stoichiometric reagents.
10. Design for degradation: Chemical products should be designed so that at the end of their functional lifetime they undergo an innocuous degradation process and do not persist in the environment.
11. Real-time analysis for pollution prevention: Analytical methodologies should be developed to allow for real-time analysis without the formation of hazardous substances.
12. Inherently safer chemistry for accident prevention: Substances involved in a chemical process should be chosen to minimize the potential for chemical accidents.

The foremost environmental impacts of CMC production are the evaporation of alcohol from the production process and the generation of waste water (Stigsson, et al., 2001). The alcohols are classified, in terms of environmental impact, as Volatile Organic Compounds (VOC), while the waste water contains substances which contribute to both the Chemical Oxygen Demand (COD) and Biological Oxygen Demand (BOD) if released without treatment (Stigsson, et al., 2001). Large quantities of alcohol are used as both a reaction and washing medium. Although the environmental impact of the process is mitigated somewhat, by the recovery and recycling of the alcohol, this in turn relies on an energy intensive distillation process.

Replacement of toxic solvents with environmentally benign alternatives is a key principal of green chemistry as solvents account for most of the mass wasted in synthetic and industrial processes (Farran, et al., 2015). Over and above this many common solvents are toxic, flammable and/or corrosive. Their volatility and solubility can contribute to air, water and land pollution as well as present serious health risks to workers. Recovery and reuse, when possible, is also often associated with energy-intensive processes such as distillation (Farran, et al., 2015). Therefore reducing the amount of solvent used, adopting an alternative more environmentally acceptable solvent or moving towards a completely solvent free process could significantly reduce the environmental impact of the CMC synthesis.

There is no “greener” solvent than water; inherently safe it is non-toxic, non-flammable and non-corrosive, it is also readily available at relatively low cost and environmentally benign (Dallinger & Kappe, 2007; Rathi, et al., 2015; Polshettiwar & Varma, 2010). A solvent free, aqueous process would therefore be the most environmentally friendly option for the CMC synthesis, however, there are several constraints on the efficiency and product quality of the dry/aqueous process which make water a problematic solvent for CMC production. Overcoming these constraints, by looking for ways to optimise the dry/aqueous process, would be the key to making water a viable solvent for the CMC synthesis.

Besides optimising the reaction conditions the use of microwave technology as an alternative heating mechanism for the reaction could be investigated.

Compared with conventional heating, microwave-assisted heating has been shown to reduce reaction time and increase product yield and purity for the carboxymethylation of various cellulose materials (Biswas, et al., 2014; dos Santos, et al., 2015; Hivechi, et al., 2015). This technology could therefore not only have a positive impact on the reaction efficiency but also improve energy efficiency of the CMC production, further improving the environmental impact of the CMC process.

1.4 Molecular Characterisation of CMC

By their very nature polysaccharides are polydisperse and contain a distribution of molecules with variations in chain lengths, structure and chemical compositions (White, 1999). This makes it very difficult to characterise polysaccharide derivatives such as CMC (Rinaudo, et al., 1993).

The use of size exclusion chromatography (SEC) in conjunction with a variety of detectors has been shown by numerous authors to be one of the most powerful methods for the characterisation of cellulose derivatives (Rinaudo, et al., 1993; Kulicke, et al., 1996; White, 1999; Clasen & Kulicke, 2001; Richardson, et al., 2002; Enebro, et al., 2007; Gaborieau & Castignolles, 2011).

1.4.1 Size Exclusion Chromatography (SEC)

Size exclusion chromatography (SEC), also commonly referred to as gel permeation chromatography (GPC), is a liquid chromatographic technique which sorts molecules according to size allowing for the calculation of molecular weight averages and molecular weight distribution (MWD) (Yau, et al., 1980). Unlike HPLC the separation mechanism for SEC is uniquely dependent on the size of the polymer molecule in solution, rather than any chemical interactions between the analyte and the stationary phase (Podzimek, 2011; Agilent Technologies, 2015).

The size of a polymer in solution is described as its hydrodynamic volume (Su, 2013) and, is dependent on a number of factors such the molar mass (M), MWD, type of substituent, DS and distribution of the substituents along the polymer backbone (Elliot & Ganz, 1974; Kulicke, et al., 1996; Clasen & Kulicke, 2001; Enebro, et al., 2007).

The hydrodynamic volume is also influenced by the number, positions and lengths of branches along the polymer chain (Gaborieau & Castignolles, 2011). An increase in the degree of branching results in a contraction of the polymer chain and corresponding reduction in the hydrodynamic volume, therefore for a branched and a linear molecule of the same molecular weight the branched polymer will have the smaller hydrodynamic volume (Gaborieau & Castignolles, 2011), Figure 1-12.

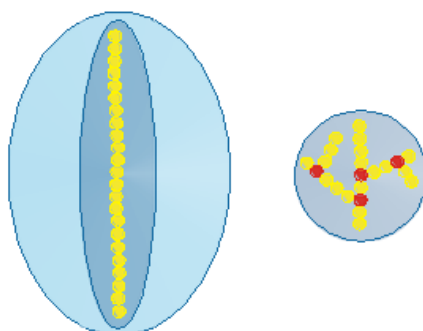


Figure 1-12 Schematic representation of the relative hydrodynamic volumes of a linear and a branched polymer with the same molecular weight.

In SEC the stationary phase is comprised of extremely small porous beads, typically polymer or silica, designed to have pores of a defined size (Agilent Technologies, 2015). The pore size of the stationary phase therefore determines the molecular size range within which the separation occurs and the manner in which the samples elute from the column (Yau, et al., 1980; Agilent Technologies, 2015; Su, 2013).

Prior to SEC analysis the polymer is prepared as a dilute solution which is then injected on to the column. As the dissolved polymer molecules are carried by the mobile phase through the column they flow past the “porous beads” and can diffuse into the internal pore structure. Larger molecules can enter only a small fraction of the pores or are excluded completely, while smaller polymer molecules penetrate to a larger extent (Agilent Technologies, 2015). The polymer molecules, therefore, elute from the column in order of their molecular size, hydrodynamic volume, with the largest emerging first (Yau, et al., 1980; Clasen & Kulicke, 2001; Richardson & Gorton, 2003; Su, 2013). As the polymer fractions exit the column they can be detected in various ways.

If a concentration sensitive detector such as a differential refractometer is used then the resulting chromatogram is a size distribution in weight concentration (Yau, et al., 1980) as depicted in Figure 1-13. Therefore, in any given elution volume all the molecules will have identical hydrodynamic volumes, but can have different molar masses, number of branch units, and chain architectures (Podzimek, 2011).

SEC offers several advantages for polymer characterisation such as relative simplicity, versatility, the ability to determine the complete distribution of molar masses, speed of measurement, and low sample demand (Podzimek, 2011).

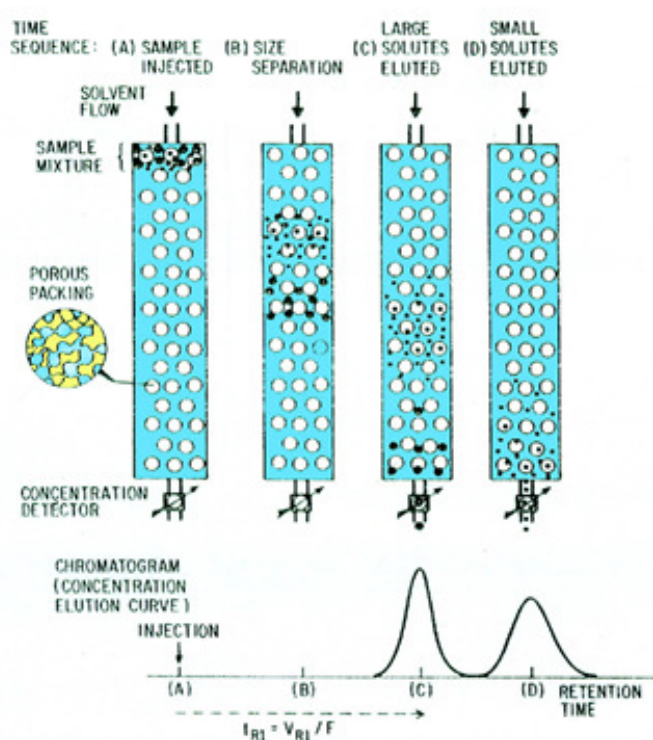


Figure 1-13 Separation of polymer molecules by hydrodynamic volume by SEC/GPC (Yau, et al., 1980)

1.4.2 Detectors

The analysis of the polymer fractions eluting from the SEC columns can be performed by a variety of detectors of which, the refractive index (RI) detector, ultraviolet (UV) detector, viscometer, light scattering (LS) detector, infrared (IR) photometer, and the evaporative light scattering detector (ELSD) are the most common (Podzimek, 2011).

The selection of the detectors is determined by the characteristics of the polymer and the required analysis. Detectors such as the RI, UV and ELSD are sensitive only to concentration (Agilent Technologies, 2015), whereas a LS detector is sensitive to both concentration and molecular mass, while a viscometer responds to the changes in viscosity of a polymer in relation to its concentration (Podzimek, 2011).

1.4.2.1 The Refractive Index Detector

The refractive index (RI) detector is one of the most common detectors used in conjunction with SEC, it is a concentration sensitive detector (Agilent Technologies, 2015), which functions by comparing the difference in refractive index between the pure mobile phase and the mobile phase containing analyte (Kamide, et al., 1993), and for this reason it is often referred to as a differential refractive index (DRI) detector. Its response is directly proportional to the sample concentration (Agilent Technologies, 2015) and can be described by the following equation (Ford, et al., 1998);

$$RI_{(signal)} = K_{(cal)} c \left(\frac{dn}{dc} \right) \quad \text{Equation 1}$$

Where $K_{(cal)}$ is the calibration constant of the detector, c is the concentration and dn/dc is the specific refractive index increment of the sample. The dn/dc is defined as the change in the refractive index of the solution with respect to the change of polymer concentration, and is obtained from the slope of a plot of these two parameters (Hong Chen & Wyatt, 1999; White, 1999; Wyatt Technology, 2010; Su, 2013). The dn/dc is a critical parameter for the calculation of a samples the absolute molecular weight using a light scattering detector (LSD). An RI detector is therefore used to determine both the concentration and the dn/dc of the polymer solution (Ford, et al., 1998).

There are several other types of concentration detector which are routinely used in conjunction with SEC such as UV, IR and ELSD (Podzimek, 2011). In comparison to the RI these detectors sometimes exhibit better baseline stability and higher sensitivity, however, the ability to measure the dn/dc of the sample is lost (Malvern Instruments Limited, 2015). This therefore makes the RI the preferred detector for use in conjunction with a LSD and for triple detection.

1.4.2.2 The Viscometer

The use of on-line viscometers as a detection technique for SEC has become widespread, especially for the analysis of synthetic polymers and polysaccharides (Striegel, 2016). There are two principal areas where viscometric detection finds application; 1. The use of universal calibration to determine the absolute, calibrant-independent molecular weight and MWD, 2. The characterisation of long-chain branching in macromolecules (Striegel, 2016).

The most common type of on-line viscometer is a differential viscometer. This viscometer determines the viscosity of a polymer by measuring the pressure drop between a capillary containing pure mobile phase and a capillary with mobile phase containing polymer (Podzimek, 2011), the basic design is shown in Figure 1-14.

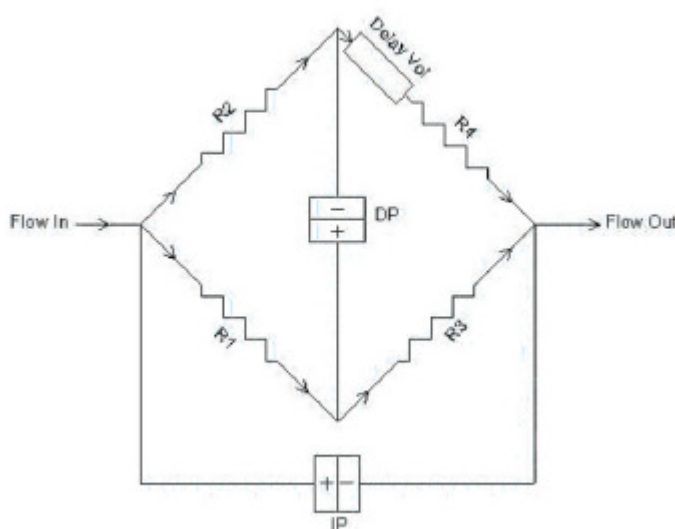


Figure 1-14 Basic design of a differential viscometer consisting of, 4 capillary tubes (R1-R4) which are arranged in a balanced bridge configuration, a differential pressure transducer (DP), an inlet pressure transducer (IP) and a delay volume (Malvern Instruments Limited, 2015).

The pressure drop across the bridge, from inlet to outlet, is measured by the inlet pressure transducer (IP) and the pressure drop through the bridge is measured by the differential pressure transducer (DP) (Striegel, 2016). The delay volume is a hold up reservoir which provides a reference flow of solvent through R4 during the analysis (Malvern Instruments Limited, 2015).

The pressure drop across the capillaries can be related to the specific viscosity of the fluid in the capillary by means of Poiseuille's Law (Haney, 1985; Agilent Technologies, 2012). Specific viscosity (η_{sp}) articulates the increase in viscosity due to the presence of polymer molecules in a solution. It is expressed as the ratio of the absolute viscosity of the dilute polymer solution (η) to that of the pure mobile phase (η_0) as per Equation 2 below (Podzimek, 2011; Malvern Instruments Limited, 2015).

$$\eta_{sp} = \frac{\eta - \eta_0}{\eta_0} \quad \text{Equation 2}$$

When used in conjunction with a concentration detector, such as RI, the intrinsic viscosity can be calculated (Haney, 1985). The intrinsic viscosity $[\eta]$ is defined as the ratio of specific viscosity (η_{sp}) to concentration (c) to the limit of infinite dilution (Podzimek, 2011; Malvern Instruments Limited, 2015).

$$[\eta] = \lim_{c \rightarrow 0} \frac{\eta_{sp}}{c} \quad \text{Equation 3}$$

The intrinsic viscosity can, in turn, be related to the number-average molecular weight (M_n) for the polymer by means of universal calibration (Gaborieau & Castignolles, 2011). It is for this reason that a viscometer is generally considered to be a mass sensitive detector.

There is, however, a great deal of evidence which indicates that universal calibration is not suitable for aqueous elution systems, due to the occurrence of non-SEC separation mechanisms such as electrostatic exclusion and selective column sorptive effects (Reed, 1995). Although it does still find application for samples with low molecular weights and/or low dn/dc , the use of light scattering detection has become the preferred method for determining molecular weight for the majority of polymers (Malvern Instruments Limited, 2015). When used in conjunction with a light scattering detector a viscometer provides valuable information on polymer size and branching characteristics (Podzimek, 2011).

1.4.2.3 The Light Scattering Detector

A light scattering detector is considered to be an absolute detector because the molecular weight and root mean square radius of a polymer can be determined without the requirement of universal calibration (White, 1999).

There are three types of light scattering detectors which are commonly available, a low-angle light scattering (LALS), right-angle light scattering (RALS) and multi-angle light scattering (MALS) (Agilent Technologies, 2015). All three detectors are static light scattering detectors which work on the principal that a beam of light will be scattered when it strikes a polymer molecule (Agilent Technologies, 2015). As the sample scatters the incident light each detector provides a response which is directly proportional to the intensity of the scattered light it receives (Wyatt Technology, 2010).

The basic equation which relates the intensity of the scattered light to the properties of the polymer is shown below (Hong Chen & Wyatt, 1999; White, 1999; Wyatt Technology, 2010; Su, 2013).

$$\frac{K^* c}{R(\theta)} \approx \frac{1}{MP(\theta)} + 2A_2 c \quad \text{Equation 4}$$

Where $R(\theta)$ is the excess Rayleigh ratio measured at concentration c and light scattering angle θ . M is the weight average molecular weight and A_2 is the second virial coefficient. $P(\theta)$ is the particle scattering function which is dependent on the structure of the scattering molecule and describes the scattered light's angular dependence, this is the term from which the root mean square radius (RMS) is derived. K^* is the optical constant described by, $K^* = 4\pi^2(dn/dc)^2 n_0^2 / (N_A / \lambda_0^4)$ where N_A is Avagadro's number, λ_0 is the vacuum wavelength of the incident light, n_0 is the refractive index increment of the solvent and dn/dc is the specific refractive index increment of the sample.

The basic light scattering equation can be summarised by two fundamental principles; firstly that the intensity of light scattered is proportional to the concentration and the molecular weight of the polymer and, secondly that the angular variation of the scattered light intensity is dependent on the size of the polymer (White, 1999; Podzimek, 2011). A more detailed derivation of the light scattering equations can be found in Kamide, et al., 1993 and Podzimek, 2011.

To determine the RMS radius of a polymer a minimum of two light scattering angles is required, as R_g is calculated from the angular dissymmetry of the scattered light intensity at different angles, a MALS-type light scattering detector is therefore required (Podzimek, 2011).

MALS detectors allow for the simultaneous determination of both molecular weight and size of a polymer and, the precision of these results increases as the number of scattering angles increases (Wyatt, 1997).

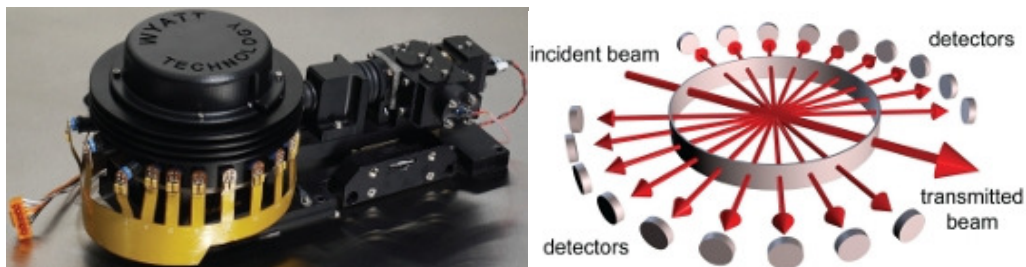


Figure 1-15 Shown on the left is the optical bench for the Dawn Helios II (Wyatt Technology) multiangle light scattering photometer (Wyatt Technology, 2010). The diagram on the right is a schematic representation of how the multiangle light scattering measurement is made (Wyatt, 2013).

1.4.2.4 Triple Detection

The term triple detection is used to describe the analysis of polymers by SEC where a RI detector, a light scattering detector and a viscometer are used in series. This is a well-established technique which is applicable to synthetic polymers as well as to natural polymers such as proteins and polysaccharides (Malvern Instruments Limited, 2015). The use of triple detection is considered to be the most advanced form of multi-detection for SEC (Agilent Technologies, 2012). The power of this technique is in the complimentary information supplied by all the detectors for each fractionated slice as it emerges from the SEC column. The RI detector provides an accurate concentration profile while the MALS determines both absolute molecular weight and the RMS, the viscometer provides the structural data allowing for the determination of branching and hydrodynamic size (Malvern Instruments Limited, 2015).

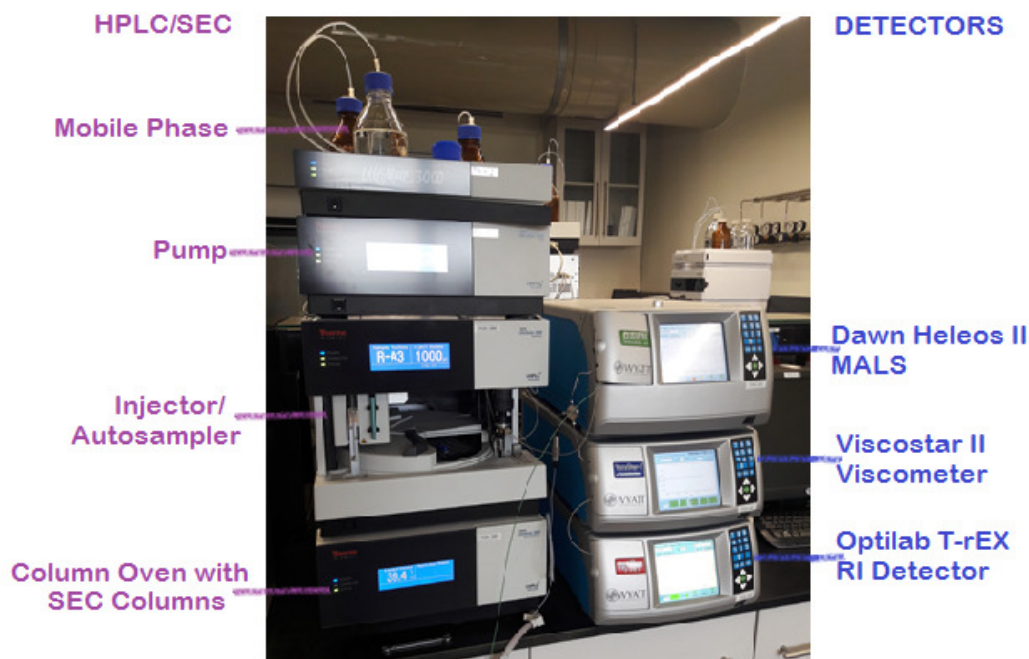


Figure 1-16 HPLC/SEC system with triple detector array

1.4.3 Molecular Weight and Molecular Weight Distributions

Polymers are composed of chains of monomer units and can vary in molecular weight from very low (a few thousand) to very high (several million). Due to the statistical variations which occur during the polymerisation process, be it natural or synthetic, polymers almost always exist as a mixture of molecular weights (Su, 2013).

It is, in fact, considered to be impossible to produce a polymer which consists of chains which are all the same length (Agilent Technologies, 2015). Unlike a low molar mass organic molecule which, can be described by a single molecular weight, polymers must be described as the average molecular weight calculated from the molecular weights of all the chains within the sample (Podzimek, 2011; Agilent Technologies, 2015b). The molecular weight and molecular weight distribution (MWD) of a polymer are related to its physical properties and industrial applications and, knowing these characteristics can allow for the prediction of polymer behaviour (Podzimek, 2011; Agilent Technologies, 2015).

The typical molecular weight averages used in polymer science are described below;

- M_n** The number-average molecular weight describes the total weight of all the molecules present in a sample divided by the total number of molecules present and is biased toward lower molecular masses (Su, 2013). The thermodynamic properties of a polymer are influenced by M_n (Agilent Technologies, 2015).
- M_w** The weight-average molecular weight is defined as the point of the distribution at which there are equal masses of high and low molecular weight to either side (Agilent Technologies, 2015). The molecular weight of each polymer chain determines its contribution to the overall average, and the chains with more mass will have a larger contribution, therefore the M_w is sensitive to higher molecular weight fractions (Agilent Technologies, 2015b). Many of the polymers physical properties, such as tensile strength, are influenced by the M_w (Podzimek, 2011).
- M_z** The Z-average and Z+1-average molecular weights are not commonly quoted for polymers. They take increasing account of the higher molecular weight components of the polymer (Agilent Technologies, 2015b). M_z influences the viscoelasticity, flex life and melt flow behaviour of the polymer (Podzimek, 2011; Agilent Technologies, 2015).
- M_p** The peak molecular weight is the molecular weight at the highest point of the distribution curve and is usually only quoted for narrowly distributed polymers (Agilent Technologies, 2015b).

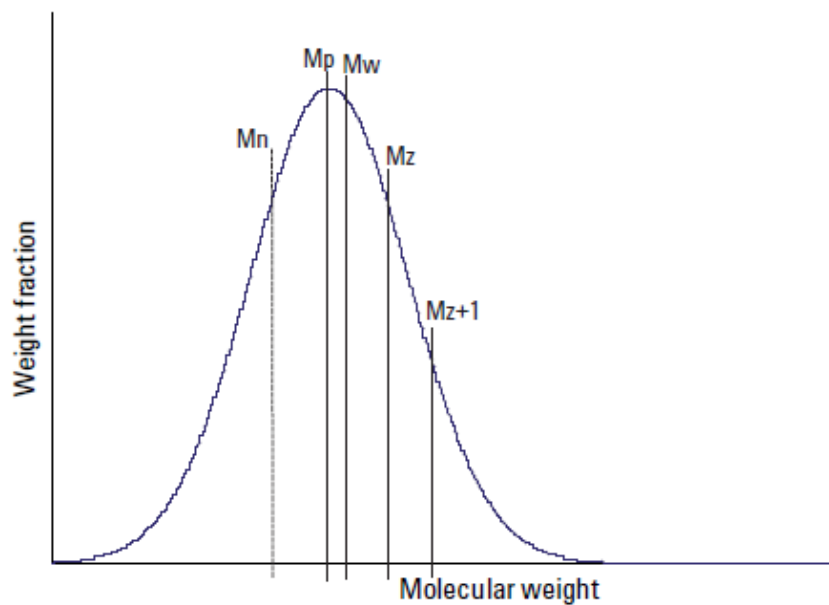


Figure 1-17 A monodisperse MWD indicating the typical positions of the molecular weight averages (**Agilent Technologies, 2015**)

There are various units and nomenclatures used to describe the molecular weight of a polymer; molar mass or molecular mass refer to mass of polymer (g) divided by the amount of polymer (mol) and is expressed in units of g/mol, relative molecular mass or molecular weight is dimensionless and represents the mass of the polymer related to 1/12 of the mass of the ^{12}C atom (Podzimek, 2011). The relative unit of Dalton (Da) can also be used. All these ways of expressing the molecular weight are numerically identical so that a polymer which has a molar mass of 10^5 g/mol has a molecular weight of 10^5 or 10^5 Da (Podzimek, 2011).

The MWD represents the frequency that any particular molecular weight in the polymer occurs (Podzimek, 2011). The range of molecular weights represented in the MWD is described by the polydispersity, which is defined as the ratio of M_w to M_n (Agilent Technologies, 2015).

$$\text{Polydispersity} = \frac{M_w}{M_n} \qquad \text{Equation 5}$$

The polydispersity therefore provides an indication of the broadness of the MWD for the polymer, so that as the distribution becomes broader the polydispersity increases (Agilent Technologies, 2015b).

The differential MWD plot is a good way to compare samples in terms of their mean molecular weight and polydispersity, these plots show the calculated differential weight fraction distributions, $dW(M)/d\log_{10}M$, plotted against the logarithm base 10 of the molecular weight (Hong Chen & Wyatt, 1999). This type of plot allows for the easy assessment and comparison of distribution symmetry and shape (Podzimek, 2011).

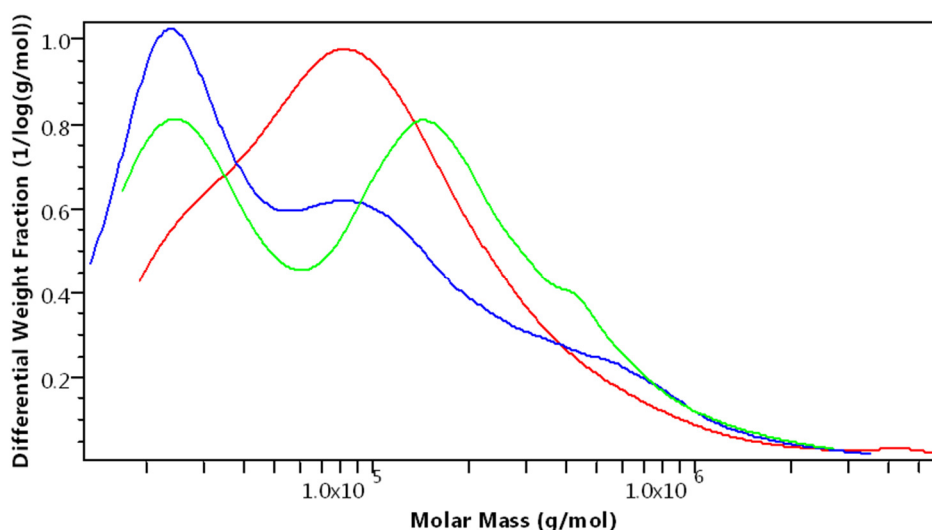


Figure 1-18 Examples of differential MWD plots, showing the different distribution symmetry and shapes which can be obtained for CMC products

1.4.4 Molecular Size and Conformation

There are two terms which can be used to describe the geometric structure of a polymer chain (Billmeyer, 1971);

1. Configuration describes the molecular structure of the polymer which arises from its chemical bonds. The configuration can only be changed if bonds are broken and reformed.
2. Conformation refers to the spatial orientation which a polymer assumes in a dilute solution due to the rotation around a single bond.

The conformation which the polymer assumes in solution depends on the thermodynamic quality of the solvent and the properties of the polymer chain (Podzimek, 2011). The polymer may adopt one of three typical arrangements, a sphere, a random coil or a rod (Billmeyer, 1971). There are however variations which can occur within these conformations (Smith, et al., 1996; Vlassopoulos, et al., 2001; Clasen & Kulicke, 2001) as can be seen in Figure 1-19.

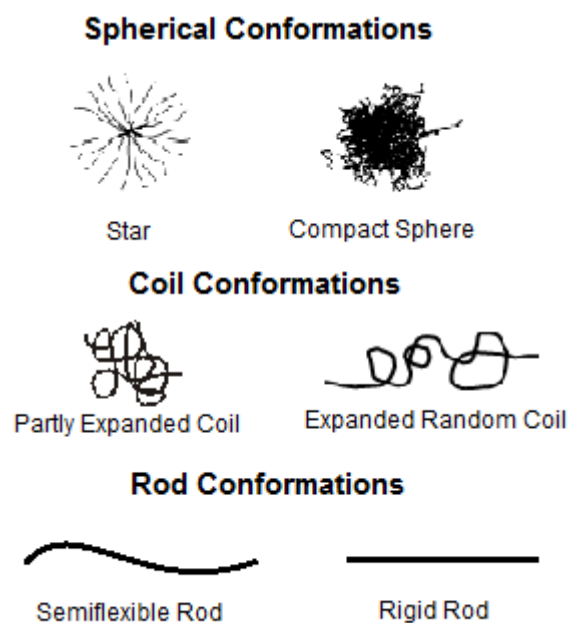


Figure 1-19 Examples of conformations which polymers can assume in solution

For a linear polymer the size in solution can be described by the mean-square end-to-end distance, $\langle r^2 \rangle$ or the square root thereof, $\langle r^2 \rangle^{\frac{1}{2}}$, while for a branched molecule the mean square radius, $\langle R^2 \rangle$, or the root mean square radius, $\langle R^2 \rangle^{\frac{1}{2}}$, can be used (Su, 2013; Podzimek, 2011). The root mean square radius (RMS), also referred to as radius of gyration (R_g), is related to the distribution of mass within the polymer in respect to its centre of gravity (White, 1999; Podzimek, 2011; Agilent Technologies, 2012). Figure 1-20 illustrates the meaning of r and R for a better understanding of these parameters.

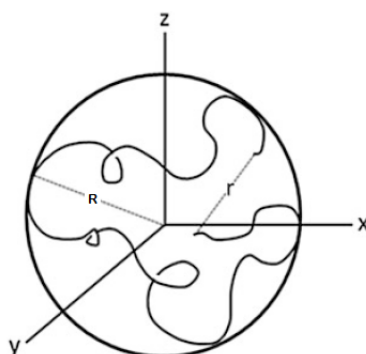


Figure 1-20 Graphic Representation of a Polymer Showing the Difference Between r = End-to-End distance and R = Mean Square Radius (Su, 2013).

The RMS radius, or R_g , can be used to describe the size of a polymer in solution of any shape as it makes no assumption of particle shape (Podzimek, 2011). It is defined as the square root of the weight-average of r_i^2 for all the mass elements as per Equation 6, where r_i is the distance of the i th mass element of mass m_i from the centre of gravity (Podzimek, 2011).

$$R_g = \left(\frac{\sum m_i r_i^2}{\sum m_i} \right)^{\frac{1}{2}} \quad \text{Equation 6}$$

The determination of R_g is done by means of light scattering (Clasen & Kulicke, 2001) and is based on the principal of angular dissymmetry (Agilent Technologies, 2012). For large molecules the intensity of scattered light is not the same in all directions due to the fact that light scattered from one part of the molecule will not travel the same distance as light scattered from another part of the molecule (Ford, et al., 1998). This results in destructive interference which reduces the intensity of the scattered light as the detection angle (θ) increases (Podzimek, 2011; Agilent Technologies, 2012). The angular dissymmetry can be quantified by defining the light scattering form factor, $P(\theta)$, as the ratio of scattered light intensity at observation angle θ to the intensity of scattered light at angle 0° (Ford, et al., 1998; Podzimek, 2011). The R_g can therefore only be determined by means of light scattering if a MALS detector is used and the polymer is large enough to create angular dissymmetry, it must therefore requires an R_g greater than 10 nm (Agilent Technologies, 2012).

The relationship between R_g and molecular weight (M) can be described by the following equation, where K and ν remain constant for a given solvent and polymer combination (Clasen & Kulicke, 2001; Agilent Technologies, 2012).

$$R_g = KM^\nu \quad \text{Equation 7}$$

If $\log R_g$ is plotted against $\log M$ this provides a straight line with an intercept of K and a slope of ν (Agilent Technologies, 2012), this type of plot is termed a conformational plot. For a highly branched polymer it is expected that the R_g would increase as a cube root of the molecular weight resulting in a slope of 0.33 whereas for a rigid rod the R_g should increase linearly with the molecular weight and the conformational plot would therefore have a slope of 1 (White, 1999; Podzimek, 2011; Agilent Technologies, 2012).

The slope of a random coil would be 0.5 as the R_g would increase as approximately the square root of the molecular weight (White, 1999; Podzimek, 2011; Agilent Technologies, 2012).

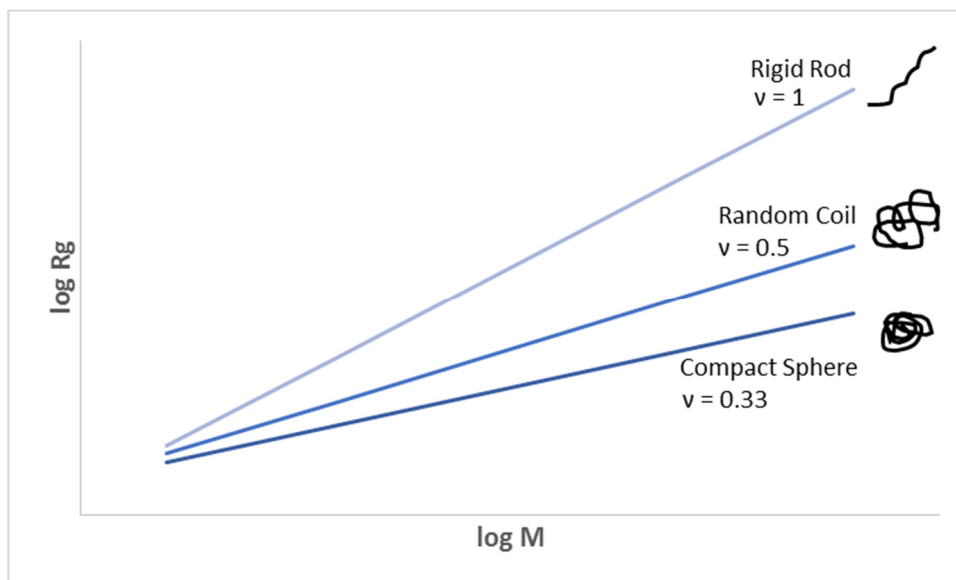


Figure 1-21 Conformational plot showing the variation in the plot slope related to changes in polymer conformation in solution

Figure 1-18 demonstrates the ideal slopes for the different conformations in solution, however as shown in Figure 1-16 there are a number of variations which can occur for the conformations. The slopes of the conformational plots therefore in reality very seldom follow the ideal case as laid out above. Table 3 below outlines the variations in slope which can occur and gives a guide as to how it relates to changes in the conformation.

Table 1-3 Relationship of conformational plot slope to the conformation. Adapted from Clasen & Kulicke, (2001)

Slope ν	Conformation
0.333	Compact Sphere
0.5	Non-Expanded Random Coil
0.5 – 0.6	Partly Expanded Random Coil
0.67	Completely Expanded Random Coil
0.67 - 1	Semi-flexible Rod
1	Rigid Rod

The second size parameter which can be determined by means of triple detection is the hydrodynamic radius, R_h , which is defined as the hypothetical hard sphere which has the same intrinsic viscosity as the polymer molecule (Podzimek, 2011). This radius is therefore indicative of the volume which a hydrated, dynamic (tumbling), polymer occupies in solution (Weiner, 2010). Traditionally the R_h is determined by dynamic light scattering, however it can also be calculated from intrinsic viscosity (Podzimek, 2011; Malvern Instruments Limited, 2015). The R_h can be determined for particles down to a size of 1 nm (Podzimek, 2011).

The R_h is a different size parameter to the R_g in that it includes effects of both shape and hydration, it also always assumes a sphere, whereas R_g is not affected by the hydration layer of the polymer and is independent of shape assumptions (Weiner, 2010). If you were to consider adding a side group to a large polymer it would hardly affect the R_h but it would have a significant effect on the R_g . The ratio of R_g to R_h can therefore, in principal, provide information about the geometry of the polymer (Ford, et al., 1998). For a sphere a ratio of R_g/R_h of 0.77 is expected while a random coil has a ratio of 1.54 (Kok & Rudin, 1981; Weiner, 2010).

1.5 Objectives

The overall objective of this study is to show that it is possible to apply the principals of green chemistry to the synthesis of CMC to reduce its overall environmental impact, while having a good reaction efficiency and producing product of comparable quality to the current solvent slurry process.

Water is the most environmentally friendly solvent, however, due to poor reaction efficiency, reproducibility and product quality it has been mostly abandoned as a reaction medium for the production of CMC on an industrial scale. Therefore the first objective of this study is to optimise the reaction conditions for the dry/aqueous CMC production process to show that the quality of this product can be improved on compared to that historically achieved while demonstrating improved reaction efficiency and reproducibility. The reaction conditions were therefore optimised in two parts. Firstly the mercerisation of the cellulose, where the swelling of the cellulose was monitored by means of changes in its crystallinity, with an aim to improving product solubility and reproducibility of the reaction.

Secondly the etherification reaction, where attention was given to the effect of the temperature during addition of the etherification reagent on the DS and reaction efficiency as well as the type of etherification reagent used.

Following on from this the use of microwave energy, as an alternative heating source, was investigated to determine if the reaction efficiency and product quality for the optimised dry/aqueous process could be further improved, while reducing the overall energy consumption of the process.

A final objective will be to show that the SEC-MALS technique can be used to determine the distribution of substituents along the cellulose backbone, offering a relatively simple alternative to the techniques currently used.

2 MATERIALS AND METHODS

2.1 Materials

The following chemicals were used in the preparation of the CMC: Isopropanol (100% A.R grade, Minema Chemicals), NaOH (48% lye, NCP Chlorchem, Crest Chemicals), Monochloroacetic acid MCA (flakes, AkzoNobel), Sodium monochloroacetate SMCA (granules, AkzoNobel), 91 Alpha cellulose dissolving pulp (SAI-Pharma Grade, Sappi).

2.2 Experimental Procedures

2.2.1 Preparation of Powdered Cellulose

The 91 Alpha cellulose pulp is a “hardwood dissolving pulp” with a maximum S10 and S14 content of 14.0% and 6.8% respectively, a viscosity range of 9 to 15 cps and a brightness of 91.0%. The pulp was milled through a two stage Herbold system which consisted of a SML 60/100 granulator fitted with a 12 mm screen followed by a SMF 500/1000 fine grinder equipped with a 0.1 mm screen to produce a powdered cellulose.

2.2.2 Preparation of CMC by the Solvent Slurry Process

The standard slurry procedure followed was adapted from Klemm, et al. (2001b). Powdered cellulose, 15 g, was added to 400 ml of isopropanol in a glass reactor equipped with a rigid overhead stirrer. The reaction mixture was mixed at 25°C for 10 min before adding 25 g of 30% (w/w) aqueous NaOH dropwise over 30 min. After stirring for another hour 8.3 g of MCA powder was added over a 30 min period. The mixture was stirred for a further 3 hours at 55°C, and then filtered and dried at 60°C.

2.2.3 Preparation of CMC by the Dry Aqueous Process

2.2.3.1 The Effect of NaOH Concentration and Swelling Temperature

The effect of NaOH solution concentration and temperature were investigated by conducting a series of reactions where 350 g of powdered cellulose was treated with 25%, 37%, 43% and 48% aqueous solutions of NaOH (w/w) at starting temperatures of 0°C, 5°C, 10°C and 20°C. The NaOH solutions were added over 30 min followed by a further 30 min swelling period after which samples were taken for XRD analysis. The reactions were performed in a lab reactor equipped with a double helical agitator and were all performed under a nitrogen blanket.

2.2.3.2 The Effect of Nitrogen

To investigate the effect of nitrogen, the same procedure as above was followed using a 25% NaOH solution at a starting temperature of 10°C without the presence of nitrogen. These results were then compared to the equivalent reaction run in the presence of nitrogen.

To further investigate the effect of the nitrogen two sets of triplicate reactions were performed with and without a nitrogen blanket respectively. An amount of 12 kg powdered cellulose was added to a 185 L pilot scale reactor (see Appendix for details), equipped with a double helical agitator, and allowed to cool to a starting temperature of 0°C. A 37% NaOH solution was added over 30 min, after which 30 min was allowed for the swelling of the cellulose. An amount of 8 kg of MCA powder was added over 30 min followed by a 30 min adsorption period. The reaction was heated to 65°C for 3 hours, the product was then discharged and dried at 60°C overnight.

2.2.3.3 SMCA versus MCA

To investigate the impact of using MCA versus SMCA, 12kg of powdered cellulose was added to the 185 L pilot scale reactor and cooled to 0°C. For the reaction where MCA was used a 37% aqueous NaOH solution was added, for the reaction where SMCA was used a 21% aqueous NaOH solution was used. The NaOH solution was added in over 30 min followed by a further 30 min for swelling. After the cellulose was swelled the appropriate etherification reagent was added, 9.9 kg and 8.0 kg of SMCA and MCA were added respectively, over 30 min followed by a 30 min adsorption period. The reaction was then heated to 65°C and reacted for 3 hours. Once the reaction was completed the product was discharged and dried at 60°C overnight. The reactions were each performed in triplicate, under a nitrogen blanket.

2.2.3.4 The Effect of Temperature during MCA Addition

To determine the effect of temperature during the MCA addition, 12 kg of powdered cellulose was added to the 185 L pilot scale reactor and cooled to a starting temperature 5°C. A 37% NaOH solution was added over 30 min, after which 30 min was allowed for the swelling of the cellulose. An amount of 8 kg of MCA powder was added over 30 min followed by a 30 min adsorption period.

During the addition and adsorption period of the MCA the peak batch temperature was varied to 18°C, 20°C, 23°C, 25°C, 28°C, 32°C, 39°C and 45°C, respectively. The reaction was then heated to 65°C for 3 hours. On completion the product was then discharged from the reactor and dried at 60°C overnight. The reactions were performed in duplicate and in a nitrogen atmosphere.

2.2.4 Microwave Reactions

To investigate the use of microwave heating, 12 kg of powdered cellulose was added to the 185 L pilot scale reactor and cooled to a starting temperature 5°C. A 37% NaOH solution was added over 30 min, after which 30 min was allowed for the swelling of the cellulose. An amount of 8 kg of MCA powder was added over 30 min followed by a 30 min adsorption period. After the completion of the adsorption period a bulk sample was taken and placed in the lab fridge. The reaction was then heated to 65°C for 3 hours. On completion the product was then discharged from the reactor and dried at 60°C overnight. This reaction was performed under nitrogen.

For the first set of reactions performed at 85 watts a 200 g sample was taken from the bulk sample and place into a 200ml Pyrex glass bowl was covered by a watch glass, to prevent evaporation. Samples were taken at the time intervals indicated in Table 2-1 and placed in an oven at 110°C to dry for 2 hours. For the remaining reactions 30 g aliquots were taken from the bulk sample and placed into a 200ml Pyrex glass bowl was covered by a watch glass, to prevent evaporation. The reactions were then performed according to the outline in Table 2-1 below, with the complete 30 g sample being removed at the required time.

Table 2-1 Outline of microwave heating reactions

Microwave Power (W)	Reaction Time
85	5 min, 10 min, 15 min, 20 min
255	2 min, 4 min, 6 min, 8 min
425	30 sec, 1 min, 2 min, 3 min
595	30 sec, 1 min, 1 min 30 sec, 2 min

Once the reaction time was completed the sample was uncovered and placed in an oven at 110°C to dry for 2 hours. These reactions were performed in a domestic AIM AM20 microwave.

2.3 Analysis Methods

2.3.1 Purity

An amount of 2.5 g of CMC was weighed into a 500 ml conical flask to which 250 ml of an 80:20, methanol (100% A.R grade) to water mixture was added. The mixture was stirred for 2 hours and then the sample was transferred into a pre-weighed fritted glass filtering crucible and washed with 3x 25 ml aliquots of the 100% methanol solution before partially drying it via suction. The crucible was then placed in an oven at 105°C for an hour. The crucible was removed from the oven and placed into a desiccator to cool. Once cool the crucible was weighed and the mass used to calculate the percent wet and dry purity of the CMC using the following equations:

$$\text{Wet Purity (\%)} = \frac{M_F - M_C}{M_s} \times 100 \quad \text{Equation 8}$$

$$\text{Dry Purity (\%)} = \frac{\text{Wet Purity (\%)}}{100 - \% \text{moisture}} \times 100 \quad \text{Equation 9}$$

Where M_F is the final dry mass of the sample and crucible, M_C is the mass of the empty crucible, M_s is the initial sample mass and the % *moisture* is the moisture content of the initial sample determined by means of a Sartorius MA30 Moisture Analyser.

2.3.2 Degree of Substitution

A purified sample (as per the method outlined in Section 2.3.1) was placed in a moisture analyser (Sartorius MA30) at 90°C until it contained 0% moisture. An amount of 0.4 g of this purified sample was then weighed into a 250 ml conical flask. A 65 ml aliquot of neutralized glacial acetic acid (A.R grade) was added to the purified CMC sample. This suspension was refluxed for 2 hours and then allowed to cool to room temperature. Four drops of quinaldine red indicator was added to the cooled suspension which was then titrated with 0.1 M perchloric acid (ACS grade) to a colourless end point. The DS was calculated as follows:

$$\text{Bonded Na (\%)} = \frac{2.3 \times C_{\text{HClO}_4} \times V_{\text{HClO}_4}}{M} \quad \text{Equation 10}$$

$$\text{DS} = \frac{1.62 \times \% \text{Bonded Na}}{2.3 - (0.8 \times \% \text{Bonded Na})} \quad \text{Equation 11}$$

Where the factor 2.3 represents the molar mass of Na divided by 10, C_{HClO_4} is the molarity of the perchloric acid (mol/L), V_{HClO_4} is the volume of perchloric acid titrated (ml), and M was the mass of the initial purified CMC sample (g). This method was based on ASTM D1439.

2.3.3 Insoluble Content

An amount of 0.5 g of CMC was weighed into a 100 ml beaker and dissolved with 50 ml of deionized water. The suspension was stirred for 2 hours and then transferred into a pre-weighed centrifuge tube. The suspension was then centrifuged (C-28A, Boeco) for 15 min at 4000 rpm to separate the insoluble material from the aqueous sample. The aqueous supernatant was decanted and the remaining residue re-suspended in 50 ml of deionized water. This centrifuge and decant procedure was repeated 3 times. The centrifuge tube containing the insoluble material was then dried overnight in an oven at 105°C and the percentage insoluble material was calculated as follows:

$$\text{Insoluble Material (\%)} = \frac{M_F - M_C}{M_S} \times 100 \quad \text{Equation 12}$$

Where M_F was the final dry mass of the sample and centrifuge tube, M_C was the mass of the empty centrifuge tube, and M_S was the initial sample mass.

2.3.4 Solution Viscosity

A 2% solution of CMC was prepared by weighing out 5.0 g of the sample and carefully adding it to 245 g of deionized water while stirring. The prepared solution was stirred on a magnetic stirrer for 5 min and then placed on a tumbler for an hour and 45 min. The solution was then placed in a water bath at 25°C for 15 min. The viscosity was measured by DV-I LV Brookfield viscometer with spindle 1 and the speed was adjusted between 30 and 60 rpm depending on the viscosity of the sample.

2.3.5 Calculation of Reaction Efficiency

The reaction efficiency is defined as the ratio of the actual DS to the theoretical DS expressed as percent (Branan, 1953).

$$\text{Reaction Efficiency} = \frac{\text{Actual DS}}{\text{Theoretical DS}} \times 100 \quad \text{Equation 13}$$

Where the *Actual DS* is the actual degree of substitution obtained, determined as per Section 2.3.2 above, and the *Theoretical DS* is defined as the number of moles of etherifying agent used per AGU.

2.3.6 SEC with Triple Detection

The CMC samples were analysed by SEC with Triple detection. The system is comprised of an Ultimate 3000 HPLC system (Thermo Scientific), which is equipped with an in-line degasser and auto sampler, the detectors comprise a Dawn Heleos II Multi Angle Light scattering detector, a Viscostar II viscometer and an Optilab T-rEX Refractive Index detector (all detectors are supplied by Wyatt Technology Corp.). The separation was carried out on 2x 30 cm OHPak SB-806M HQ mixed bed columns (Shodex) at a flow rate of 1 ml/min and an injection volume of 100 µl. The mobile phase contained 0.1 N NaNO₃, 0.01N NaH₂PO₄·2H₂O and 0.2% NaN₃ at a pH of 7.00. The CMCs were dissolved to a concentration of 2.5 mg/ml in mobile phase and allowed to stir for 4 hours. All samples were filtered through a 0.45 µm syringe filter (Millipore) before the analysis. The data from the detectors were processed using ASTRA 7 software (Wyatt Technology Corp.). Refractive index increment dn/dc of 0.146 was used for the calculations.

2.3.7 XRD Analysis

Samples of the alkali cellulose were taken for XRD analysis after the completion of the swelling phase of the reaction. These samples were dried in a conventional oven at 60°C overnight.

The analysis was performed at Mintek in a Bruker D8 XRD with a cobalt x-ray source. Samples were scanned from 10°- 80° 2θ with a step size of 0.021° 2θ, with a Bragg-Brentano geometry. The phases were identified in EVA, the peak identification software from Bruker.

2.3.8 Hysteresis Loop Analysis

A purified sample (as per the method outlined in Section 2.3.1) was used to prepare 1 and 3% solutions by weighing out 2 g and 6 g of purified sample and adding it into 198 g and 194 g of deionised water respectively. The prepared solution was stirred on a magnetic stirrer for 5 min and then placed on a tumbler for an hour and 45 min. The solution was then placed in a water bath at 25°C for 15 min. The hysteresis loop was measured by a Brookfield RST-CC Rheometer fitted with a CCT-45 bob and cup. The measurement was conducted with a Shear rate of 1-100 (10-1000) /s for the ascending and 100-1 (1000-10) /s for the descending curves, with a time interval of 120 s in each direction and a measuring frequency of 60 points. Brookfield Rheo3000 Software, version 2.1, was used to perform the data analysis.

3 THE COMBINED INFLUENCE OF SODIUM HYDROXIDE CONCENTRATION AND TEMPERATURE ON FIBRE SWELLING DURING MERCERISATION

3.1 Background

The swelling of the cellulose is a vital step in the carboxymethylation process as the degree of the swelling will eventually determine the distribution of the substituents introduced in the subsequent etherification reaction, and therefore impact on the quality of the final product (Thielking & Schimdt, 2012). The effect of NaOH concentration, mercerisation temperatures and reaction times have been studied extensively (Roy, et al., 2001; Sameii, et al., 2008; Miura & Nakano, 2015; Alban Reyes, et al., 2016).

A review conducted by Budtova and Navard (2016) summarised the effect of NaOH concentration as follows; all alkaline hydroxides are able to swell cellulose however, the efficiency of the swelling is dependent on the nature of the metal ion with the given order as $\text{Li} > \text{Na} > \text{K} > \text{Rb} > \text{Cs}$. This was explained in terms of the size of the alkali ion where the larger the ion, the more difficult it was for it to penetrate the cellulose fibre. This concept can also be applied to explain the effect of NaOH concentration on the swelling of the cellulose.

When anhydrous NaOH interacts with water a series of hydrates are formed, as a result the phase diagram for the NaOH water mixture is very complex, as shown in Figure 3-1. The regions below 20% and above 70% show relatively simple behaviour while in the region between several stable and metastable hydrates are present.

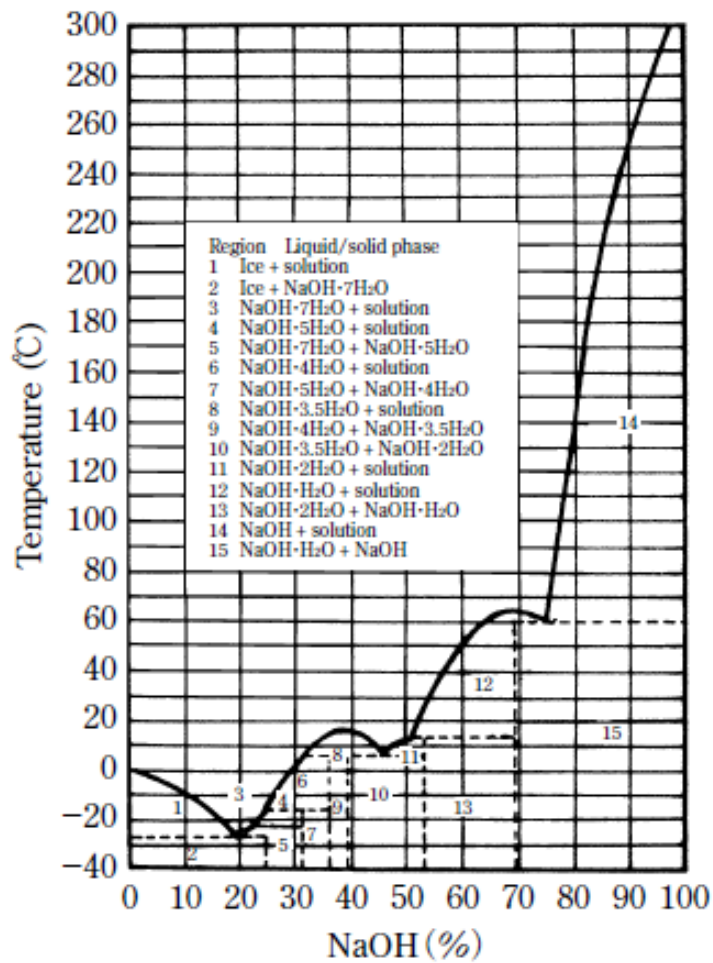


Figure 3-1 Binary phase diagram of NaOH and water (Wang, 2008)

The most complex region of the diagram falls between 20 and 40%, where the highest number of hydrates have been identified. The composition of these hydrates varies with temperature, as shown in Table 3-1.

Table 3-1 Composition and temperature range of NaOH – water hydrates. Adapted from Budtova & Navard (2016)

Hydrates	NaOH Concentration (w/w, %)	Temperature Range (°C)
NaOH, 3.5 H ₂ O	38.0 – 38.8	5.1 to 6.2
NaOH, 4.0 H ₂ O	34.8 – 35.7	-18 to 5.1
NaOH, 5.0 H ₂ O	30.2 – 30.9	-24 to -18
NaOH, 7.0 H ₂ O	22.8 – 24.1	-28 to -24

The structure of these hydrates is an important factor for the swelling of the cellulose. When the ions go into solution they can have different solvated forms depending on their concentration and temperature. The water which surrounds the ions is bonded in the form of cages, the primary cage represents the strongly bonded water, while the more loosely bound water forms the secondary cage.

Yamashiki, et al. (1988) proposed that for a 9% (w/w) NaOH solution the cages occurred as separate ion pairs where the four water molecules surrounded each ion to form the primary solvation cage and the secondary cage was composed of 23 water molecules split between the two ions, Figure 3-2.

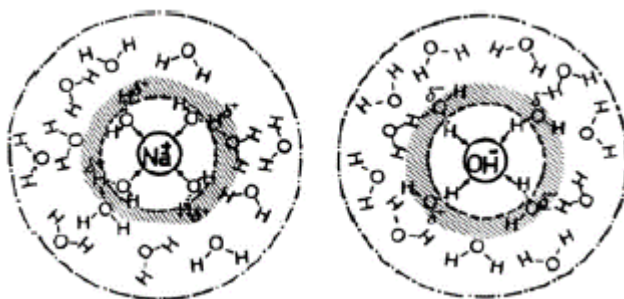


Figure 3-2 Representation of the organisation of an 9% aqueous NaOH solution (w/w)
(Yamashiki, et al., 1988)

Figure 3-3 shows how for low alkali hydroxide concentrations the number of water molecules incorporated in the solvation cages result in the formation of hydrated ion pairs (Egal, 2006; Budtova & Navard, 2016). The large hydrodynamic diameter of which cannot easily penetrate the cellulose fibre, thus leading to relatively low degrees of swelling. As the concentration of the alkali solution increases the number of water molecules decreases and solvated dipole hydrates are formed. The hydrodynamic diameter therefore decreases and the ions are better able to penetrate into the amorphous and crystalline regions of the cellulose fibre, allowing for improved swelling (Egal, 2006; Budtova & Navard, 2016).

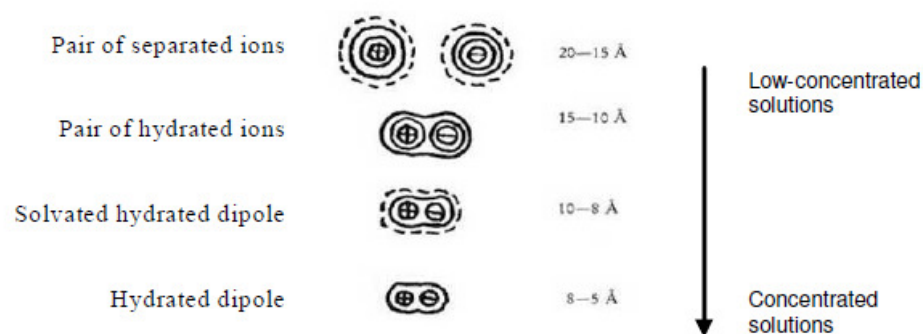


Figure 3-3 Various forms and corresponding hydrodynamic diameters of alkali hydrates (Egal, 2006)

The degree of swelling for the cellulose can be considered as being determined by two factors, firstly the number of water molecules carried into the fibre by the alkali ions or ion dipoles and secondly the depth of the penetration of these ion dipoles. The first factor decreases with increasing NaOH concentration while the second increases with NaOH concentration (Klemm, et al., 2001a).

At this point it is important to recall that the purpose of the mercerisation process is to convert the Cellulose I crystal structure of the raw cellulose into the more reactive Na-cell forms. As per Section 1.3.1 five different forms of alkali cellulose have been identified of which Na-cell I and Na-cell II are the most important. The form of Na-cell is determined by the concentration and temperature of the NaOH solution.

At room temperature no binding of NaOH into the crystal structure of the cellulose occurs below a NaOH concentration of 9% (Klemm, et al., 2001b; Ambjornsson, et al., 2013). As the concentration increases from 9% the chain conformation of the cellulose starts to change until at 15% NaOH the transformation to Na-cell I is complete. A uniform chain conformation persists up to a NaOH concentration of 22%. The conversion to the three-fold helix of Na-cell II is completed by 25%. The order of the supramolecular structure continues to decrease as the NaOH concentration increases up to a maximum of 50% (Klemm, et al., 2001b; Ambjornsson, et al., 2013).

In 1939 Sobue et al. published a phase diagram of the different Na-cell forms indicating their dependence on NaOH concentration and temperature, this is shown in Figure 3-4.

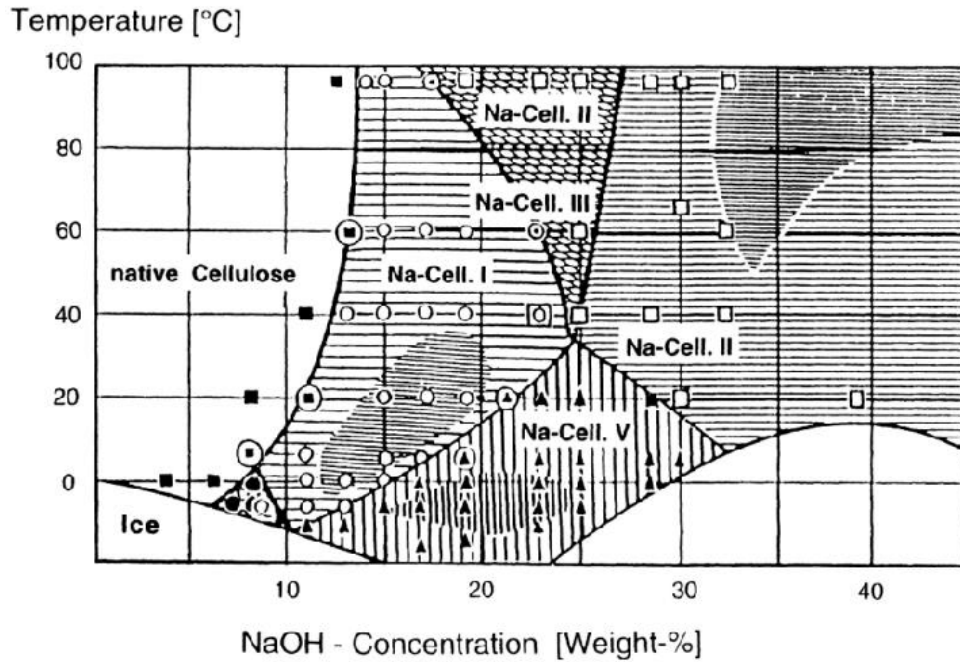


Figure 3-4 Phase diagram of the various Na-cellulose forms.
(Sobue et al.1939 as presented in (Klemm, et al., 2001b))

More recently Porro, et al. (2007) presented evidence that Na-cell I and Na-cell II were the only two stable allomorphs which could be distinguished. An alternative phase diagram was put forward which indicated that Na-cell II was predominantly formed at NaOH concentrations above 10% in the temperature range -13 to 26°C and, that the likelihood of forming Na-cell II increased with increasing NaOH concentration and temperature.

Most of the available aqueous mercerisation studies focus on conditions which are more applicable to the viscose process and very little attention has been given to conditions which would be practical and cost effective for an industrial dry/aqueous process to produce CMC's.

3.2 Objective and Approach

The aim of this portion of the optimisation work was to identify conditions that would be applicable for an industrial dry/aqueous process, at which good swelling of the cellulose could be achieved. This is important because the degree and uniformity of the swelling influences the eventual distribution of the substituents along the cellulose backbone in the final product (Thielking & Schimdt, 2012).

Improving the distribution of substituents should therefore improve the solubility and consistency of the CMC, which was a major drawback of the original dry/aqueous process.

The approach which was followed was to study the swelling of the cellulose at NaOH concentrations of 25 to 48% (w/w) and temperatures ranging from 0 to 20°C. In order to identify where the optimal swelling was achieved the changes in the crystal structure were examined using XRD analysis, which is a technique that has been well defined (Nishimura & Sarko, 1987; Zugenmaier, 2008).

The decision to use high concentrations of NaOH was based on the requirement to reduce the amount of water present in the reaction and thereby reduce the occurrence of the side reactions. Also numerous authors agree that NaOH concentrations above 25% provided more swelling of the cellulose (Klemm, et al., 2001a; Porro, et al., 2007; Ambjornsson, et al., 2013) and therefore increase the likelihood of forming the highly swollen Na-cell II intermediate.

In order to maintain the reaction as “dry” and remove the requirement for filtration of excess NaOH, which had been found to be problematic in the traditional process, a ratio of 2.4 mol of NaOH per mole AGU was used (Omiya, 1984; Fink, et al., 1986; Klemm, et al., 2001a; Stigsson, et al., 2006). This low stoichiometric ratio would also assist with reducing the side reaction and improve the efficiency of the overall etherification reaction.

Traditionally mercerisation is performed at temperatures between 20 and 40°C (Budtova & Navard, 2016), however, Nakano, et al. (2013) as well as Miura & Nakano (2015) found that applying cooling decreased the concentration at which Cellulose I was converted to Cellulose II for NaOH concentrations ranging from 0 to 20%. Alban Reyes, et al. (2016) also found a correlation between temperature and transformation of the crystal structure. They found that for NaOH concentrations between 15 and 21% there was a decrease in transformation as the temperature increased from 20 to 70°C. For higher NaOH concentrations of 45 to 55% it was found that temperatures between 30 and 60°C had little impact on the swelling of the cellulose (Alban Reyes, et al., 2017). Temperature conditions between 0 and 20°C were therefore selected for the study.

The experimental methods used are outlined in Chapter 2.

3.3 Results and Discussion

The XRD scan for the raw unswelled cellulose is shown in Figure 3-5 below.

The results of the XRD analysis of the cellulose swelled at different NaOH concentrations and temperatures can be seen in Figures 3-6 to 3-09. The cellulose peaks of interest fall between 10 and 30 degrees 2-Theta, peaks which appear after 30 degrees in the NaOH treated samples can be attributed to the NaOH which was not washed out of the samples prior to analysis.

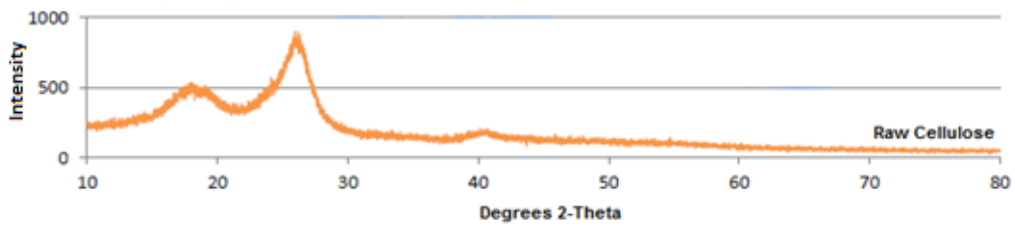


Figure 3-5 XRD scan of raw unswelled cellulose

At a swelling temperature of 0°C, Figure 3-6, the cellulose treated with 48% NaOH has a peak profile which still contains elements of the raw cellulose and the swelling, therefore, appears to be incomplete. The 25% NaOH peak is the sharpest peak which indicates that it is the most crystalline, while the 37% NaOH peak is the broadest and therefore the most amorphous. The peak for the cellulose treated with 43% NaOH is indicative of a mixture of crystalline and amorphous material.

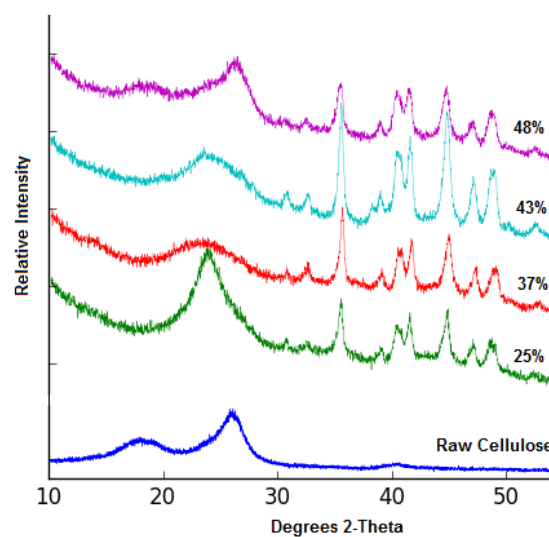


Figure 3-6 Stacked overlay of XRD scans for alkalisated cellulose at a swelling temperature of 0°C for NaOH concentrations of 25%, 37%, 43% and 48%

For the swelling conducted at 5°C, Figure 3-7, the XRD peaks for the cellulose treated with 37% and 43% NaOH are almost identical, which infers that they have similar amorphous phases. The peak for the cellulose swelled with 25% NaOH once again indicates a highly crystalline structure. The swelling of the cellulose treated with 48% NaOH has improved in comparison to that obtained at 0°C and the peak profile now indicates a mixture of crystalline and amorphous material.

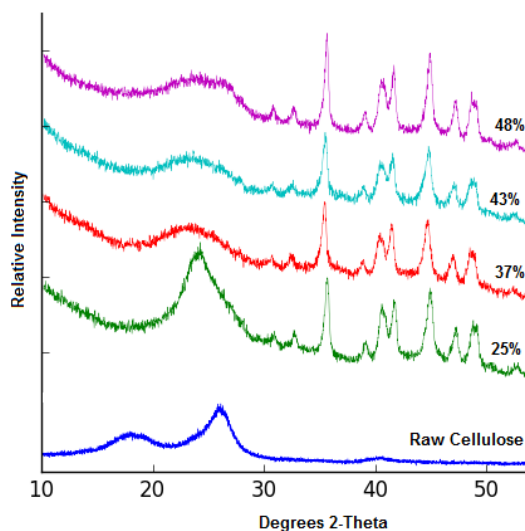


Figure 3-7 Stacked overlay of XRD scans for alkalised cellulose at a swelling temperature of 5°C for NaOH concentrations of 25%, 37%, 43% and 48%

At 10°C the XRD peaks for the cellulose swelled with 37%, 43% and 48% NaOH have identical broad peaks which indicate an amorphous structure. The peak for the 25% NaOH remains unchanged from that seen at 0 and 5°C and it therefore has the most crystalline structure.

At a swelling temperature of 20°C the peak profile for the cellulose swelled with 48% NaOH again becomes indicative of a mixture of crystalline and amorphous structures. The peak for the 43% NaOH has become sharper indicating an increase in the crystallinity of the cellulose. The cellulose swelled with 25% NaOH still has the sharpest peak which indicates that it has the highest crystallinity. The peak for the 37% NaOH remains the broadest peak representing the sample with the most amorphous structure.

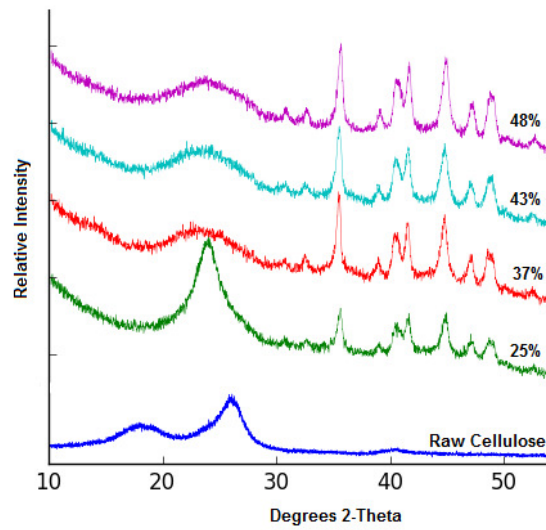


Figure 3-8 Stacked overlay of XRD scans for alkalised cellulose at a swelling temperature of 10°C for NaOH concentrations of 25%, 37%, 43% and 48%

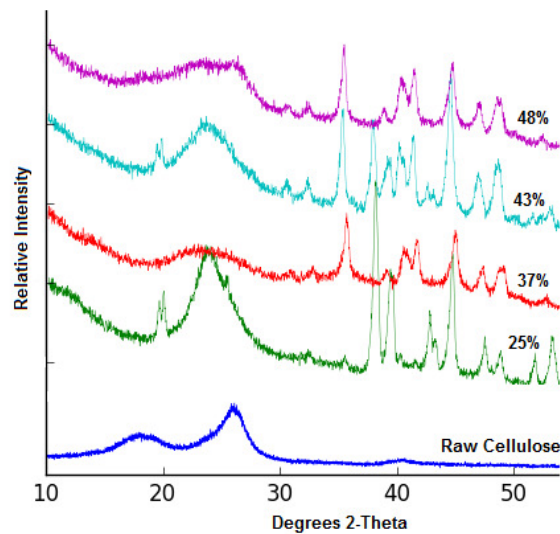


Figure 3-9 Stacked overlay of XRD scans for alkalised cellulose at a swelling temperature of 20°C for NaOH concentrations of 25%, 37%, 43% and 48%

At all temperatures studied it was found that the cellulose treated with 25% NaOH resulted in the most crystalline structure of the alkali cellulose. A possible explanation for this is that at this concentration the hydrodynamic size of the alkali hydrates is large enough to prevent the hydrate from easily penetrating the cellulose fibre and has thus resulted in a lower degree of swelling (Budtova & Navard, 2016).

The 43 and 48% NaOH solutions provided better swelling of the cellulose fibres in comparison to the 25% NaOH. This would therefore be consistent with the assumption that the hydrate size has decreased with increasing NaOH concentration and allowed for better penetration of the cellulose fibre. It was, however, found that these two concentrations exhibited a degree of temperature dependence. The 43% NaOH providing the best swelling at 5 and 10°C, while 48% provided good swelling at only 10°C and at 0°C showed incomplete swelling. These findings appear to contradict those of Alban Reyes, et al. (2017), however, a significant difference between the two studies was the temperatures under investigation. In the temperature range of 30 to 60°C Alban Reyes, et al. (2017), found that temperature had little significant impact on the swelling of the cellulose for NaOH concentrations of 45 to 55%. From the results of this investigation it is clear that for the range of 43 to 48% NaOH the temperature does have a significant impact on the swelling of the cellulose.

Wang (2008) suggested that the adsorption of NaOH into the cellulose fibre was increased in the region of the phase transition interface, Figure 3-1, for the NaOH water system. His theory was that at the phase transition line ice would begin to appear and as the temperature continued to drop the NaOH concentration in the liquid phase would start to increase, this would result in a corresponding decrease in the alkali hydrate size, thus improving the cellulose swelling. This he had shown was beneficial for low concentrations of NaOH.

The phase transition for 43 and 48% NaOH occurs between 10 and 12°C, and this could therefore explain why these concentrations showed a temperature dependence for their swelling behaviour in comparison to the 25% NaOH which has a transition temperature of approximately -17°C.

It could also contribute to the low degree of swelling found for the 25% NaOH; as the transition phase for this concentration was never approached it could be put forward that the NaOH.5H₂O was not formed and therefore supports the assumption that the size of the alkali hydrate was too large to allow for good penetration of the cellulose fibre.

The phase transition for 37% NaOH occurs at approximately 14°C, not much higher than for the 43 and 48% NaOH concentrations; however this concentration shows the best swelling across all the temperatures investigated during this study. It therefore appears that the temperature and resulting hydrate size are not the only factors that are contributing to the swelling of the cellulose under these conditions. Another factor which needs to be considered is that the swelling of the cellulose is not purely dependant on NaOH but also on the amount of water present. At high concentrations of NaOH the hydration of the alkali ions could be insufficient to break the hydrogen bonding within the cellulose fibre thus resulting in poor swelling (Kuo & Hong, 2005). At a NaOH concentration of 37% the size of the hydrate formed at the temperatures under investigation must be sufficiently small, as per Table 3-2, to allow for good penetration of the cellulose fibre while having sufficient water present to allow for the distruption of the hydrogen bonding thereby resulting in an amorphos cellulose structure.

This investigation therefore found that at all the temperatures investigated the cellulose treated with the 25% NaOH resulted in the most crystalline structure for the alkali cellulose. On the other hand the cellulose treated with 37% NaOH consistently gave the boardest peak indicating it was in a more desirable amorphous form at all the temperatures studied. The cellulose treated with 43% and 48% NaOH showed a temperature dependant variation in the crystallinity of the alkali cellulose. These results therefore substatiate that both the concentration of the NaOH, as well as the temperature at which the swelling is performed, have an impact on the degree to which the highly ordered crystalline structure of the raw cellulose is converted to the more reactive amorphous structure.

3.4 Conclusion

From this investigation it can therefore be concluded that use of 37% NaOH in the temperature range of 0 to 20°C resulted in the most consistent swelling of the raw cellulose. This therefore represents the optimum conditions for the swelling of the cellulose for the dry/aqueous reaction; firstly because efficient swelling of the cellulose will improve the overall quality of the final product and, secondly because the large temperature range over which the 37% NaOH can be used improves the robustness of the industrial process.

4 THE INFLUENCE OF A NITROGEN ATMOSPHERE ON FIBRE SWELLING DURING MERCERISATION

4.1 Background

One of the primary uses of CMC is as a viscosity modifier for aqueous solutions (Klemm, et al., 2001b; Stigsson, et al., 2004), therefore its solution viscosity and rheological properties are of great importance. These properties have been shown to be affected by the molecular weight, molecular weight distribution, DS and distribution of substitution (Stigsson, et al., 2004; Enebro, et al., 2007). The control of the molecular weight and molecular weight distribution is therefore a critical parameter during the production of CMC (Stigsson, et al., 2005).

Cellulose, because of its polyhydric alcohol structure, can be oxidised by a variety of reagents (McBurney, 1954). Oxidation of cellulose by atmosphere oxygen does not readily occur under neutral and acidic conditions, however if in contact with aqueous alkali it will be rapidly degraded by a set of autoxidation reactions (Klemm, et al., 2001a). This reaction will occur readily at temperatures between 20 and 40°C, and an increase in temperature will result in an increase in the rate of the reaction. Even in the absence of oxygen a severe chain degradation will occur at temperatures above 100°C (Klemm, et al., 2001a). The alkaline oxidation of cellulose can be catalysed by transition metals such as cobalt, iron and manganese (McBurney, 1954).

This type of cellulose degradation is routinely employed for the controlled reduction of the degree of polymerisation and intrinsic viscosity of the cellulose during the viscose process (Strunk, et al., 2012). For the carboxymethylation process the mercerisation would proceed with only a small amount of chain degradation if the swelling time was kept short and/or oxygen was excluded from the reaction (Klemm, et al., 2001a). Stigsson, et al. (2005) demonstrated how the use of nitrogen and cobalt (II) could be used to control the viscosity of the CMC final product.

The viscosity modification of the CMC final product did not fall within the scope of this project. However, it was decided to investigate if the use of a nitrogen blanket it had any impact over and above the prevention of depolymerisation.

4.2 Objective and Approach

The carboxymethylation reaction is traditionally performed in the presence of a nitrogen gas blanket to prevent uncontrolled oxidation of the cellulose backbone. In order to determine if the use of a nitrogen blanket during the mercerisation of the cellulose had any impact on the swelling of the cellulose, changes in the crystalline structure of the cellulose were determined using XRD analysis for alkali cellulose samples, swelled with 25% NaOH at a starting temperature of 10°C, with and without the presence of nitrogen during the mercerisation.

The experimental methods used are outlined in Chapter 2.

4.3 Results and Discussion

The results of the XRD analysis for these samples can be seen in Figure 4-1. The cellulose swelled in the presence of nitrogen showed a less intense peak at 25 degrees 2-Theta than that of the cellulose swelled without the nitrogen present. This indicates that the use of a nitrogen blanket during the mercerisation of the cellulose has resulted in a more amorphous crystalline structure and thus improved the degree to which the cellulose has swelled.

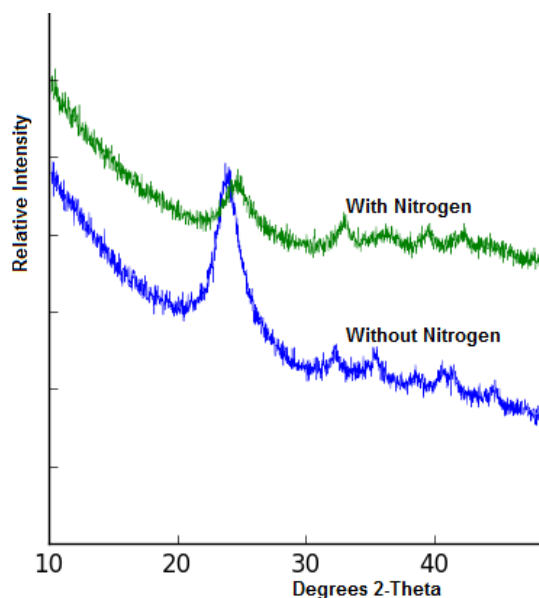


Figure 4-1 Stacked overlay of XRD scans for alkali cellulose at a swelling temperature of 10°C and NaOH concentration of 25% with and without the presence of a nitrogen blanket during mercerisation.

This was an unexpected outcome for the study and comparable results could not be found in the literature as a bench mark. As nitrogen is an inert gas and not expected to take part in the reaction there is no likely chemical explanation which can be put forward to explain these results. The nitrogen must therefore have an impact on the physical reaction conditions. When the temperature curves of the two reactions were compared, Figure 4-2, it was found that although all the same set points and reaction conditions were applied the temperature of the bulk reaction mixture for the reaction where the nitrogen blanket was used was several degrees lower than the reaction run without it. Temperature has been shown, in the previous section, to impact on the degree of swelling of the cellulose and this could therefore explain the differences in the crystallinity between the two samples.

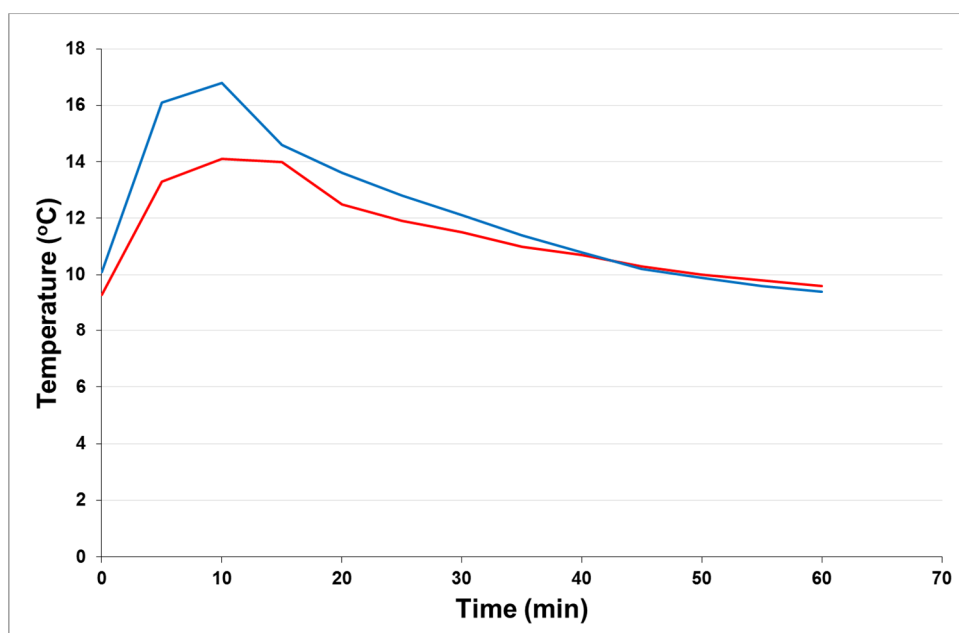


Figure 4-2 Temperature profile overlay for the mercerisation of cellulose with a starting swelling temperature of 10°C and NaOH concentration of 25%, with (—) and without (—) the presence of a nitrogen blanket during mercerisation.

In order to verify the results of the above investigation it was decided to run a set of complete carboxymethylation reactions where the same reaction conditions were used with and without the presence of a nitrogen blanket during the reaction. The results of the complete carboxymethylation reactions performed with and without the presence of nitrogen are tabulated in Table 4-1, and shows that the % dry purity, the DS and the % insoluble content of the two reaction products are very consistent.

Table 4-1 Analytical characterisation results of carboxymethylation reactions performed with and without the presence of a nitrogen blanket.

	With Nitrogen Blanket	Without Nitrogen Blanket
Dry Purity (%)	69.17	69.17
DS	0.74	0.75
2% Solution Viscosity	259	81

There is however a significant difference in the 2% solution viscosities. This is in-line with the findings of Stigsson, et al. (2005), who found that the viscosity of the CMC final product increased when the synthesis was performed in the presence of nitrogen.

Solution viscosity is, fundamentally, a measure of the hydrodynamic size of a polymer in solution (Billmeyer, 1971; Clasen & Kulicke, 2001). The hydrodynamic size can be influenced by the molecular mass, branching and conformation that a polymer assumes in solution (Section 1.5). From Table 4-2 it can be seen that the CMC product produced without the presence of the nitrogen blanket has a lower weight average molar mass (M_w) than the CMC product produced with the nitrogen present. This would be expected as in the presence of atmospheric oxygen in air, alkaline oxidation of the cellulose would occur thus reducing the overall molecular weight (Stigsson, et al., 2005).

Table 4-2 SEC-MALS characterisation results of carboxymethylation reactions performed with and without the presence of a nitrogen blanket. *The Z-average data is used for the R_g and R_h .*

	With Nitrogen Blanket	Without Nitrogen Blanket
M_w (kDa)	324	254
R_g (nm)	109	86
R_h (nm)	85	81
Conformational Slope	0.36	0.32

The shift differential MWD, resulting from the alkaline oxidation, for these two products can be clearly seen in Figure 4-3.

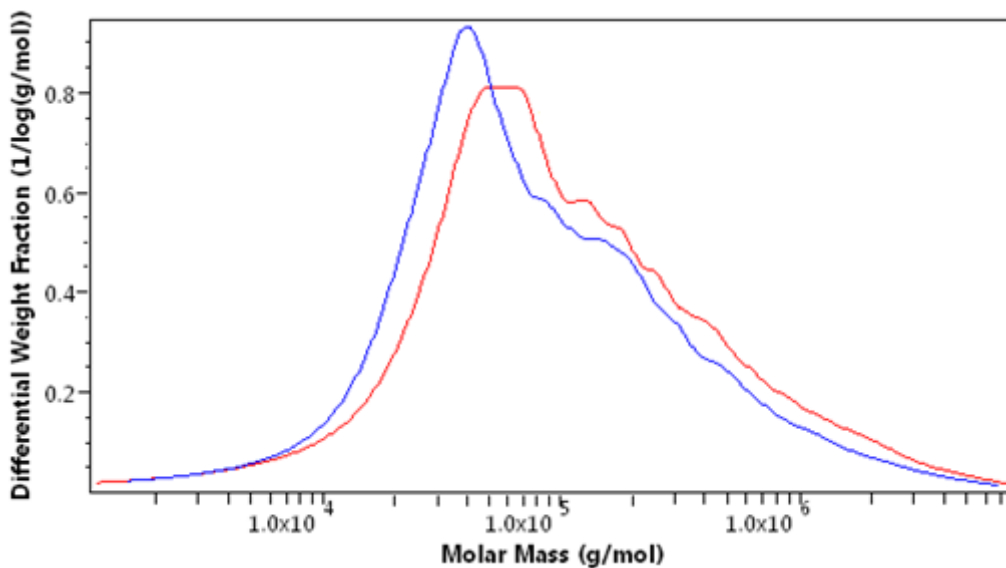


Figure 4-3 Differential MWD overlay of CMC products produced with (—) and without (—) the presence of a nitrogen blanket

This reduction in molecular weight and the downward shift in MWD of the CMC produced in the presence of atmospheric oxygen can therefore be related to its lower solution viscosity in comparison to that of the CMC product produced under a nitrogen atmosphere. This agrees with the findings of Kulicke, et al. (1996), Clasen & Kulicke (2001) and Prusova, et al. (2002) who demonstrated the relationship between M_w , MWD and solution viscosity.

The results in Table 4-2 also indicate that there is a difference in the R_g and conformational slopes of the two products, while the R_h values are similar. As discussed in Section 1.5 the R_g , R_h , and the conformational plots supply information about the size of the polymer and the conformation that it assumes in solution. These results indicate that the use of nitrogen has not just had the expected impact on the M_w but also has affected the conformation which the polymer assumes in solution.

The R_g for the CMC product produced under nitrogen is significantly larger than that of the CMC produced under atmospheric conditions, this follows the difference in the M_w and MWD for these products and therefore makes sense. The conformation plot overlay for these two products, shown in Figure 4-4, indicates that there is a difference in the conformation that the two CMC's assumed in solution.

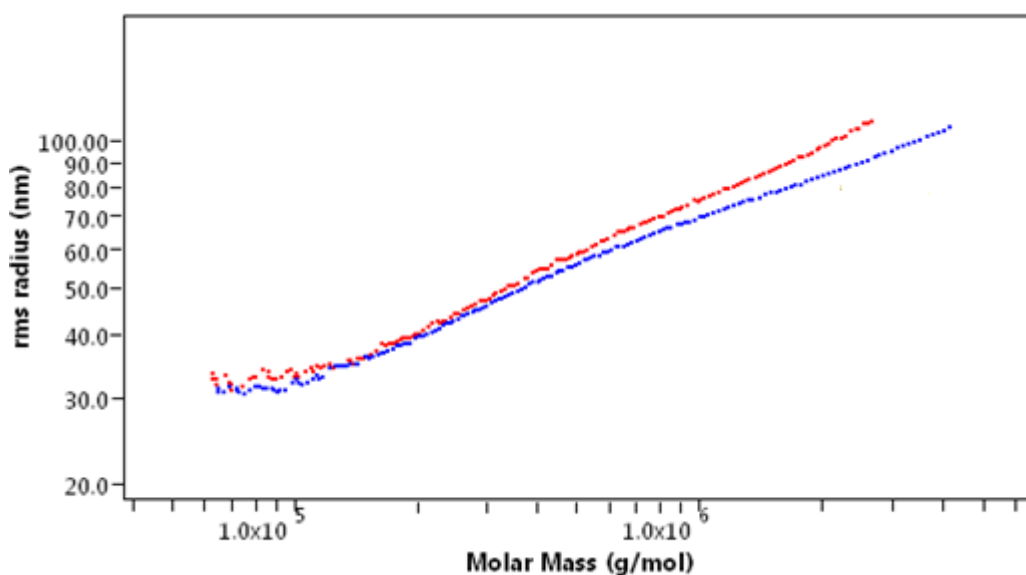


Figure 4-4 Conformational plot overlay of CMC products produced with (-) and without (-) the presence of a nitrogen blanket

The conformational plot shows how the R_g changes with regards to the M_w . Although both products can be interpreted as having a compact spherical conformation in solution, the CMC produced under nitrogen has a slightly steeper slope which indicates a more extended structure.

It therefore follows that for the reaction under nitrogen (which resulted in a more amorphous crystalline CMC structure according to the XRD analysis), there was a corresponding extension of the conformation that polymer assumed in solution. Li, et al. (2010) found that adsorption of NaOH and the degree of crystallinity of the cellulose impacted on the uniformity of the substituent distribution in the CMC. It is therefore proposed that the changes seen in the conformational plots of these products is indicative of a change in the uniformity of the substituents distribution. This concept will be investigated further in a later chapter.

It was found that when the temperature profiles from the start of the NaOH addition to the end of the MCA adsorption period were compared, the reaction conducted under nitrogen had a lower overall temperature than the reaction run in air.

There are two possible reasons why the reaction performed under the nitrogen blanket would have lower temperatures, firstly nitrogen has a greater heat capacity than oxygen which makes it a more efficient coolant and secondly in order to maintain the nitrogen blanket there was a constant, but very low flow from the top of the reactor, of nitrogen to maintain the blanket. Under atmospheric conditions the reactor was not completely sealed so there would have been some movement of air in the reactor, it would however have been minimal. Though small this flow of nitrogen would make a significant difference in the heat transfer of the nitrogen blanket.

4.4 Conclusions

The novel conclusion can therefore be drawn that the nitrogen blanket serves as an added cooling mechanism during the mercerisation and absorption phases of the carboxymethylation reaction. The reduction in the temperature of the reaction, especially during the NaOH swelling period, has resulted in a more amorphous structure and improved swelling of the alkali cellulose, as was evident from the XRD study. The improved swelling, has in turn, resulted in a more uniform distribution of substitution as indicated by the more extended conformation in solution of the CMC final product.

The solution viscosity, M_w , MWD, and R_g were all lower for the CMC product produced under atmospheric conditions, demonstrating the effect of the oxidative degradation on these parameters. The DS of the two products was the same so the presence of oxygen had no impact on the efficiency of the reaction.

5 THE INFLUENCE OF THE FORM OF ETHERIFICATION AGENT

5.1 Background

The investigations performed in Chapters 3 and 4 show how the swelling conditions of the aqueous process can be optimised. The next step is to optimise the etherification step of the carboxymethylation reaction. The etherification reagent is the most expensive reagent and so it is with regard to this reagent that the reaction efficiency needs to be optimised.

There are two possibilities when it comes to the etherification reagent, either monochloroacetic acid (MCA) or its sodium salt SMCA can be used. As the S_N2 reaction describes the reaction between the alkali cellulose and the SMCA, if MCA is used it must first be neutralised in-situ to form its sodium salt. Klemm, et al. (2001a) reported that if SMCA was used then approximately 0.8 mol of NaOH was required to swell the cellulose for the reaction, however, if MCA was used an extra equimolar amount of NaOH needed to be added to neutralise the acid. Alban Reyes, et al. (2017) showed that under the dry/aqueous conditions it required 1.8 mol of NaOH per mol of AUG to swell the cellulose sufficiently. Stigsson, et al. (2006), however, reported that for their solvent slurry investigation they used a molar ratio of 2.3 NaOH/AGU.

For the optimisation of the swelling conditions for the dry/aqueous reaction, performed in Chapter 3, a molar ratio of 2.4 NaOH/AGU was used and shown to provide sufficient swelling of the cellulose. Using the same molar ratio of NaOH/AGU will however pose a problem if SMCA is used as the etherification reagent, because an excess of NaOH will promote the side reaction resulting in the formation of sodium glycolate and poor reaction efficiencies. It can therefore be seen that the same reaction conditions can not be applied for the two different etherification reagents if reaction efficiency is the main concern.

A second consideration is the quality of the final product, it has been stated previously that the swelling of the cellulose determines a number of the characteristics of the final product because it impacts on the distribution of the substituents. The distribution of the substituents is, however, also impacted by the conditions of the etherification reaction.

Xiquan, et al. (1990) studied the kinetics of the carboxymethylation reaction of cotton linters in an isopropyl slurry system and found that the etherification reaction could be divided into two first order reactions with different rate constants. The first stage described the reaction in the alkalised amorphous region on the surface of the crystalline chain sheets or on the surface of the microfibrils, while the second stage described the transformation of the more crystalline regions as the etherification reagent diffuses across the microfibrils. The first stage was found to be faster with an activation energy of 52.2 kJ/mol for the activated cellulose while the second stage was dependant on the diffusion rate and the reaction controlled by the diffusion process. Olaru, et al. (1998) supported these results with their findings for the ethanol, acetone and ethanol/acetone solvent system. The rate of the substitution reaction is therefore faster than the diffusion of the MCA into the cellulose fibres (Omiya, 1984).

The rate at which the etherification reagent diffuses into the cellulose fibre is influenced by both thermodynamic and kinetic factors as well as physical barriers (Wu, et al., 2009). Diffusion can generally be said to obey Fick's First Law which is expressed as follows;

$$J_x = -D \left(\frac{\delta C}{\delta x} \right) \quad \text{Equation 14}$$

Where C is the concentration or number density, x is the distance perpendicular to the gradient of concentration and D is the diffusion constant. The diffusion constant can be related to the temperature of the system, the viscosity of the fluid and the size of the particle. Studies have shown that solutes with higher molecular weights have a slower rate of penetration (Wu, et al., 2009). Therefore it would be expected that the lower molecular weight MCA would diffuse more readily into the swollen cellulose fibre than the bulkier SMCA and thus promote a more even distribution of substituents and improve product quality.

5.2 Objective and Approach

The objective of this investigation is to compare the benefits of using either SMCA or MCA in regards to reaction efficiency and product quality.

A concern for the SMCA reaction was around the amount of NaOH to be used; having a large excess of NaOH present during the reaction could potentially reduce the efficiency of the reaction, while on the other hand reducing the concentration of the NaOH could negatively impact the swelling of the cellulose. It was decided to opt for reducing the amount of NaOH and maintaining the water content, to ensure that enough moisture was present to allow the reaction to occur. Therefore a lower NaOH concentration was used. This approach was adopted so that the emphasis could be placed on reaction efficiency.

For the reaction where MCA was used as the etherification reagent a molar ratio of 2.4 NaOH/AGU was used under the optimised swelling conditions determined previously.

For the reaction where SMCA was used the a molar ratio of 1.2 NaOH/AGU was used, thus removing the excess NaOH not required for in-situ neutralisation.

The water content of both the reactions was kept the same, for the MCA reaction a 37% solution of NaOH was used and for the SMCA reaction a 21% solution. Both reactions were performed using a nitrogen blanket and identical reaction conditions.

The experimental methods used are outlined in Chapter 2.

5.3 Results and Discussion

Table 5-1 shows the results for the two reaction products using SMCA and MCA respectively. It can be seen that the purity of the two products is not significantly different and that the DS of the products, and hence the calculated reaction efficiencies are the same. This substantiates the decision to reduce the NaOH to AUG ratio for the CMC_{SMCA} reaction to promote reaction efficiency. The % insoluble content for the CMC_{SMCA} reaction product was found to be more than double that of the CMC_{MCA} reaction product. This maybe as a result of the differences in the NaOH concentrations used during the swelling process that has

impacted on the solubility of the final products. There is also a significant difference in the 2% solution viscosity of the two products.

Table 5-1 Analytical characterisation results of carboxymethylation reactions performed with SMCA and MCA.

	SMCA	MCA
Dry Purity (%)	63.32	64.66
DS	0.74	0.74
2% Solution Viscosity	118	259
% Insoluble Content	0.93	0.43
% Reaction Efficiency	62%	62%

As was discussed in Chapter 4 the differences in the solution viscosities indicate that there are differences in the molecular characteristics of the two final products and, as can be seen from the SEC-MALS characterisation results shown in Table 5-2, this is in fact the case.

Table 5-2 SEC-MALS characterisation results of carboxymethylation reactions performed with SMCA and MCA as etherification reagents. *The Z-average data is used for the R_g and R_h .*

	SMCA	MCA
M_w (kDa)	196	323
R_g (nm)	75	110
R_h (nm)	72	86
Conformational slope	0.30	0.37

The CMC_{SMCA} product has a lower M_w than the CMC_{MCA} product and the corresponding shift in the MWD can be seen in Figure 5-1 below.

This shift to the lower molecular weight region for the MWD and M_w was unexpected. Both reactions were performed under a nitrogen blanket which would have limited the amount of oxidative hydrolysis; it was therefore expected that the two reaction products would either have similar M_w or that the MCA reaction product would have the lower M_w because more NaOH was present during the reaction.

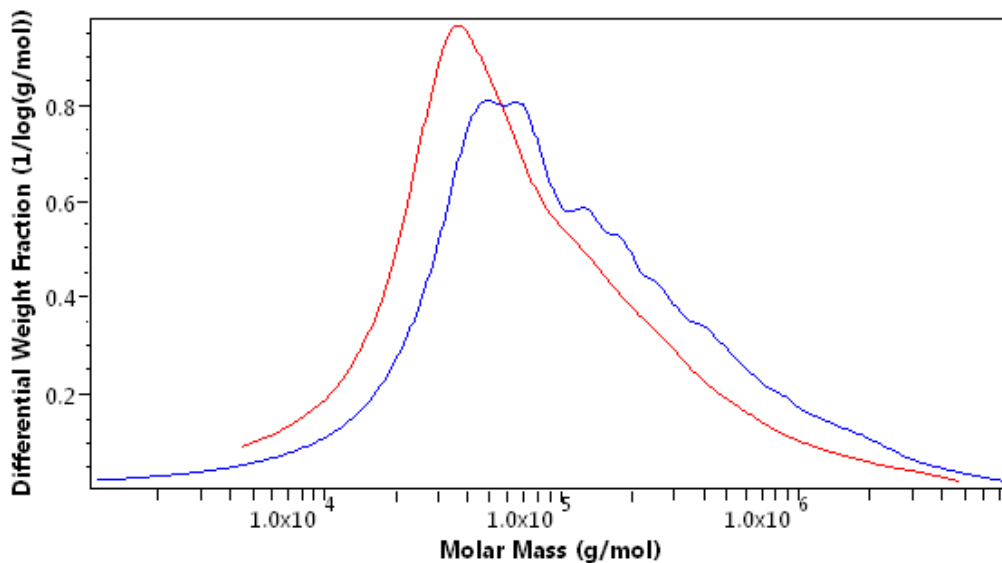


Figure 5-1 Differential MWD overlay for CMC_{SMCA} (-) and CMC_{MCA} (-)

One possible explanation for this result is linked to the difference in solubility of the two products. The solubility of the CMC is controlled by its DS, the uniformity of substitution and the molecular weight (Feddersen & Thorp, 1993). As the DS of these two reaction products is the same, the differences in solubility must therefore be as a result of either the uniformity of the substitution or the molecular weight. Both these products were produced from the same cellulose starting material under conditions where oxidative hydrolysis was limited therefore large differences in M_w and MWD distribution were not expected. It must therefore be concluded that the differences in the solubility must be related to differences in the uniformity of the substitution. How then does this translate into the differences in M_w and MWD observed?

In polymer samples the insolubles consist of the high molecular weight part of the sample (Podzimek, 2011) which have not been adequately substituted to allow them to go properly into solution. The variation in substituent distribution between individual chains can also result in non-substituted cellulose fibres still being present in the solution (Thielking & Schimdt, 2012). The solubility of the polymer sample is an important factor for the SEC-MALS characterisation that we use in this study (Yau, et al., 1980; Gaborieau & Castignolles, 2011). These insoluble fractions would be removed by the filtration step during the sample preparation for the SEC-MALS characterisation.

It should be recalled from Section 1.5.3 that M_w is sensitive to the higher molecular weight fractions and therefore, the removal of small amounts high molecular weight material from the polymer sample will have a significant impact on the M_w and the MWD. It is therefore concluded that the CMC_{SMCA} product has a lower M_w and MWD than the CMC_{MCA} product due to an increase in the insoluble content of the CMC. This also explains the lower solution viscosity for the CMC_{SMCA} product, as longer polymer chains tend to give a disproportionate increase in viscosity due to chain entanglements (Feddersen & Thorp, 1993).

The results shown in Table 5-1 also indicate that there are conformational differences between the CMC_{SMCA} and CMC_{MCA} products where the slopes of the conformational curves are 0.30 and 0.37 respectively. The lower slope value for CMC_{SMCA} is indicative of a compact sphere whereas the higher value for CMC_{MCA} indicates more of an extended coil conformation. Figure 5-2 shows the difference in the conformational plots for the two products in more detail.

The curve for CMC_{MCA} is linear which shows that the conformation for the CMC is the same for the entire molecular weight distribution. The curve for CMC_{SMCA} , however, shows two inflection points (indicated by arrows on the figure) at around 500 kDa and 1500 kDa which are indicative of a change in the conformation of the CMC as the molecular weight increases. Below 500 kDa the slopes of the conformational plots are approximately the same, 0.36 and 0.37 for the CMC_{SMCA} and CMC_{MCA} respectively. Therefore in this low molecular weight region both products have an expanded conformation which is no longer a compact sphere but not quite a random coil. Above 500 kDa the slope of the conformational plot, for CMC_{SMCA} , changes to 0.23 which is indicative of a very compact sphere. At around 1500kDa there is a second inflection point on the CMC_{SMCA} curve, where the slope of the remaining high molecular weight portion of the conformational plot becomes 0.43, a slope which is indicative of a random coil conformation. These changes in the slope of the conformational plot for CMC_{SMCA} suggest that the distribution of substituents is not uniform across all the polymer chains. It also highlights why it is important to examine the plots and not just rely on the average results.

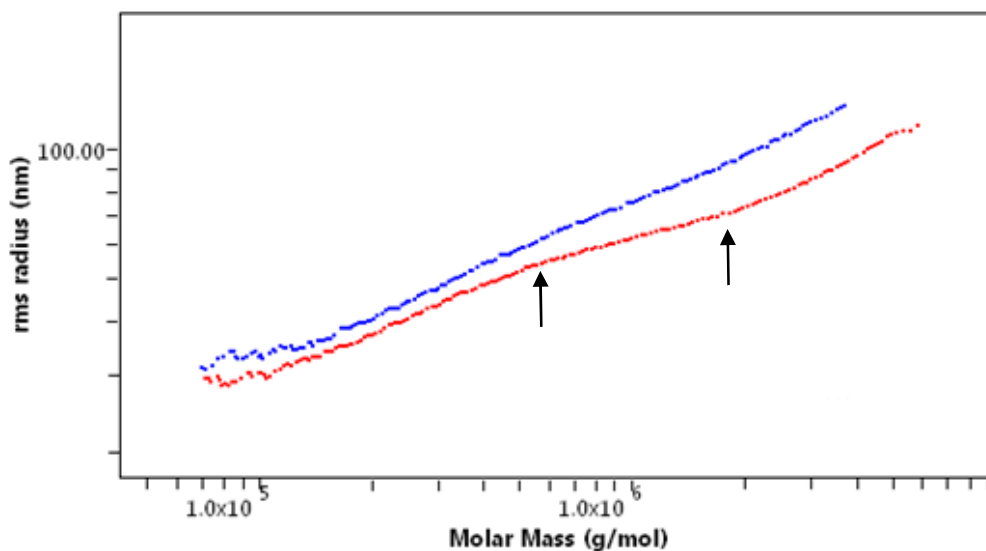


Figure 5-2 Conformational Plot Overlays for CMC_{SMCA} (-) and CMC_{MCA} (-)

Over and above the changes in the slope values for the conformational plot the same trend is evident, as was found during the investigation in Chapter 4, that conditions where improved swelling conditions are used results in an increase in the slope of the conformational plot. This lends support to the hypothesis that the changes in conformational slope are indicative of changes in the uniformity of the substituent distribution in the CMC final product.

5.4 Conclusions

It was found that, for reactions where etherification reagents MCA or SMCA were used the same reaction efficiencies were obtained. This result was achieved when the amount of NaOH decreased for the SMCA etherification reaction to bring it to parity with that used in the MCA reaction having taken into account the amount required for *in-situ* neutralisation. The water content of both reactions was maintained at around 36%.

It was found that the use of these conditions resulted in the CMC_{SMCA} product having a higher insoluble content, which impacted on the Mw and MWD of the product and ultimately contributed to a lower solution viscosity. It was also found that the conformational plot of the CMC_{SMCA} product contained inflection points which indicated that the conformation changed for different molecular weights fractions of the CMC polymer. This was indicative of a non-uniform distribution of the carboxymethyl substituents along the cellulose backbone.

The conclusion can therefore be made that the distribution of substituents for CMC_{SMCA} is less uniform than for CMC_{MCA} product due to different NaOH concentrations used during the initial swelling of the cellulose. This finding therefore confirms that sufficient swelling of the cellulose is critical to adequately destroy the crystalline structure of the cellulose in order to allow reagents to diffuse into the fibres. This confirms the statement made by Feddersen & Thorp (1993) that “the first element in preparing a uniformly substituted polymer is the preparation of a uniform alkali cellulose”, as well as the findings of Chapters 3 and 4 of this investigation.

Although the reaction efficiency is an important parameter for this investigation the improvement of the overall product quality also needs to be taken into account. It is therefore recommended that MCA should be used as the etherification reagent in conjunction with the dry aqueous reaction conditions.

6 EFFECT OF TEMPERATURE DURING MCA ADDITION

6.1 Background

In the previous Chapter it was found that MCA was the more beneficial etherification reagent for the dry/aqueous process, due mostly to the fact that it can be used in conjunction with the optimised swelling conditions. Temperature has already been shown to play a significant role in achieving optimum swelling of the cellulose under dry/aqueous conditions. The question now centers around the effect of temperature during the addition of the MCA and the subsequent adsorption period during the dry aqueous process.

The addition of the etherification reagent is one aspect where there is a significant difference in the reaction between the solvent slurry and the dry aqueous processes. For the solvent slurry process, after the NaOH addition and swelling period, the MCA is added and the reaction temperature is allowed to increase to the required reaction temperature where it is then maintained (Stigsson, et al., 2004; Stigsson, et al., 2005; Stigsson, et al., 2006). Thus the heat of neutralisation is partially used to heat the reaction to the desired temperature (Salmi, et al., 1994). For the historical dry/aqueous process a contact period of 1 to 2 hours at temperatures of 35 to 45°C is allowed depending on whether the etherification reagent is added as an aqueous solution or a dry powder (NIIR Board, 2003).

For the slurry process the presence of the organic solvent, as well as the low solids content, promotes a more even distribution of the reactants during the reaction (Stigsson, et al., 2006), the MCA is also highly soluble in the solvent and can therefore be more readily adsorbed by the cellulose fibres. These factors reduce the requirement for an adsorption period during the slurry process. On the other hand for the dry/aqueous process, time needs to be allowed for the MCA, to hydrate and be adsorbed by the cellulose especially if used in a powder form. It is for this reason that a 30 minute adsorption period is allowed after the addition of MCA powder to the alkali cellulose in the reaction process.

As discussed in Chapter 5 the rate of the substitution reaction is faster than the diffusion of the MCA into the cellulose fibres (Omiya, 1984). Branam (1954), proposed that the etherification reaction can be essentially arrested by maintaining the reaction temperature below 30°C.

This promotes the penetration of the MCA into the cellulose fibre, resulting in a more uniform distribution and an improved reaction efficiency (Branan, 1954). Results published by Salmi, et al. (1994) found that while the rate of the carboxymethylation reaction increased with increasing temperature the distribution of substitution becomes less uniform and that monosubstituted units dominated at temperatures of 30 to 40°C, thus supporting Branan's (1954) statement. On the other hand Stigsson, et al. (2004) stated that increasing the temperature of the etherification reaction favoured the substitution reaction increasing the reaction efficiency but had no significant effect on the distribution of substitution.

The kinetics of the etherification reaction and side reaction may offer some explanation as to why the reaction efficiency would improve with lower reaction temperatures. Xiquan, et al. (1990) proposed an activation energy of 52.2 kJ/mol for the etherification reaction where the etherification reagent reacts with the alkalised amorphous regions and the surface of the cellulose microfibrils in a temperature range of 45 to 65°C. While Li, et al. (2010) found that temperature had a greater impact on the formation of sodium glycolate during the carboxymethylation of cellulose than NaOH concentration. It was found that after 15 minutes at 45°C the conversion to sodium glycolate was only 10% but this increased to over 80% when the temperature was increased to 85°C. The formation of sodium glycolate was found to be a second order reaction with an activation energy of 103 kJ/mol (Li, et al., 2010).

The activation energy of the side reaction therefore appears to be higher than that of the first stage of the substitution reaction, it therefore follows that a lower temperature during the adsorption stage of the dry aqueous reaction could increase the reaction efficiency because it would limit the formation of sodium glycolate. Whether this has any additional impact on the distribution of substitution will need to be established.

6.2 Objectives and Approach

For this investigation the ratio of reactants was kept the same for all reactions as were the swelling and reaction temperatures. Temperatures during the addition of the MCA and subsequent adsorption period were varied from 17 to 45°C. The main objective of the study was determine the effect of the temperature on the reaction efficiency and product quality.

The experimental methods used are outlined in Chapter 2.

6.3 Results and Discussion

In order to accurately determine the impact of the temperature during the MCA addition and adsorption period it was important to keep the NaOH addition and swelling conditions as consistent as possible. The temperature profiles for this series of reactions is shown in Figure 6-1.

The NaOH addition and swelling period of the carboxymethylation reaction falls between 0 – 60 min on the graph where the first temperature peak occurs. This rise in temperature is due to the re-arrangement of the cellulose crystal structure and formation of the alkali-cellulose which are both exothermic processes (Wang, 2008). It can be seen from Figure 6-1 that for this series of reactions the temperature profiles for this period of the reaction do not show significant variation.

The MCA addition and adsorption period of the carboxymethylation reaction falls between 60 – 120 min on the graph where the second much larger temperature peak occurs. This temperature peak occurs because the in-situ neutralisation of MCA to SMCA with NaOH is highly exothermic. The temperature during this period was controlled by varying the degree of cooling applied to the reactor so that the temperature varied from 17 to 45°C. The temperature for each set of reactions is taken from the highest temperature obtained during the adsorption period i.e. CMC₁₇ has a maximum adsorption period temperature of 17°C, whereas CMC₂₈ has a maximum temperature of 28°C.

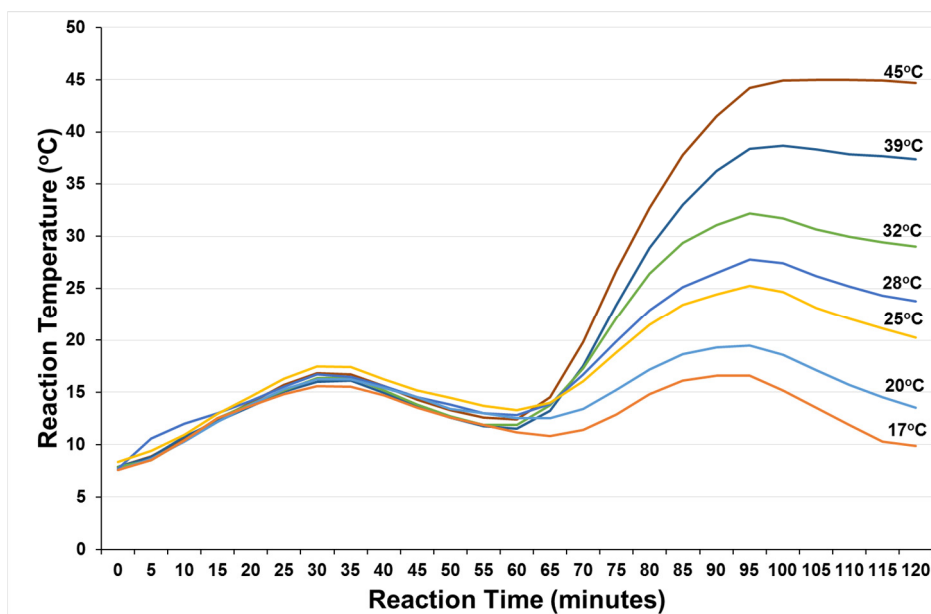


Figure 6-1 Overlay of temperature profiles for the NaOH addition and swelling period as well as the MCA addition and adsorption period for reactions CMC₁₇ to CMC₄₅, showing the temperature variations for the MCA addition and adsorption period.

The results for the analytical characterisation for these products is shown in Table 6-1.

Table 6-1 Analytical characterisation results for reactions CMC₁₇ to CMC₄₅ performed with variations in temperature for the MCA addition and adsorption Period.

	Max Absorption Temp (°C)	Dry Purity (%)	2% Solution Viscosity (cps)	Insoluble Content (%)	DS	Reaction Efficiency (%)
CMC₁₇	17	67.44	164	0.41	0.69	58
CMC₂₀	20	68.10	170	0.47	0.73	61
CMC₂₅	25	68.26	164	0.30	0.76	64
CMC₂₈	28	67.72	127	0.41	0.77	65
CMC₃₂	32	68.69	123	0.51	0.74	62
CMC₃₉	39	68.57	120	0.37	0.74	62
CMC₄₅	45	68.84	130	0.48	0.72	61

The dry purity and insoluble contents are very consistent for all the products. On the other hand the 2% solution viscosity does show some variation and this could again be indicative of differences in the molecular characteristics of the products as has been found previously. It appears that slightly higher viscosities are achieved below 25°C.

The molecular characterisation results for these products are shown in Table 6-2. Unlike what was found in Chapter 4 and 5 there is not a large variation in the M_w and in fact they fall in a very narrow range between 374 to 436 kDa, which indicates that there has been very little overall change in the average molecular weight for these products.

Table 6-2 SEC-MALS characterisation results for reactions CMC₁₇ to CMC₄₅ performed with variations in temperature for the MCA addition and adsorption period.

	Max Temp (°C)	M_w (kDa)	R_g (nm)	R_h (nm)	Conformational Slope
CMC ₁₇	17	436	146	81	0.39
CMC ₂₀	20	380	138	77	0.39
CMC ₂₅	25	373	137	78	0.38
CMC ₂₈	28	374	134	76	0.38
CMC ₃₂	32	428	143	82	0.39
CMC ₃₉	39	383	135	82	0.39
CMC ₄₅	45	381	139	80	0.40

An overlay of the differential MWD for these products, Figure 6-2, shows that there is some variation in the peak intensities for these products but the shape and polydispersity of the curves are, however, the same. In order to determine how significant these differences are a cumulative MWD can also be examined.

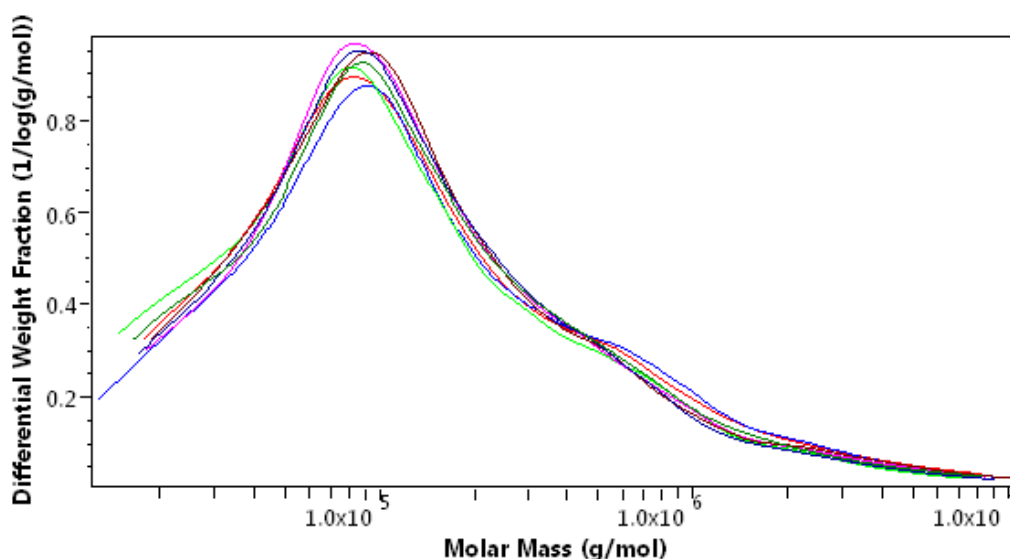


Figure 6-2 Differential MWD overlays for CMC₁₇ (—), CMC₂₀ (—), CMC₂₅ (—), CMC₂₈ (—), CMC₃₂ (—), CMC₃₈ (—) and CMC₄₅ (—)

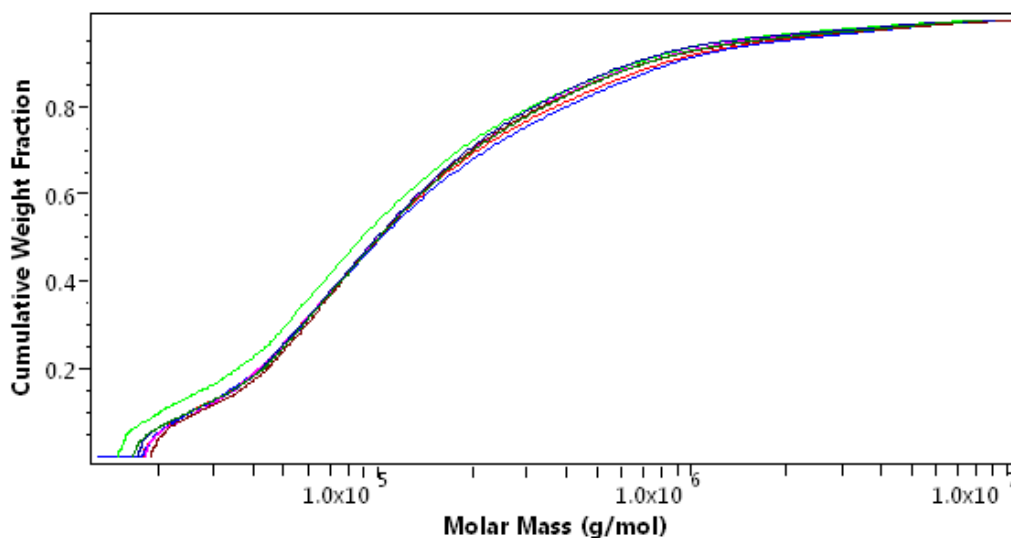


Figure 6-3 Cumulative MWD overlays for CMC₁₇ (—), CMC₂₀ (—), CMC₂₅ (—), CMC₂₈ (—), CMC₃₂ (—), CMC₃₈ (—) and CMC₄₅ (—)

Figure 6-3 shows the cumulative MWD for these products and from this it can be seen that the differences in the distributions do not appear to be significant. CMC₂₅ is the only product which shows some deviation, in that it has a higher proportion of low molecular weight material in comparison to the other products.

The results for R_g and R_h shown in Table 6-2 indicate no significant difference between the CMC products of these reactions, this is also true for the conformation in solution. The slopes of the conformational plot vary between 0.38 and 0.40 which is indicative of an expanded conformation which is no longer a compact sphere but not quite a random coil. Figure 6-4 shows the overlays of the conformational plots for these products and illustrates that there is no significant change in the conformation in solution in relation to changes in the temperature during the MCA addition and adsorption periods.

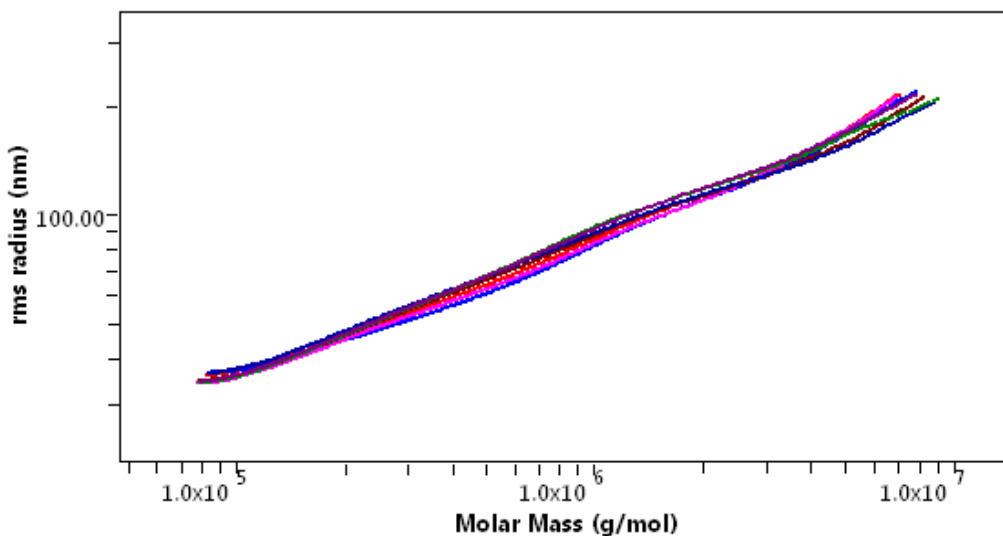


Figure 6-4 Conformational plot overlays for CMC₁₇ (—), CMC₂₀ (—), CMC₂₅ (—), CMC₂₈ (—), CMC₃₂ (—), CMC₃₈ (—) and CMC₄₅ (—)

In Chapter 4 and 5 it was discussed that changes in the conformation in solution of the CMC polymer could be indicative of changes in the distribution of substituents along the polymer backbone. If this hypothesis is true then the result indicates that changes to the temperature of the MCA addition and adsorption periods have not influenced the distribution of substituents.

From the results shown in Table 6-1 it appears that the most significant impact of the changes in temperature during the MCA addition and adsorption period is the moderate changes in the DS and subsequent impact on the reaction efficiency.

The lowest DS, 0.69, is observed at 17°C for CMC₁₇, as the temperature increases to 20°C the DS also increases to 0.73 for CMC₂₀. This trend continues for CMC₂₅ and CMC₂₈. The highest DS, 0.77, is observed at 28°C for CMC₂₈ but this is, however, only marginally higher than CMC₂₅ which has a DS of 0.76. The efficiency of the reaction starts to decrease as the temperature continues to increase from 28°C, CMC₃₂ and CMC₃₉ both have DS values of 0.74 and, at 45°C the DS obtained for CMC₄₅ is only 0.72.

Figure 6-4 is a plot of reaction efficiency versus maximum observed temperature during the MCA addition and adsorption period. The optimum reaction efficiency is obtained between 25 and 30°C. This therefore concurs with the findings of Branam (1954).

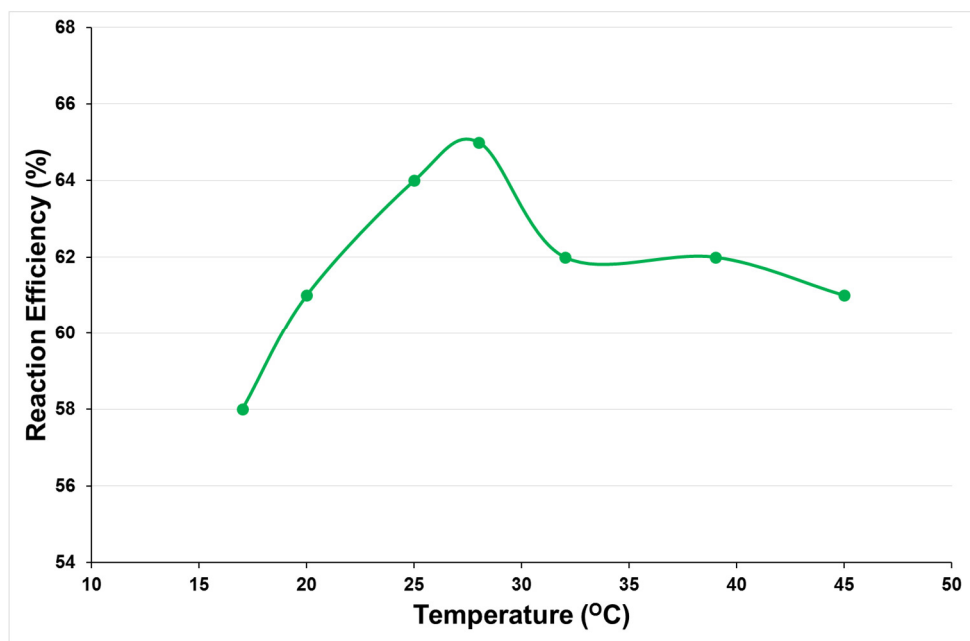


Figure 6-5 Plot of reaction efficiency versus maximum temperature during the MCA addition and adsorption period for the reactions CMC₁₇ to CMC₄₅

The dissolution of MCA is an endothermic process (Benoit, et al., 1991) and it therefore follows that if the temperature of the reaction system is too low there is insufficient energy available for the MCA to solubilise, this explains why the reaction efficiency is lower below 25°C. As the temperature increases, the side reaction, which results in the formation of sodium glycolate, may start to be favoured, due to its higher energy of activation. This would result in a decrease in reaction efficiency, however, this can not be proved conclusively because the purity of the CMC products does not show a trend to support this statement. It may however be that the purity method used is not sensitive enough to detect small changes in the salt contents of the CMC.

6.4 Conclusions

It was found that the change of temperature during the MCA addition and adsorption phase had no significant impact on the purity, viscosity and % insoluble content of the CMC final products. The Mw and MWD also showed no significant changes. Previously it had been proposed that changes in the slopes of the conformational plots were indicative of changes in the distribution of substitution, in this case all the conformations in solution of the CMC products were found to be similar and therefore no changes in distribution could be inferred.

The only significant changes which were observed between the products were the DS and the derived reaction efficiency. The optimum reaction efficiency was achieved between 25 and 30°C. This supports the findings of Branam (1954) that temperatures below 30°C increase the reaction efficiency and verify the statement made by Stigsson, et al. (2004) that increasing the temperature of the etherification reaction favoured the substitution reaction increasing the reaction efficiency but had no significant effect on the distribution of substitution.

7 MICROWAVE REACTIONS

7.1 Background

One of the aspects of many chemical processes which has an indirect impact on the environment is the consumption of large amounts of energy for the heating and cooling of reactions (Dallinger & Kappe, 2007). Designing more energy efficient processes is therefore one of the key principals of green chemistry (Anastas. & Warner, 1998). Two alternative energy sources which have received a lot of attention in the last few years are the use of ultrasound and microwave irradiation (Dallinger & Kappe, 2007).

Conventional means of heating reactions, such as oil baths, heating mantles or reactor jackets are indirect heating methods, where heat is transferred by means of thermal conduction and convection, from an outside source into the reaction vessel and then to the reaction mixture (Dallinger & Kappe, 2007; Rathi, et al., 2015). The efficiency and rate of heating depends on the thermal conductivity, specific heat capacity and density of the reaction vessel components and reaction mixture (Nomanbhay & Ong, 2017). It is a heterogeneous heating effect that results in non-uniform temperatures and high thermal gradients between the reaction vessel and the reaction mixture (Nomanbhay & Ong, 2017). A large portion of the heat energy is also lost to the environment, this is therefore, a comparatively inefficient and slow way of transferring energy to a reaction system (Dallinger & Kappe, 2007; Rathi, et al., 2015; Nomanbhay & Ong, 2017).

Microwave irradiation, on the other hand, provides more direct heating by coupling the microwave energy with dipole or ionic molecules present in the reaction mixture resulting in a near instantaneous heat transfer (Dallinger & Kappe, 2007; Rathi, et al., 2015). Microwaves consist of two components, electric and magnetic fields, which are responsible for the microwave dielectric heating and magnetic loss heating respectively (Nomanbhay & Ong, 2017). The majority of the work done in the organic chemistry field refers to dielectric heating, which can be explained by two primary mechanisms, dipolar polarization and ionic conduction (Polshettiwar & Varma, 2010; Nomanbhay & Ong, 2017).

The efficiency of the microwave irradiation is therefore dependent on the ability of the molecules within the reaction mixture to absorb the electromagnetic radiation and convert it to heat energy (Polshettiwar & Varma, 2010), this is defined as dielectric loss (Dallinger & Kappe, 2007). For this reason polar solvents with high dielectric loss, such as ethylene glycol and ethanol, are frequently selected (Rathi, et al., 2015). Water is a polar molecule and thus also suitable as a solvent for microwave reactions. Due to its suitability as a benign reaction medium, the use of water as a solvent in combination with microwave heating is very desirable for green chemistry applications and is the subject of a number of investigations (Dallinger & Kappe, 2007; Rathi, et al., 2015; Polshettiwar & Varma, 2010).

Under controlled conditions microwave heating has been found to reduce reaction times, improve reaction homogeneity as well as increasing product yield and purity (Dallinger & Kappe, 2007; Biswas, et al., 2014; dos Santos, et al., 2015; Hivechi, et al., 2015; Rathi, et al., 2015). Figure 7-1 below illustrates the differences between conventional heating and microwave heating. For solid state reactions microwave heating would be more beneficial than conventional heating as you don't get convection in a solid.

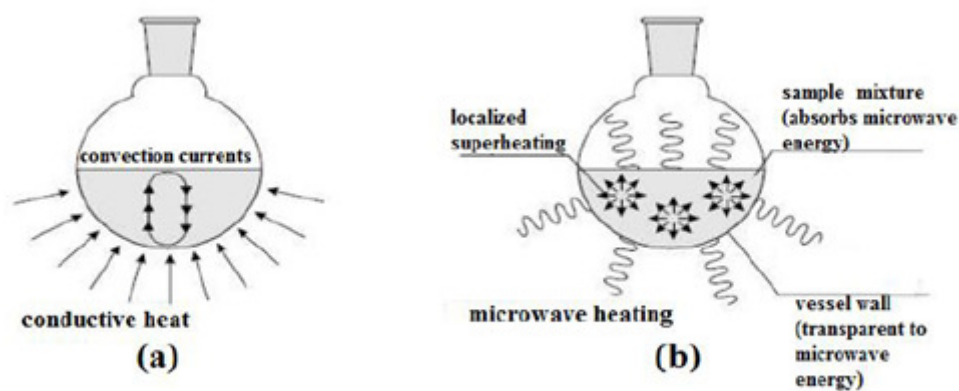


Figure 7-1 Illustration of the heating mechanisms for (a) conventional heating and (b) microwave heating (Nomanbhay & Ong, 2017)

Early microwave experiments were conducted in domestic microwave ovens without the ability to measure temperature or stir the reaction mixtures (Roberts & Strauss, 2005).

Uniform heating is difficult to control in a domestic microwave oven where the irradiation power is generally controlled by on-off cycles of the magnetron (Dallinger & Kappe, 2007) and therefore, the “reaction time” of the sample does not necessarily equate to the “irradiated time” (Leonelli & Veronesi, 2015).

Dedicated microwave reactors for chemical synthesis, have been developed over the last 20 years, which offer precise temperature and pressure control, continuous monitoring of process parameters and stirring of the reaction mixture (Dallinger & Kappe, 2007; Leonelli & Veronesi, 2015). The use of these reactors is however limited due to the size restrictions of the cavity and reactor, there are larger scale reactors available but these have intrinsic limitations (Leonelli & Veronesi, 2015; Rathi, et al., 2015). Besides size the dedicated microwave reactors are on the whole designed to handle liquid reactions and use magnetic stirrers or continuous flow systems to mix reactants (Rathi, et al., 2015).

A number of previous investigations have been conducted on the microwave-assisted functionalisation and modification of polysaccharides (Koroskenyi & McCarthy, 2002; Markin, et al., 2015). More specifically the use of microwave-assisted heating for the carboxymethylation of various sources of cellulose were investigated which included pine wood (Cheprasova, et al., 2012; Markin, et al., 2014), cotton stalk waste (Zhang, et al., 2011), brewer’s spent grain (dos Santos, et al., 2015) and agricultural waste materials such as wheat straw, barley straw and rice hull (Biswas, et al., 2014). In most cases the slurry process, or a modification thereof, was used with solvents such as ethanol and isopropanol.

In only two cases were aqueous reaction conditions investigated. Biswas, et al. (2014), investigated the carboxymethylation of agricultural waste with both water and isopropanol as solvent. They found that in an aqueous environment the achieved DS was low (0.1) and optimised the reaction by minimising the amount of water present and moving to isopropanol as solvent. With the optimised reaction conditions they were able to achieve DS results of 0.8 to 1.1, they further found that conventional and microwave heating produced CMC’s with comparative DS values, however, the microwave reactions had a significantly shorter reaction time (Biswas, et al., 2014).

On the other hand Cheprasova, et al. (2012) investigated the carboxymethylation of pine and aspen wood, in a number of different solvents including water, and found that the percent of carboxymethyl groups (CMGs) present in the final product increased when water was used as the solvent in comparison to isopropanol. The findings of this work are somewhat questionable, they are also difficult to interpret and relate to other work because they do not include DS values.

The possible benefits associated with the use of microwave heating in regards to the improved energy efficiency i.e. reduced reaction time and more efficient use of energy could further the “greenness” of the dry aqueous production of CMC. If an improved reaction efficiency and product quality can also be obtained this may bring the dry aqueous process even closer to solvent slurry process and increase its viability as an alternative process.

7.2 Objectives and Approach

The objective of this investigation was to determine if microwave heating could be used for the dry aqueous reaction to improve the energy efficiency of the etherification reaction by reducing the required reaction time and also improve the reaction efficiency. Although not ideal, this series of reactions was performed in a domestic microwave oven; this was due to the large sample size required to perform the chemical analysis exceeding the volume of available laboratory microwave reactors. A closed reaction vessel was used to limit the amount of evaporation during the reaction.

A standard pilot plant batch of CMC was performed where the optimum reaction conditions were used. Once the MCA addition and adsorption period had been completed, a bulk sample was taken for the purpose of the microwave reactions, while the remainder of the pilot plant batch was allowed to run to completion via the conventional process in parallel to the microwave process. A series of microwave reactions were performed at 85, 255, 425 and 595 W respectively.

The experimental methods used are outlined in Chapter 2

7.3 Results and Discussion

The microwave reactions were carried out using two different methods to determine which would be the most effective. For the first set of reactions, performed at 85 W, a 200 g sample was taken from the bulk sample and placed into a Pyrex glass bowl and covered to prevent evaporation. 30 g samples were taken at 5, 10, 15 and 20 minute intervals and placed in an oven at 110°C to dry for 2 hours.

It was noted during the course of these reactions that as the condensate dripped back into the reaction mixture it formed areas of partially solubilised CMC, which had a gel like consistency. The same phenomenon occurred along the wall of the vessel where condensate collected and then ran back into the reaction mixture. This can be explained by considering that as the etherification reaction proceeds the CMC becomes more soluble and therefore starts to partially hydrate when it comes into contact with the water. This effect indicates that stirring is required during the reaction to ensure that water returning to the reaction system is evenly distributed. Because the reaction mixture is essentially “dry” obtaining effective stirring within the microwave reactor maybe challenging, the current pilot and lab reactors utilise a double helical agitator. Of the available dedicated lab and pilot scale microwave reactors studied none appeared to be suitable for this type of dry solid reaction (Esveld, et al., 2000; Leonelli & Veronesi, 2015; Rathi, et al., 2015).

The results for the microwave reactions run under these conditions, MW 04 – MW 07, are shown in Table 7-1. The pilot scale reaction which was completed by conventional heating, CH 03, was reacted at 65°C for 2 hours and had a final DS of 0.68. At 5 and 10 minutes, reactions MW 04 and MW 05 respectively, the DS achieved using microwave heating was 0.67 and for MW 06, with a reaction time of 15 minutes, the DS achieved was 0.69. These results are therefore comparative to what was achieved with the conventional heating. This confirms the findings of Koroskenyi & McCarthy (2002), and Biswas, et al. (2014), that the use of Microwave energy results in comparative DS values at significantly reduced reaction times.

The microwave reaction which produced the highest DS was achieved at a reaction time of 20 minutes. The reaction efficiency of this reaction, MW 07, was 59.17%, which is higher than the 56.67% achieved by the reaction that used conventional heating. This result confirms the findings of Hivechi, et al. (2015), who showed that the use of microwave heating resulted in a increase in the effective MCA utilisation per gram of cellulose.

The concern with this reaction method was that as each subsequent sample was removed from the original sample the remaining reaction mixture would be subjected to increased radiation per mass. This is a difficulty observed when using domestic microwave ovens (Roberts & Strauss, 2005; Leonelli & Veronesi, 2015).

Table 7-1 Reaction conditions and DS values for the CMC reactions performed using conventional and microwave heating

Sample	Energy	Power (W)	Time	DS	Reaction Efficiency (%)
CH 03	Heat		2 h	0.68	56.67
MW 04	Microwave	85	5 min	0.67	55.83
MW 05	Microwave	85	10 min	0.67	55.83
MW 06	Microwave	85	15 min	0.69	57.50
MW 07	Microwave	85	20 min	0.71	59.17
MW 08	Microwave	255	2 min	0.56	46.67
MW 09	Microwave	255	4 min	0.55	45.83
MW 10	Microwave	255	6 min	0.56	46.67
MW 11	Microwave	255	8 min	0.56	46.67
MW 12	Microwave	425	30 sec	0.58	48.33
MW 13	Microwave	425	1 min	0.60	50.00
MW 14	Microwave	425	2 min	0.61	50.83
MW 15	Microwave	425	3 min	0.63	52.50
MW 16	Microwave	595	30 sec	0.58	48.33
MW 17	Microwave	595	1 min	0.57	47.50
MW 18	Microwave	595	2 min	0.55	45.83

For the remaining reactions, MW 08 to MW 18, the reaction method was therefore changed. Aliquots of 30 g were taken from the bulk sample and placed into Pyrex glass bowls and covered to prevent evaporation. At the end of the allotted reaction time the whole 30 g sample was removed and dried.

During the course of these reactions it was found that the reaction mixture began to lose moisture so that it became hard and in some cases a small amount of charring was observed. As the power of the microwave oven increased this effect occurred at shorter times. For the reactions performed at 255 W the reaction mixture had a dry appearance at 6 minutes and appeared to be completely dry at 8 minutes. For the reactions performed at 425 W the reaction mixture started to dry out at three minutes and at 595 W the sample appeared to be completely dry, with some charring evident, after only two minutes.

None of the ten higher powered reactions obtained a comparable DS to the conventional heating reaction. Of these reactions MW 15, performed at 425 W for three minutes provided the best DS of 0.63 and a resulting reaction efficiency of 52.50%. It is felt that these reactions probably required longer reaction times but due to the loss of moisture this could not be done. This is consistent with the observations made by Koroskenyi & McCarthy, (2002), where they found that the loss of solvent during the microwave reaction prohibited long reaction times and therefore resulted in lower DS values.

The change in the reaction procedure was therefore not found to be positive. The best results were obtained with the original procedure and the most successful reaction was MW 07 where a DS of 0.71 was achieved at a power setting of 85 W and a reaction time of 20 minutes. It is felt that this reaction procedure was more successful because the larger reaction volume allowed more moisture to be retained in the reaction mixture, the lower power setting of the microwave also contributed to the moisture retention.

7.4 Conclusions

It can therefore be concluded that the retention of moisture during the microwave heating of the etherification is critical for the completion of the etherification reaction. Under reflux conditions, where moisture levels are maintained, the reaction mixture needs to be agitated so that water returning to the system is evenly distributed through the product and does not form gel-like lumps which compromise the quality of the final product. It was shown that the use of microwave heating can improve the energy efficiency as well as the reaction efficiency of the dry/aqueous production of CMC.

8 THE APPLICATION OF GREEN CHEMISTRY TO THE PRODUCTION OF CMC

8.1 Background

The core principal of 'green chemistry' is to protect the environment by developing new chemistry and chemical processes that minimise potential pollution (Anastas. & Warner, 1998). There are twelve core principles which can be used to evaluate the greenness of a process, these were discussed in Chapter 1 and are summarised in Figure 8-1 below. It is unlikely that any chemical process will satisfy all the green chemistry principles but the more it satisfies the greener the overall process will be (Polshettiwar & Varma, 2010).

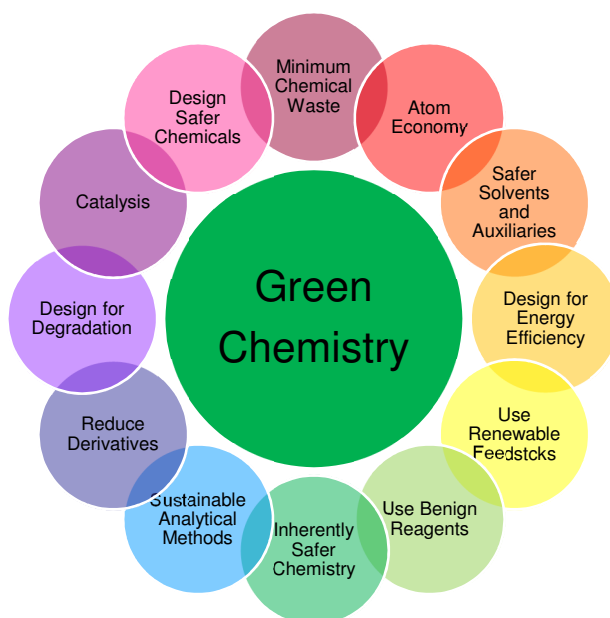


Figure 8-1 Core Principles of Green Chemistry

If the CMC process is considered in relation to the green chemistry principals then it scores well for at least two of the principals, the use of renewable feedstocks and the design for degradation. The starting material cellulose, is one of the principal components of plant cell walls and as such, it is considered to be an almost inexhaustible raw material with a total production of 1.5×10^{12} tons per year (Klemm, et al., 2005). The final product, CMC, is non-toxic and readily biodegradable by a consortia of microorganisms and represents a negligible environmental risk (van Grinkel & Gayton, 1996).

Stigsson, et al. (2001), identified that the main environmental impacts of the solvent slurry process for the production of CMC are the evaporation of alcohol during the production process and the generation of waste water. For the production of purified grade CMC's large volumes of alcohol are used not only during the reaction, but also during the washing process. Isopropyl alcohol (IPA) is the predominant alcohol used during the reaction process as it has been found to offer the highest reaction efficiency, however, other solvents such as ethanol are also used commercially for economical reasons (Stigsson, et al., 2006). During the washing of CMC to produce the purified grades, ethanol and methanol are typically used because they offer more efficient washing of the final product than IPA (Stigsson, et al., 2001). The washing liquor needs to be recovered and reused for economical as well as environmental reasons and this is typically performed by means of distillation, where the water and salts which are removed are treated separately (Stigsson, et al., 2001). Replacing toxic, volatile and highly flammable solvents with a benign alternatives is one of the best ways to make a process greener (Polshettiwar & Varma, 2010). But how does one measure how "green" a solvent is?

Capello, et al. (2007) proposed a framework to evaluate solvents which looked at aspects of environmental performance as well as important health and safety issues (EHS assessment) in combination with a life-cycle assessment (LCA). The EHS assessment looks at identifying possible hazards associated with the use of a particular solvent, for example organic solvents can be highly flammable, explosive, toxic and persistent in the environment. There are nine categories by which the solvents are evaluated:

- Safety hazards: release potential, fire/explosion and reaction/decomposition
- Health hazards: acute toxicity, irritation and chronic toxicity
- Environmental hazards: persistency, air hazard and water hazard

For each effect an index between zero and one is calculated, this results in an overall score of between zero and nine for each solvent (Capello, et al., 2007).

Using Capello, *et al's* methodology Connelly (2015) completed a comparative EHS investigation on methanol, ethanol and IPA (amongst others). His findings are shown in Figure 8-2. All three of these chemicals are considered to be highly flammable with flash points between 12 and 17°C and volatile, for this reason they are given very high scores in terms of safety.

For health effects ethanol was found to be the least harmful although it does have a level of chronic toxicity, it is much less so than methanol. IPA was determined to be more harmful because of its irritant properties, however, it is far less toxic than methanol. In terms of environmental impacts ethanol and IPA scored more poorly than methanol. Connelly’s final conclusion was that ethanol was best of the three solvents with the lowest EHS score however it does not negate its negatives in terms of environmental impact. To put it into perspective, if water was rated on the same system it would have a score of zero.

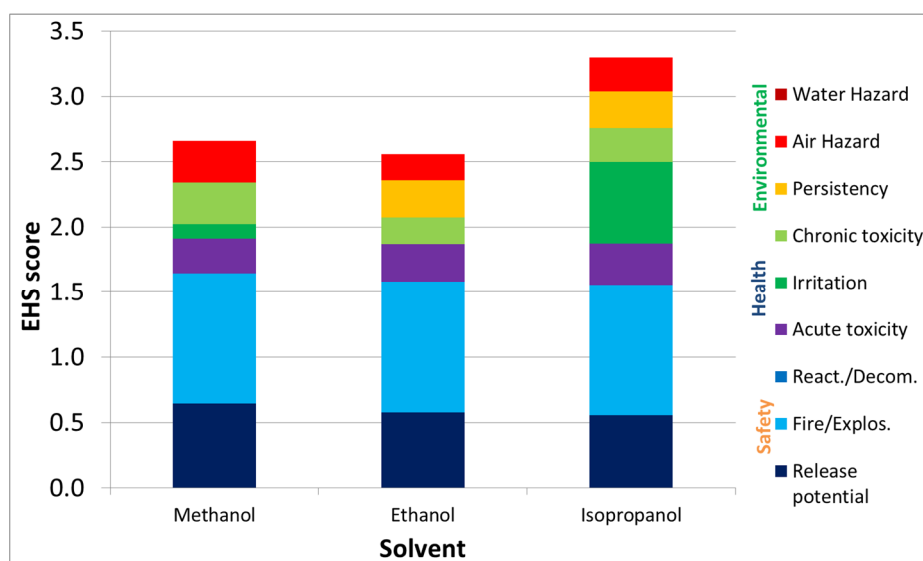


Figure 8-2 EHS scores for Methanol, Ethanol and IPA adapted from Connelly (2015)

The use of solvents is also associated with a number of indirect environmental impacts such as non-renewable resource depletion, air emissions due to solvent incineration or high energy requirements for solvent recovery, to quantify these impacts a LCA can be used (Capello, et al., 2007). A LCA provides a systematic way to evaluate environmental performance based on potential impacts from all stages of the product life cycle, it includes manufacture, product use and end-of-life management (von Blottnitz & Curran, 2007). Figure 8-3 illustrates the LCA methodology.

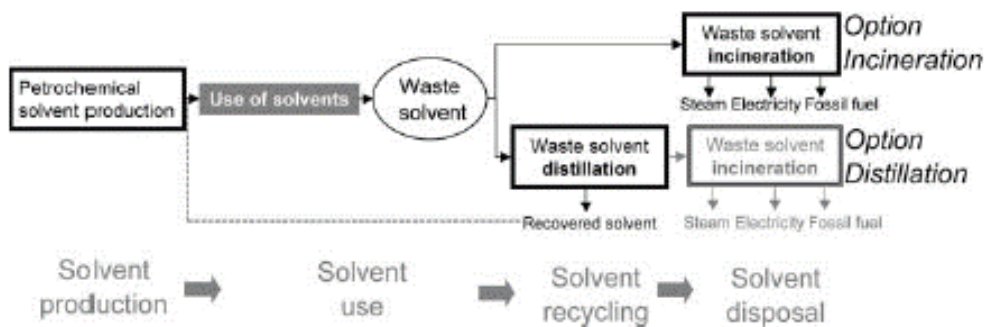


Figure 8-3 System model used for the life-cycle assessment method (Capello, et al., 2007)

In a LCA conducted by Capello, et al. (2007) it was found that ethanol and methanol had very similar scores with ethanol scoring only slightly better than methanol, as was found in the EHS assessment, IPA was again some what worse off. When the scores of the EHS and LCA were combined ethanol and methanol were two of the lowest scoring solvents as shown in Figure 8-4 (Capello, et al., 2007).

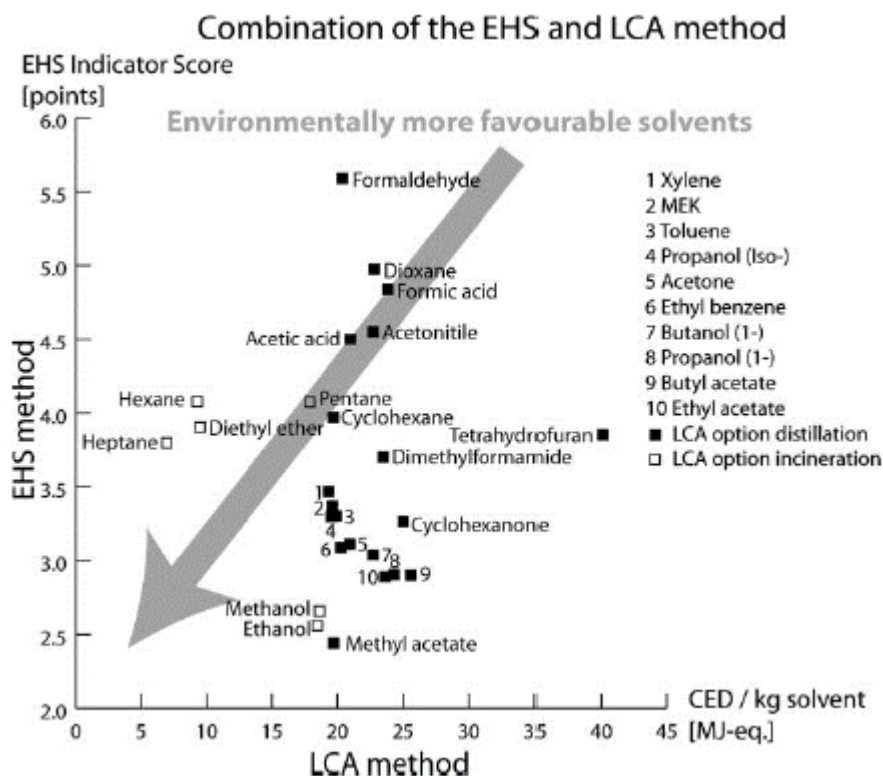


Figure 8-4 Combination of EHS and LCA method outcomes for the environmental assessment of 26 organic solvents (Capello, et al., 2007)

One downfall of some LCA studies is that they do not take full account of solvents produced from a bio-based origin (Byrne, et al., 2016). Ethanol, for example, is already produced at a commercial scale almost exclusively from biomass feed stocks as a fuel additive to reduce exhaust greenhouse gas emissions (Balat & Balat, 2009). Currently ethanol is considered to be a first-generation biofuel as its production is almost entirely dependent on existing food crops such as corn (USA, China and Canada), wheat (China, Europe and Canada), sugar beet (Europe) and sugar cane (Brazil) (Balat & Balat, 2009; Nigam & Singh, 2011). This may seem beneficial but the drawback of depending on starch and sugars from existing food crops is that they are expensive, due to competition with food supplies, and also raise environmental concerns about destruction of vital soil resources (Balat & Balat, 2009; Nigam & Singh, 2011). In fact several LCA studies indicated that, due to the acidification, human toxicity and ecological toxicity impacts which occur during the harvesting and processing of the agricultural crops, the results were often unfavourable for bio-ethanol (von Blottnitz & Curran, 2007). Therefore sustainability of bio-based solvents is dependent on the nature of the feed stocks and this drives the search for non-edible biomass sources (Nigam & Singh, 2011). As ethanol can also be generated from waste biomass this offers the opportunity for it to become a second generation biofuel in the future.

Solvents like methanol can also be produced commercially from biomass, but this is currently not the primary feedstock while IPA is also highly feasible for bio-based production but is not currently produced at a commercial scale (Byrne, et al., 2016).

A considerable amount of research has been conducted into the use of unconventional solvents that offer a reduced environmental impact, these include supercritical fluids, ionic liquids, flurous solvents, deep eutectic solvents, biomass derived solvents as well as solvent-free systems (Farran, et al., 2015). However these alternative solvents are only of value if they can be successfully used at an industrial level (Polshettiwar & Varma, 2010) and their relative “greenness” is also a topic of some debate (Dallinger & Kappe, 2007).

Water as an alternative solvent for organic synthesis has received a lot of attention of late (Dallinger & Kappe, 2007; Polshettiwar & Varma, 2010; Farran, et al., 2015) and for the production of CMC it offers a lot of potential. It is in fact difficult to conceive any greener solvent than water. Water is the most abundantly available liquid solvent as it constitutes almost 70% of the earth's surface, it is also non-toxic, non-corrosive and non-flammable as well as environmentally benign (Dallinger & Kappe, 2007; Polshettiwar & Varma, 2010).

Although the use of large quantities of solvents results in a significant environmental impact for the solvent slurry process, it does however offer substantial benefits in terms of the atom economy and energy efficiency of the solvent slurry process. The use of an organic solvent improves the reaction efficiency in a number of ways, firstly it promotes the homogeneous mixing of the reactants which results in a more uniform reaction (Branan, 1953; Ambjornsson, et al., 2013), it therefore removes the necessity of using excessive amounts of water to distribute the reactants. The presence of large quantities of water during the reaction is known to be detrimental to the reaction efficiency as it promotes the hydrolysis of the MCA to glycolic acid or its sodium salt (Branan, 1953). Control of the water content during the reaction is therefore important for promoting reaction efficiency (Stigsson, et al., 2001) and is the second way in which the use of an alcoholic medium promotes the atom economy of the carboxymethylation reaction.

The third mechanism by which the organic medium promotes the atom economy of the process is by creating an environment which promotes the substitution reaction over the formation of the sodium glycolate, this has been shown to be dependant on the polarity of the solvent and its affinity for the NaOH (Klemm, et al., 2001b). When the organic solvent used is IPA a two phase system occurs where the NaOH will be predominantly in the water phase, due to its low solubility in non-polar solvents (Almlöf, 2010), but the MCA will occur predominantly in the solvent phase which reduces the probability of side reactions occurring. If the solvent used is ethanol then a homogeneous system occurs where all the reactants are present in the aqueous co-solvent system (Stigsson, et al., 2006). IPA is therefore considered to be the better solvent system (Olaru & Olaru, 1992).

The energy efficiency of the solvent slurry process also represents a two edged sword. On the one hand the use of the solvent during the mercerisation and etherification reaction assists with heat transfer during the reaction, allowing for better control of the reaction temperature and exotherms. These then in turn impact on the reaction efficiency and therefore the overall atom economy of the process. On the other hand the recovery and recycling of the solvent then requires an energy intensive distillation process.

Based on these discussions it can therefore be seen that when considering the production of CMC there are aspects both for and against the solvent slurry process from a “green chemistry” perspective. One of the key objectives of this investigation was to look at the use of water as an alternative, more benign solvent for the industrial production of CMC based on the the historical dry/aqueous process. The atom economy of this process was its biggest downfall, in order to achieve homogeneous reactions excessive amounts of both NaOH and SMCA/MCA were used in order to obtain water soluble products (Branan, 1953; Grassie & Wallis, 1954). Controlling the water content of the reaction was also very difficult as it was required to ensure the homogeneous mixing of the other reactants (Stigsson, et al., 2001). The quality of the CMC products produced via this route varied considerably in terms of DS, solubility and viscosity (Hodge, et al., 1953) and were considered to be inferior (Cordrey, et al., 1963). The challenge which was faced when evaluating water as a industrially sustainable alternative to a solvent slurry process was, therefore, to overcome the poor atom economy and product quality concerns of the historical dry/aqueous process.

From an energy efficiency point of view, the low liquid content of the dry/aqueous process may make controlling the temperature during the reaction more difficult and therefore may require larger heating and cooling capacity in order to control the reaction temperatures effectively. This may have a negative impact on the energy efficiency of the process so alternatives such as microwave radiation would need to be considered.

8.2 Objectives and Approach

The overall objective of this study was to evaluate water as an alternative solvent for the production of technical grade CMC on an industrial scale, with the aim of reducing the environmental impact of this process by eliminating the requirement for large quantities of solvent. The approach which was taken was to optimise different aspects of the historical dry/aqueous procedure in order to improve its atom economy and reproducibility as well as the consistency and quality of the final products.

In regards to the energy efficiency of the process the use of an alternative heating source in the form of microwave radiation was investigated. Although this technology is not currently implementable at an industrial scale, it was felt that an assessment of its applicability to this type of “dry” reaction would be beneficial in establishing its merit going forward.

In this Chapter the results of the optimisation investigations will be summarised and the optimised dry/aqueous process will be compared to the traditional slurry process as well as evaluated against the historical process in terms of reaction efficiencies and overall product quality. The improved process will also be evaluated from a green chemistry perspective and final conclusions will be drawn about the success of the project.

8.3 Results and Discussion

In order to be able to evaluate the optimised dry/aqueous process which has been developed for the production of CMC's, from both a green chemistry and a product quality perspective, it is necessary to establish a baseline against which to measure it. The optimised process therefore needs to be compared to both the current industrial standard, which is the solvent slurry process, and the historical dry/aqueous process. For the historical process information has been drawn from patents to establish this baseline, while for the solvent slurry process reactions were performed at a laboratory scale (methods are shown in Chapter 2) using published methods for direct comparison.

Several patents were selected which, used various methods for the aqueous production of technical grade CMC's, for evaluation of the historical dry/aqueous process. As can be seen from Table 8-1 these included the use of aqueous solutions of MCA, SMCA powder and MCA powder as the etherification reagent, the reaction conditions also varied considerably. The results published by Triggs (1949), seem to suggest that relatively high reaction efficiencies were achieved, however it should be noted that the moisture content of the cellulose was not taken into account when these were calculated by the author. Assuming a moisture content of 5.5% (which is a typical average for cellulose) these reaction efficiencies would decrease to 63.59% and 60.10% for the MCA aqueous and SMCA powder reactions respectively. The % insoluble content for these products is reported to be 8.4% and therefore illustrative of the poor quality of these types of products. Some of the other examples mentioned in this particular patent reported insoluble contents of up to 12% (Triggs, 1949).

Table 8-1 Comparative reaction efficiencies for solvent slurry and aqueous CMC production

	Process Description	Theoretical DS	Achieved DS	Reaction Efficiency (%)	Insoluble Material (%)
CMC_{Aqu1}^a	Aqueous (Optimised)	0.75	0.56	74.8	1.92
CMC_{Aqu2}^{a, b}	Aqueous (Optimised)	1.19	0.77	64.7	0.41
CMC_{Aqu3}^a	Aqueous (Optimised)	1.40	0.87	62.0	0.32
Triggs (1949)	Aqueous (MCA Liquid)	1.07	0.72	67.3 ^c	8.4
	Aqueous (SMCA Powder)	1.13	0.72	63.6 ^c	8.4
Branan (1953)	Aqueous (MCA Powder)	0.83	0.50	60.1	not stated
Branan (1954)	Aqueous (MCA Powder)	0.83	0.54	65.1	not stated
	Aqueous (MCA Powder)	1.10	0.71	64.6	not stated
	Aqueous (MCA Powder)	1.40	0.78	55.7	not stated
CMC_{Solvent}^d	Solvent Slurry (IPA)	0.99	0.76	76.8	1.05
Stigsson (2006)	Solvent Slurry (IPA)	1.30	0.99	76.2	not stated

^a *This study optimised pilot scale reaction*

^b *This study pilot scale reaction as reported in Chapter 6*

^c *moisture of the cellulose was not taken into account in the efficiency calculation by Triggs (1949) and hence the efficiency is an overestimate*

^d *This study lab scale solvent slurry reaction*

Branan published two patents in the early 1950's which outlined a process utilising powdered cellulose, reduced quantities of NaOH at a concentration of 35% and a

two stage addition of MCA (Branan, 1953; Branan, 1954). In his 1954 patent Branan discusses the use of temperature control to control the uniformity of the substituent distribution and limit the side reaction by maintaining the temperature below 30°C. Of the historical processes this is the one which is most similar to our current optimised dry/aqueous process. The highest reaction efficiency reported by Branan was 65.1%, for a CMC product with a DS of 0.54. As the theoretical DS of the CMC increases the reaction efficiency decreases so that for the highest DS product the reaction efficiency is only 55.7%. In the patent Branan describes the solubility of the CMC as being “essentially completely soluble” but, unfortunately, provides no actual figures (Branan, 1954).

How then does this compare to the optimised dry/aqueous process which has been developed in the present study?

The theoretical DS which was used as a standard throughout this investigation was 1.19. The highest DS achieved during the investigation of 0.77 (Chapter 6, CMC₂₈), and as can be seen from Table 8-1 this equates to a reaction efficiency of 64.7%. This is equivalent to the reaction efficiency of Branan’s CMC with a DS of 0.71. This result seemed to indicate that the optimisation process which had been undertaken had not been able to significantly improve upon the overall reaction efficiency of the historical dry/aqueous process. It was, however, noted from Branan’s results that the reaction efficiency decreased with increasing theoretical DS.

A comparative range of CMC’s with higher and lower DS respectively were then prepared using the developed optimised dry/aqueous process. Using the a theoratial DS of 1.40, the same as was used to produce the DS 0.78 CMC product in Branan’s 1954 Patent, resulted in a DS of 0.87 for CMC_{Aqu3} which equates to a reaction efficiency of 62.0%. This is a 6.3% increase in reaction efficiency. An even greater increase in the reacion efficiency was achieved for the low DS product, CMC_{Aqu1}, which had a DS of 0.56 and a reaction efficiency of 74.8%. This represented an increase of 9.7% in reaction efficiency from the historical dry/aqueous process.

The quality of the final product for the dry/aqueous CMC products has also been improved significantly. Where Triggs (1949) had reported an insoluble content of 8.4% for a CMC with a DS of 0.72 the product produced with the optimised dry/aqueous process, CMC_{AQU2} , with an equivalent DS of 0.77 was found to have an insoluble content of 0.41%. Unfortunately Branan (1954) did not publish the insoluble content of his products for comparison. The lower DS product CMC_{AQU1} has a higher insoluble content of 1.92% which is also significantly lower than what Triggs (1949) reported. CMC_{AQU2} and CMC_{AQU3} had solutions which were clear to the naked eye with no particulate matter and their relative insoluble contents are equivalent to what would be expected for a commercial CMC product produced via the solvent slurry process.

Also shown in Table 8-1 are the results for the lab scale solvent slurry reaction which was performed. $CMC_{solvent}$ had a DS of 0.76 which equated to a reaction efficiency of 76.8%. This result was verified by comparing it to the results published by Stigsson, et al. (2006), who used a similar methodology for performing their solvent slurry work and achieved a reaction efficiency of 76.2%, although the DS achieved was higher. Analysis of the insoluble content of $CMC_{solvent}$ was found to 1.05% which was higher than anticipated, typical commercially available CMC products which are produced via the solvent slurry process and have a similar DS are reported to have an insoluble content of 0.1%.

The reaction efficiencies for the various reactions are shown graphically in Figure 8-5.

It is uncertain why the reaction efficiency for the products with a DS of 0.7 is similar for both the optimised and historical process, but improvements have definitely been achieved for the lower and higher DS regions. Overall the efficiency curve for the optimised dry/aqueous process is higher relative to that of the historical process. The efficiency of the solvent slurry process is however only approached for the lower end of the DS range, where the use of a more stoichiometric ratio of reactants is possible.

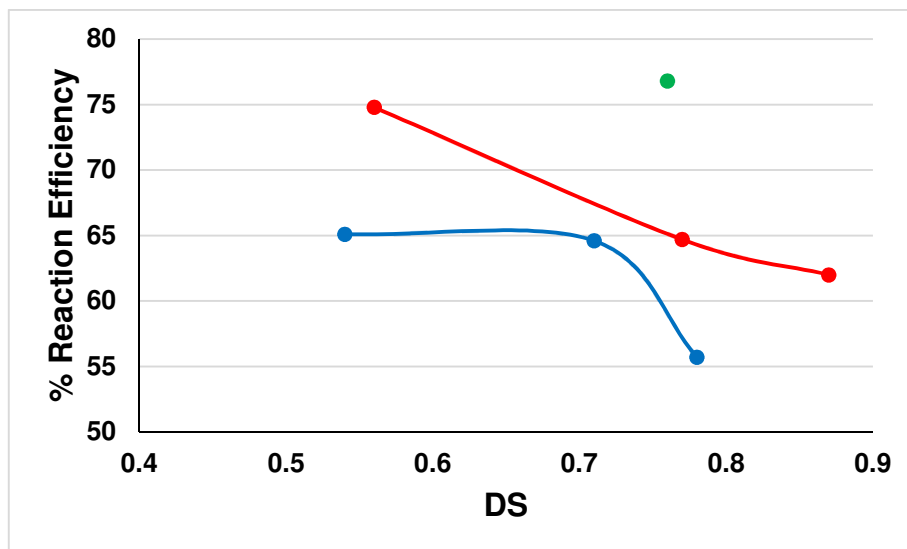


Figure 8-5 Plot Showing the Relative Reaction Efficiencies of the Optimised Dry/aqueous Process (-) relative to the Historical Dry/aqueous Process (-) and the Solvent Slurry Process (•)

On the negative side at the low DS the quality of the product is not as good as the higher DS products, most likely due to limitations in the homogeneous mixing of the reactants. The higher DS products, produced with the optimised dry/aqueous process, had excellent solution clarities and low % insoluble content and were found to be equivalent to CMC's produced by means of the solvent slurry process.

8.4 Conclusions

When considering the results of this investigation in relation to the green chemistry objectives, the reaction efficiency and, therefore, the atom economy of the historical dry/aqueous process has been improved. Although the efficiency achieved does not yet match that of the solvent slurry process the gap has been closed considerably. The overall quality of the product has been significantly improved and has been found to be equivalent to the solvent produced CMC's for the higher DS products. These results have been found to be reproducible over the course of the investigation, and it is therefore felt that the dry/aqueous process is in fact a viable alternative for the industrial production of technical grade CMC's.

9 DETERMINING THE DISTRIBUTION OF SUBSTITUTION OF CMC USING SEC-MALS ANALYSIS: A SIMPLIFIED ANALYSIS FOR APPLICATION IN INDUSTRY

9.1 Background

The distribution of substituents can be described on several different structural levels as shown in Figure 9-1. At a monomer level it refers to the number of substituents and position that those substituents occupy within the anhydroglucose unit (Richardson & Gorton, 2003). At a polymer chain level it refers to how the substituents are distributed along the polymer backbone (Adden, 2009). The distribution can also be described in regards to the crystalline and amorphous regions as well as the surface and interior of the cellulose fibre (Richardson & Gorton, 2003).

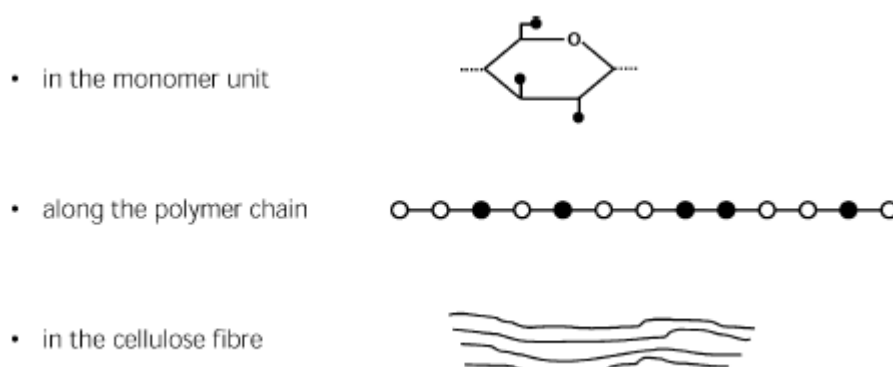


Figure 9-1 Distribution of substituents in CMC on different structural levels
(Richardson & Gorton, 2003)

The distribution of substitution at a monomer level is most commonly used for the determination of relative rate constants for the carboxymethylation reaction (Adden, 2009). The most commonly used analytical methods for determining this type of distribution are NMR spectroscopy (Baar, et al., 1994), GC/MS, HPLC and high pH anion exchange chromatography with pulsed amperometric detection (HPAEC-PAD); a prerequisite for all these methods is the complete degradation of the CMC to its monomer units (Richardson & Gorton, 2003). Adden (2009) proposed seven possible substitution patterns at the monomer level as shown in Figure 9-2.

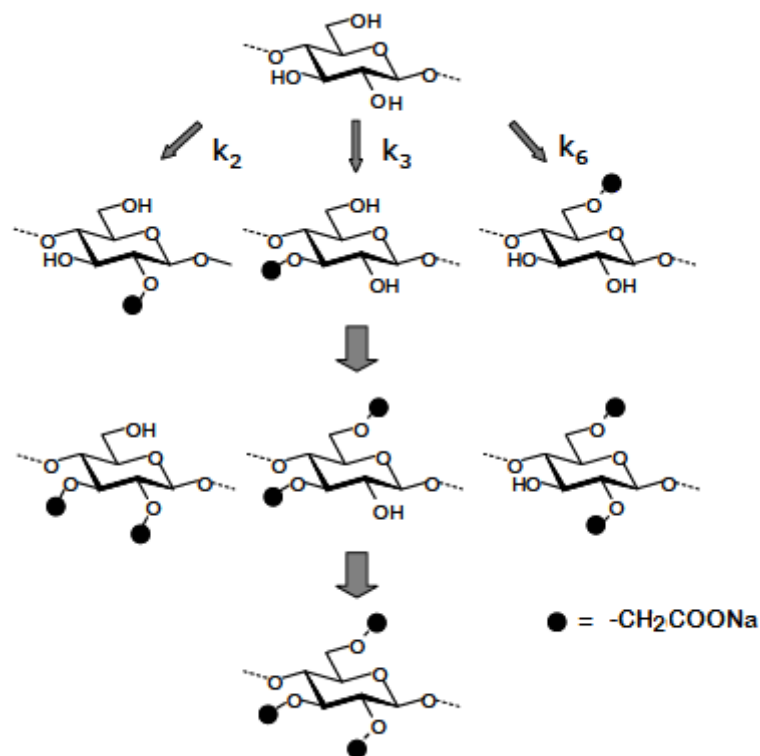


Figure 9-2 Possible distribution of substituents at a monomer level (Adden, 2009)

Determining the distribution of substituent groups along the cellulose backbone is one of the most challenging aspects of characterising CMC's (Richardson & Gorton, 2003; Enebro, et al., 2007; Adden, 2009; Li, et al., 2010) and has proven to be more difficult than determining the distribution at a monomer level (Richardson & Gorton, 2003). It has been recognised for many years that the uniformity of the substituents along the polymer chain as well as at a fibre level have a great influence on a number of the characteristics of the final CMC such as solubility, shear stability and rheological behaviour (Elliot & Ganz, 1974; Feddersen & Thorp, 1993; Cheng, et al., 1998) to name but a few.

The substituent distribution along the polymer chain is determined by the accessibility of the AUGs during the carboxymethylation reaction (Richardson & Gorton, 2003; Adden, 2009), as discussed in Section 1.3.4. The different substitution possibilities are shown in Figure 9-3, for a homogenous reaction system would result in a random distribution while for a heterogeneous system a heterogeneous or block like pattern would be expected (Adden, 2009).

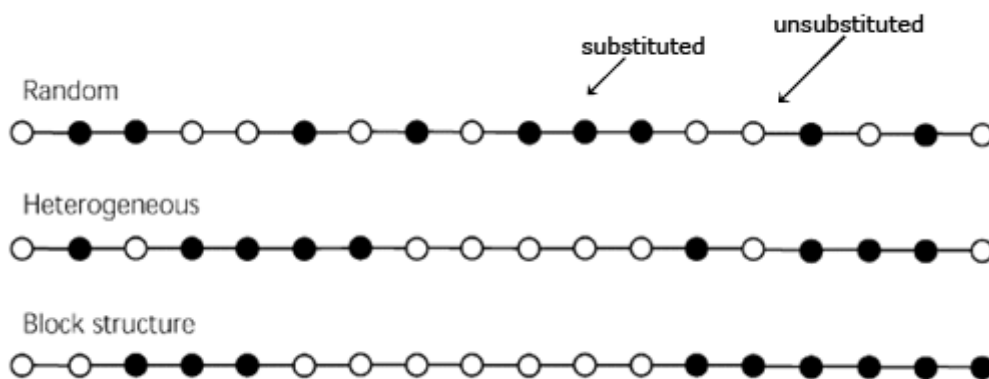


Figure 9-3 Possible Distribution of Substituents at a Polymer Chain Level
(Richardson & Gorton, 2003)

Methods employed for the determination of distribution of substitution along the polymer chain usually entail three key steps (Richardson & Gorton, 2003). Firstly the partial hydrolysis of the CMC which can be performed either randomly, by chemical means, or selectively by the use of enzymes (Cheng, et al., 1998). Secondly the hydrolysis products need to be characterised by using techniques such as MS (Enebro, et al., 2007), HPAEC-PAD (Stigsson, et al., 2006) or SEC-MALS (Rinaudo, et al., 1993; Richardson, et al., 2002; Enebro, et al., 2007; Li, et al., 2010). Finally the experimental data needs to be interpreted, either by comparing it to the unmodified polymer or by comparing it with a calculated statistical pattern (Richardson & Gorton, 2003).

A problem with a number of the methods reviewed was that they are very complex and time consuming to perform, interpretation of the experimental data is also often complex and standards with known structures, to allow accurate interpretation of results, are not readily available. For an industrial application most of these methods would therefore not be feasible. One method, which was of interest, utilises a combination of selective enzyme hydrolysis with characterisation of the hydrolysed product by means of SEC-MALS.

Richardson, et al. (2002), employed this technique for the characterisation of ethyl(hydroxyethyl) cellulose (EHEC). Two different endoglucanases from *Trichoderma reesei* were used to hydrolyse two different samples of EHEC, the hydrolysis products were then analysed by means of SEC-MALS. It was found that the Mw of the EHEC samples was reduced to differing degrees by the enzyme treatment.

The amount of glucose released from the enzyme hydrolysis was determined by HPAEC-PAD and indicated that one of the polymers had a more uniform distribution of substituents than the other (Richardson, et al., 2002).

This same technique was also employed by Enebro, et al. (2007) to characterise the substituent distribution in CMC and relate these differences to changes in rheological properties. Enebro et al.'s (2007) investigation found that changes in the Mw of the CMC before and after enzyme hydrolysis could be related to differences in the distribution of substituents and this could also be related to changes in the rheological behaviour of the CMC. It was concluded that CMC which showed the least change in Mw after enzyme treatment had the more blocky distribution and this resulted in a higher viscosity in the linear viscoelastic region (Enebro, et al., 2007).

The concern with both the studies of Richardson, et al. (2002) and Enebro, et al. (2007) was that a second technique was required to analyze the hydrolytes for the presence of glucose and, cellotetraose and cellopentaose, respectively to allow for the interpretation of the SEC-MALS results. This, again, adds to the complexity of the the method and makes it difficult to use in an industrial application, however, because the SEC-MALS is already used to characterise the molecular weight characteristics of the CMC this method remains appealing.

Stigsson, et al. (2004) recommended the use of the viscosity hysteresis behaviour of a CMC as a rapid analytical technique more suited to industrial application. The hysteresis loop method proposed by Green (1949) and later adapted for aqueous CMC solutions (deButts, et al., 1957) involves the use of a viscometer which can rapidly change the rate of rotation in known increments.

The stresses and shear rate readings are recorded as the shear rate first gradually increases and then as it decreases, this allows a rheogram to be plotted (Ghannam & Esmail, 1997). For pseudoplastic behaviour the up-and-down curves coincide whereas for thixotropic behaviour these two curves diverge to form a hysteresis loop (deButts, et al., 1957). The degree of thixotropy is estimated from the area between the up and down curves (Triantafillopoulos, 1988) and the larger this area is the stronger the thixotropic properties are considered to be (Benchabane & Bekkour, 2008).

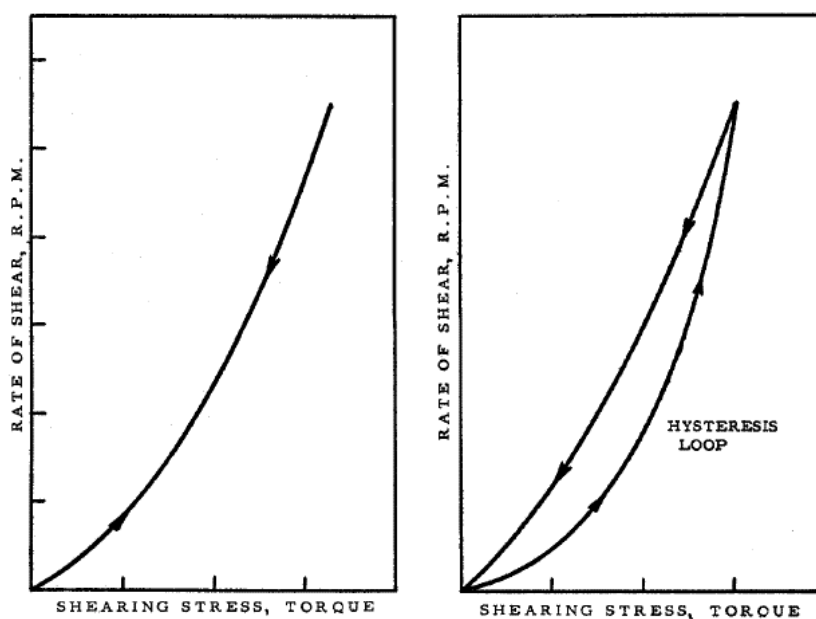


Figure 9-4 Rheogram of pseudo plastic CMC solution behaviour on the left and thixotropic behaviour on the right (deButts, et al., 1957)

Thixotropy is defined as a fluid which decreases in viscosity with time when a constant shear rate is applied (Ametek Brookfield, 2017). Therefore an alternative method for evaluating the thixotropy of a solution is to apply a constant shear rate and to measure the decrease in viscosity as a function of time until an equilibrium value is reached (Barnes, 1997; Benchabane & Bekkour, 2008).

The thixotropic behaviour of CMC solutions is thought to result from the presence of unsubstituted crystalline residues in the CMC (deButts, et al., 1957). A number of investigations have shown that solutions of uniformly substituted CMC showed less thixotropic behaviour than their less evenly substituted counterparts (deButts, et al., 1957; Francis, 1961; Elliot & Ganz, 1974; Li, et al., 2010).

It is known that unsubstituted glucose residues, and segments thereof, can form associations in solution by intermolecular interactions as shown in Figure 9-5. According to Enebro, et al. (2007) and Li, et al. (2010) this results in an increase in the apparent viscosity of the unevenly substituted CMC products.

This type of behaviour has been shown to indicate increased blockiness in CMC products and therefore less homogeneous reaction conditions (Liebert & Heinze, 2001; Enebro, et al., 2007; Li, et al., 2010).

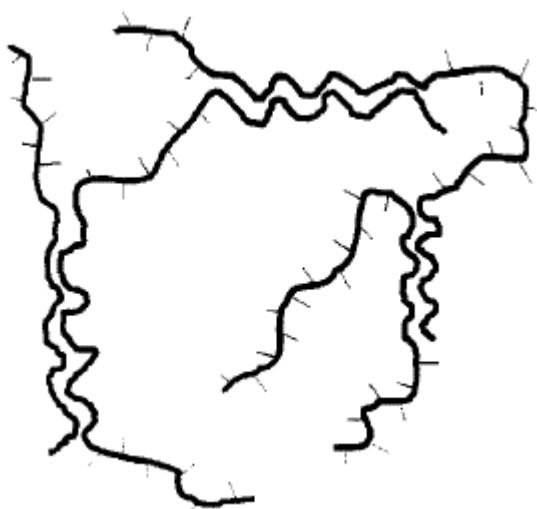


Figure 9-5 Schematic representation of the intermolecular interactions which can occur between unsubstituted areas of the CMC (Liebert & Heinze, 2001)

There is therefore a well-documented link between the thixotropic behaviour of CMC solutions and the distribution of substituents along the polymer chain. It is therefore proposed that the degree of thixotropic behaviour can be used as an indicative measure of the distribution of substitution for the CMC products and this can therefore, in turn, be used to establish whether the changes observed in the conformation in solution of the CMC's can be related back to their distribution of substitution.

9.2 Objectives and Approach

The objective of this investigation was to determine if the slope of the conformational plot could be used as an indication of the distribution of substituents along the cellulose backbone for CMC. The hysteresis loop analysis for several CMC products was compared to the slopes of the conformational plots of these products to determine if there was a correlation between the results.

Solution strengths of 1 to 3% were tested and the hysteresis loop analysis conducted using a one-cycle, up and down curve, for shear rates between 10-1000 s^{-1} . A 3% solution was found to provide the best thixotropic response however, in some cases, a solution strength of 1% needed to be used due to viscosity properties of the samples.

The experimental methods used are outlined in Chapter 2.

9.3 Results and Discussion

It was shown by Ghannam & Esmail (1997) and Edali et al. (2001) that the thixotropic behavior of CMC solutions increases with increasing solution strength. To establish a baseline for the hysteresis analysis and to confirm the effect of concentration a study was performed using CMC_{Aqu2}, which has a DS of 0.77 and was produced using the optimised dry/aqueous reaction conditions (Table 8-1). Solutions with concentrations of 1, 2 and 3% by weight, were prepared and hysteresis loop analysis performed for shear rates of 10 – 1000 s^{-1} . The results for this investigation are shown in Figure 9-6 and confirm the findings of Ghannam & Esmail (1997) and Edali et al. (2001).

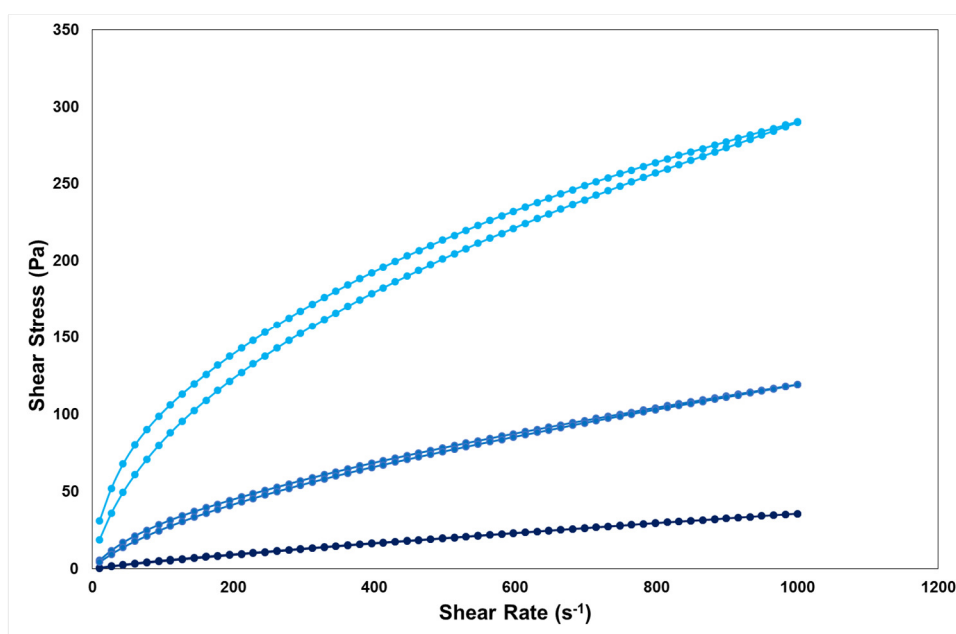


Figure 9-6 Hysteresis loop response for CMC_{Aqu2} at solution concentrations of 1% (—●—), 2% (—■—) and 3% (—▲—) solutions.

The area of the hysteresis loop increases as the solution strength increases. The results for the 1% and 2% solutions show very little thixotropic behaviour as the up and down curves very nearly overlay the 3% solution, however, shows a more significant thixotropic response. The calculated hysteresis area for these curves is 209 Pa/s, 2184 Pa/s and 11282 Pa/s for the 1%, 2% and 3% solutions respectively.

The 3% solution would therefore be the solution of choice for these studies however it was found that due to the viscosity characteristics of the some of the samples the hysteresis loops could not be obtained at 2% and 3%. The studies were therefore conducted at a solution strength of 1% and where possible at 3%.

In order to first confirm the correlation between the hysteresis loop area and the distribution of substituents along the polymer chain hysteresis loop tests were conducted for 1% solutions of CMC_{Aqu1} , CMC_{Aqu2} and CMC_{Aqu3} . The products have DS's of 0.56, 0.77 and 0.87 respectively and have all been produced using the optimised dry/aqueous process (Table 8-1). The reason for using this particular range of products is because CMC's with a higher DS are inherently more uniformly substituted than those with a lower DS (Elliot & Ganz, 1974). It is therefore expected that these products will show an increased thixotropic area as the DS decreases. The results of the initial study performed at a solution concentration of 1% are shown in Figure 9-7 below. From this it would appear that the two higher DS products CMC_{Aqu2} and CMC_{Aqu3} display negligible thixotropy in relation to the lower DS product, CMC_{Aqu1} .

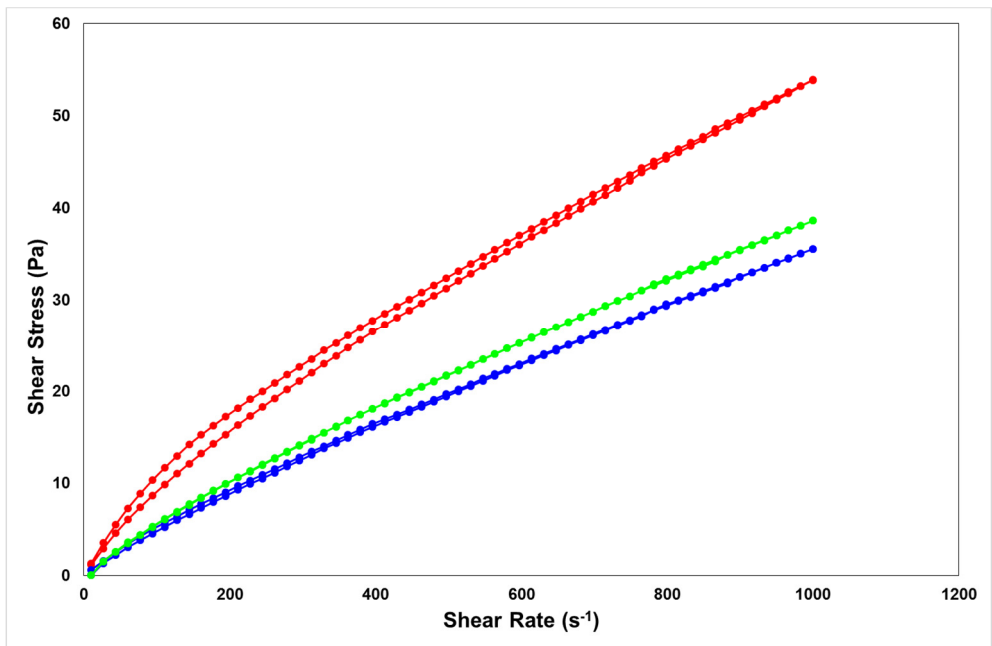


Figure 9-7 Hysteresis loops for CMC_{Aqu1} (—●—), CMC_{Aqu2} (—●—) and CMC_{Aqu3} (—●—) at a solution concentration of 1%

The hysteresis loops were repeated at a solution concentration of 3%, however, due to the high viscosity of the CMC_{Aqu1} solution results could not be obtained. The results for CMC_{Aqu2} and CMC_{Aqu3} are shown in Figure 9-8.

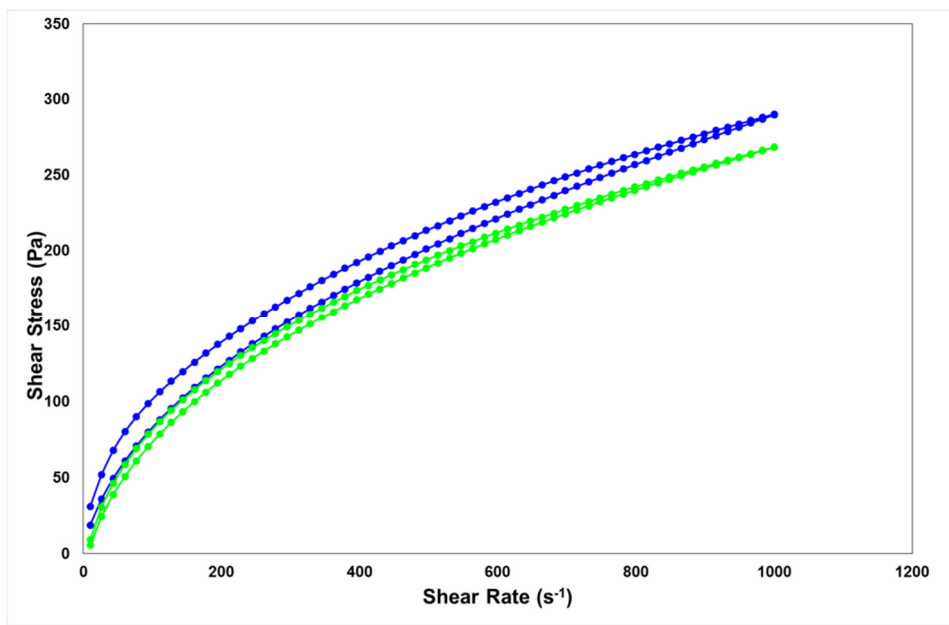


Figure 9-8 Hysteresis loops for CMC_{Aqu2} (—●—) and CMC_{Aqu3} (—●—) at a solution concentration of 3%

At the higher solution concentration both CMC_{Aqu2} and CMC_{Aqu3} display some thixotropic behaviour. The thixotropic area for CMC_{Aqu2} is larger than that of CMC_{Aqu3} indicating that it is more thixotropic. From these results it can, therefore, be said that the degree of thixotropy for these CMC products decreases as the DS of the products increases. This therefore confirms the statement made by Elliot & Ganz (1974) that as the degree of substitution increases the CMC becomes more uniformly substituted. The key now is to relate this further to the slope of the conformational plot and observe if the same trend holds true. Figure 9-9 shows the conformational plots for CMC_{Aqu1} , CMC_{Aqu2} and CMC_{Aqu3} .

A visual inspection of the conformational plots shown in Figure 9-9 highlights that the plot for CMC_{Aqu1} has a distinct inflection point, which is in of its self an indication that the polymer does not have an even distribution of substituents. The higher molecular weight region, above approximately 500k Da, has a slope similar to that of CMC_{Aqu2} but for the lower molecular weight region the slope is significantly lower. The plots for CMC_{Aqu2} and CMC_{Aqu3} are more linear.

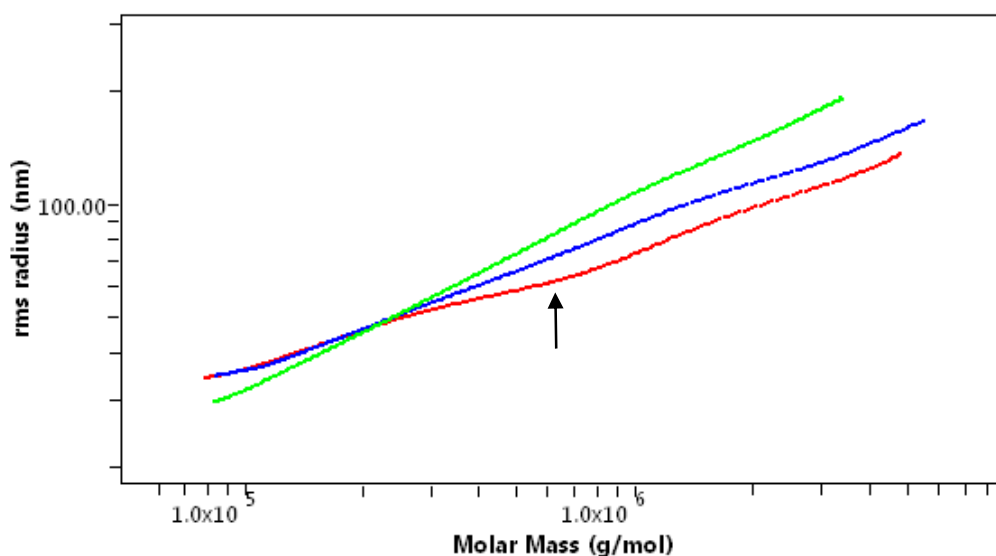


Figure 9-9 Conformational plot overlays for CMC_{Aqu1} (—), CMC_{Aqu2} (—) and CMC_{Aqu3} (—)

The average conformational plot slope for CMC_{Aqu1} , the lowest DS product, is 0.34 which is indicative of a compact sphere conformation in solution. CMC_{Aqu2} has a conformational plot slope of 0.38 which indicates that the conformation the polymer is assuming in solution is opening up and becoming more random coil like.

Finally the product which has the highest DS, CMC_{Aqu3} , is a random coil in solution with a conformational plot slope of 0.51. It can therefore be said that the slope of the plots increases as the DS of the CMC product increases.

To determine if there is any correlation of the results for the hysteresis loop study and conformational plot slopes these are summarised in Table 9-1. It can be seen that as the DS and conformational plot slope increases the thixotropic area, which is an indication of the distribution of substitution, decreases.

Table 9-1 Summary of results for CMC_{Aqu1} , CMC_{Aqu2} and CMC_{Aqu3}

Sample	DS	Conformational Plot Slope	Thixotropic Area ($Pa\ s^{-1}$)	
			1% Solution	3% Solution
CMC_{Aqu1}	0.56	0.34	1021	-
CMC_{Aqu2}	0.77	0.38	209	11282
CMC_{Aqu3}	0.87	0.51	13	4676

The thixotropic behaviour of CMC solutions is attributed to the disentanglement and re-entanglement processes which occur during shearing as well as the tendency of the polymers to align along the direction of shear (Benchabane & Bekkour, 2008). Unsubstituted segments of glucose residues along the CMC polymer chain form aggregates in solution by means of intermolecular interactions, as depicted in Figure 9-5. These areas are remnants of the original crystalline cellulose structure which hold these regions together by means of hydrogen bonding (deButts, et al., 1957). The entangled and overlapping coils act as cross-linking centres which are able to entrap other CMC chains resulting in the formation of superstructures in solution (Elliot & Ganz, 1974). When a solution of this nature is subjected to shear the superstructures are dispersed, this process occurs over a time interval, and on standing the superstructures will re-aggregate (deButts, et al., 1957). The increased thixotropy of a CMC with a low DS, in relation to a high DS product, is therefore expected because of the presence of larger regions of unsubstituted glucose which, results in a higher degree of aggregation and, in turn results in the increased formation of superstructures in solution (Elliot & Ganz, 1974).

In comparison to the solutions used for thixotropic studies SEC-MALS analysis employs dilute solutions where polymer molecules are more dispersed and polymer-solvent interactions prevail over polymer-polymer intermolecular interactions (Podzimek, 2011). This reduces the likelihood of the formation of superstructures in solution although chain aggregation will still be present. It is important to clarify that this aggregation does not occur in solution, it is a consequence of insufficient swelling of the cellulose that these regions maintain their crystallinity and therefore the polymer chains do not act independently.

The hypothesis would therefore be that the highly aggregated CMC chains would behave like highly branched polymers and would therefore result in a conformational slope equivalent to a sphere in solution. As the degree of aggregation decreased the polymers would behave more like long chain linear polymers (the substituent groups in this case would be too small to be classified as branches) and the conformation in solution would become more like a random coil. This concept is depicted in Figure 9-10.

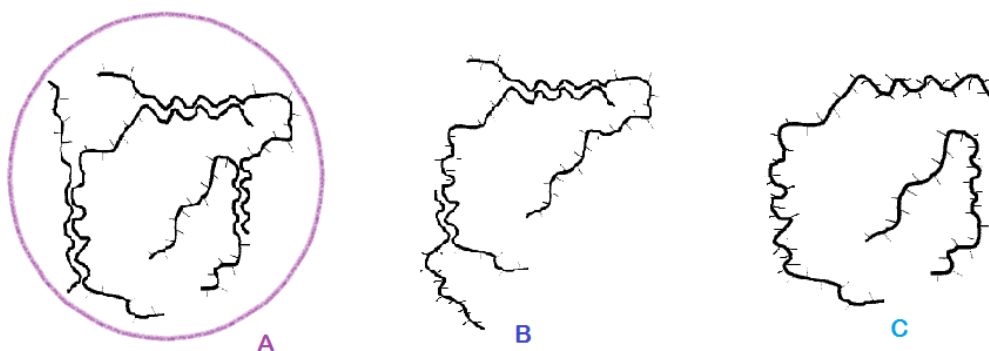


Figure 9-10 The change in conformation in solution relative to the change in chain aggregation resulting from unsubstituted segments of the CMC polymer. **A.** High degree of chain aggregation corresponding to a spherical conformation in solution. **B.** Reduced chain aggregation corresponding to non-expanded random coil conformation in solution. **C.** Low chain aggregation corresponding to expanded random coil conformation in solution.

To further confirm the correlation between the thixotropic area, distribution of substitution and the slope of the conformational plot the effect of the different solvent/reaction systems can be evaluated.

The solvent slurry process is a more homogeneous reaction system and it would therefore be expected that the product would have a more uniform distribution of substitution than the aqueous process equivalent. $CMC_{Solvent}$ was produced via the solvent slurry process and CMC_{AQU2} the optimised dry/aqueous process, they have similar DS's of 0.76 and 0.77 respectively. For these two products any differences in the distribution of substitution would therefore be as a result of the different solvent/reaction systems rather than the DS.

Figure 9-11 shows the hysteresis loops for these two products which were performed at a solution concentration of 3%. Of the two products CMC_{AQU2} has the greater thixotropic area while the $CMC_{Solvent}$ product shows a negligible degree of thixotrophy. This indicates that the solvent produced product has a more uniform distribution of substitution than the dry/aqueous product. This confirms what was expected.

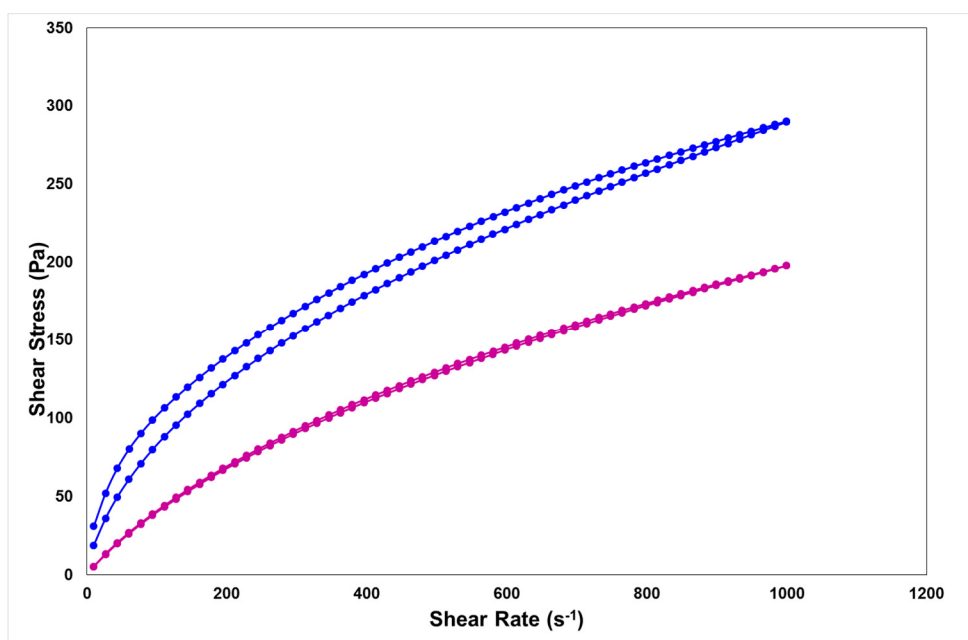


Figure 9-11 Hysteresis loops for CMC_{AQU2} (—●—) and $CMC_{Solvent}$ (—●—) at a solution concentration of 3%

The conformational plots for $CMC_{Solvent}$ and CMC_{AQU2} are shown in Figure 9-12. The slope of the $CMC_{Solvent}$ product is 0.55 indicating a random coil conformation in solution, while that of the CMC_{AQU2} product is 0.38 suggesting a partly expanded coil.

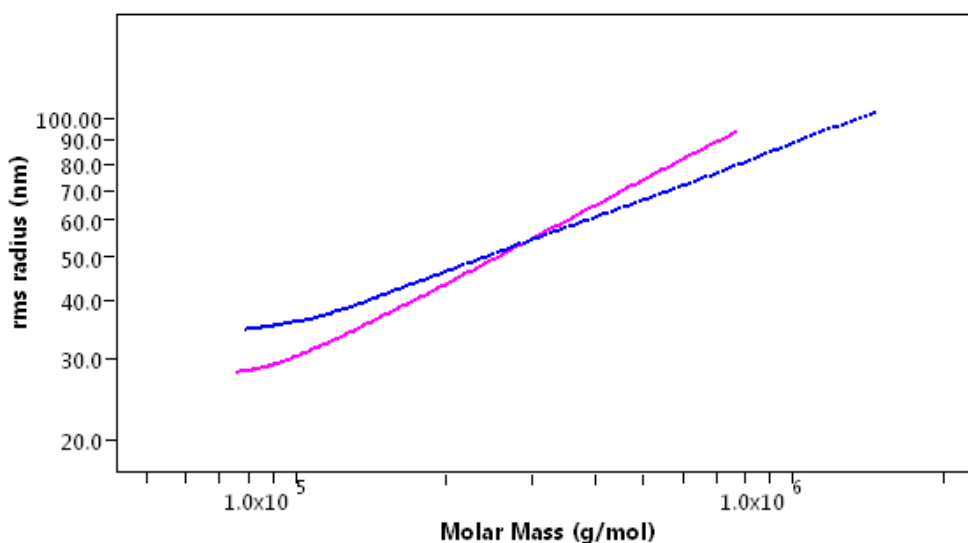


Figure 9-12 Conformational plot overlays for CMC_{Aqu2} (—) and $CMC_{Solvent}$ (—)

The results are summarised in Table 9-2 and show that as the degree of thixotropy decreases, the slope of the conformational plot increases.

Table 9-2 Summary of results for $CMC_{Solvent}$ and CMC_{Aqu2}

Sample	DS	Conformational Plot Slope	Thixotropic Area ($Pa\ s^{-1}$) 3% Solution
$CMC_{Solvent}$	0.76	0.55	1384
CMC_{Aqu2}	0.77	0.38	11282

This indicates that as the distribution of substitution becomes more uniform the conformation that the polymer assumes in solution tends more towards a random coil conformation. This result is therefore in agreement with the previous findings and confirms that the slope of the conformational plot can be related to changes in the distribution of substitution.

The results of Chapter 4 and 5, where differences in the slopes of the conformational plot were found in relation to changes in reaction conditions can now be re-examined.

In Chapter 4 the effect of using a nitrogen blanket during the reaction was investigated. It was found that the use of the nitrogen blanket had no impact on the overall reaction efficiency but that the solution viscosity, molecular weight and MWD were all higher when it was used.

This was due to the reduced degree of oxidative degradation when a nitrogen blanket is used. XRD analysis showed that cellulose swelled in the presence of the nitrogen blanket had a lower degree of crystallinity than the cellulose swelled without the nitrogen blanket. This was thought to be due to increased cooling of the temperature sensitive swelling stage by the flow of nitrogen through the reactor. In conjunction with this it was also found that the two products produced with (CMC_{WNB}) and without (CMC_{NNB}) the nitrogen blanket had different slopes for the conformational plots of 0.36 and 0.32 respectively (Figure 4-4). It was proposed that this change in the slope of the conformational plots indicated that, the improved swelling of the CMC_{WNB} resulted in a more uniform distribution of substituents along the cellulose backbone. To confirm this the hysteresis loops were determined for CMC_{WNB} and CMC_{NNB} and are shown in Figure 9-13.

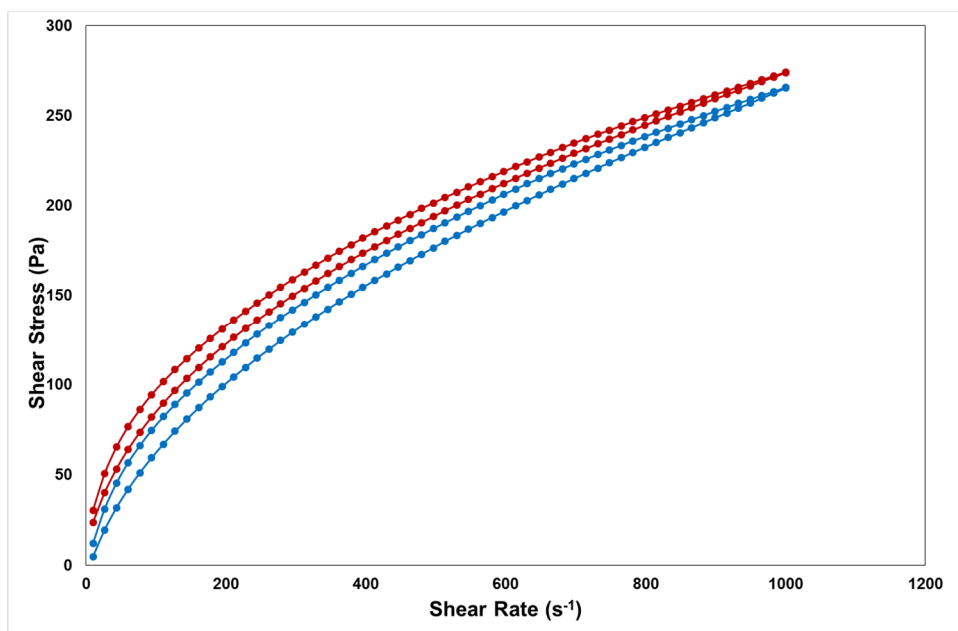


Figure 9-13 Hysteresis loops for CMC_{WNB} (—●—) and CMC_{NNB} (—●—) at a solution concentration of 3%

In this case both products exhibit some degree of thixotropy although CMC_{WNB} does have a slightly smaller hysteresis area in comparison to CMC_{NNB} . This therefore indicates that CMC_{WNB} has the more uniform substituent distribution of the two products. The results for these products are summarised in Table 9-3. As has been previously shown the decrease in the degree of thixotropy corresponds to an increase in the slope of the conformational plot.

Based on the previous examples it can therefore be concluded that the CMC_{WNB} product has a more uniform distribution of substituents than the CMC_{NNB} product. As the DS of these two products is similar and both were produced via the dry/aqueous process with, the only variation being the use of the nitrogen blanket, the further conclusion can be deduced that the use of a nitrogen blanket during the carboxymethylation reaction (in particular the swelling stage) results in an improved distribution of substitution in the final CMC product.

Table 9-3 Summary of results for CMC_{WNB} and CMC_{NNB}

Sample	DS	Conformational Plot Slope	Thixotropic Area (Pa s ⁻¹) 3% Solution
CMC _{WNB}	0.74	0.36	7051
CMC _{NNB}	0.75	0.32	9586

In Chapter 5 the use of the two different etherification reagents, namely SMCA and MCA, was investigated to determine if any offered a significant benefit over the other. What was critical during this part of the investigation was that the amount of NaOH, which was used in the SMCA reaction, needed to be adjusted to account for the lack of in-situ neutralisation required. This meant that the swelling conditions during these reactions were different in terms of the NaOH solution strength used which, for CMC_{MCA} was 37% and for CMC_{SMCA} was 21%. The results found that there was no difference in the reaction efficiency, however, there were differences in the molecular weight and MWD which was related to the insoluble contents of the products. It was observed from the overlay of the conformational plots (Figure 5-2) that the plot for CMC_{SMCA} contained inflection points which were indicative of changes in the conformation in solution of the polymer relative to its molecular weight, this indicated uneven distribution of substitution. The slopes of the conformational plots for CMC_{MCA} and CMC_{SMCA} were also observed to be different, 0.37 and 0.30 respectively and proposed to be related to changes in the distribution of substitution.

Hysteresis loop analysis was performed for CMC_{MCA} and CMC_{SMCA} at a solution concentration of 1% due to the high viscosity of the CMC_{SMCA} product. The results can be seen in Figure 9-14 where it can be seen that the CMC_{MCA} product exhibits a negligible amount of thixotropy in comparison to the CMC_{SMCA}. The results for all the analysis are summarised in Table 9-4.

Table 9-4 Summary of results for CMC_{MCA} and CMC_{SMCA}

Sample	DS	Conformational Plot Slope	Thixotropic Area (Pa s ⁻¹) 3% Solution
CMC _{MCA}	0.74	0.37	66
CMC _{SMCA}	0.74	0.30	1136

The results of the thixotropy analysis confirm what was deduced from the shape of the conformational plot slopes that, CMC_{SMCA} does not have even distribution of substituents. The relationship between the slope of the conformational plot and the thixotropic area is once again evident and so it can be concluded that CMC_{MCA} is more evenly substituted than CMC_{SMCA}.

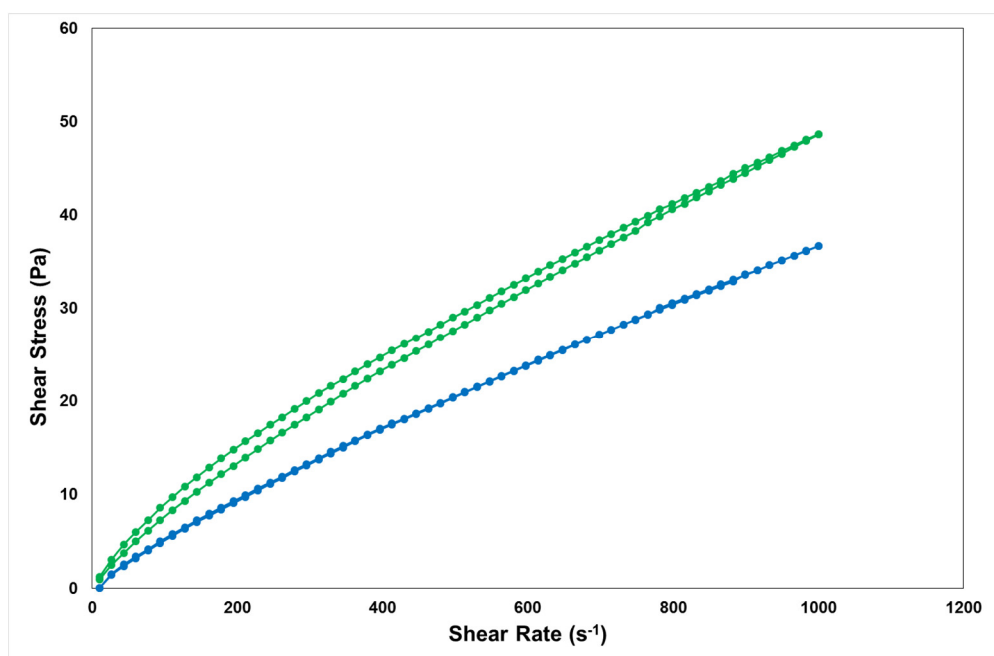


Figure 9-14 Hysteresis loops for CMC_{SMCA} (—●—) and CMC_{MCA} (—●—) at a solution concentration of 1%

9.4 Conclusions

The results discussed in this Chapter have shown that a correlation does exist between the thixotropic area of a polymer solution and the slope of the conformational plot. It was found that as the slope of the conformational plot increased the degree of thixotropy of the polymer solution decreased which indicated a more uniform distribution of substituents along the polymer chain.

A hypothesis was proposed to explain the relationship between these two methods of analysis. Through analysis of examples it was shown that the changes in the slope of the conformational plot could be related to the distribution of substitution of the CMC final products.

The use of conformational plots, as determined by SEC-MALS, as a simplified analysis for the distribution of substitution has therefore been shown to be very promising. This represents a new and novel application of this type of analysis for the determination of the distribution of substitution along the CMC polymer chain. As the use of SEC-MALS for the determination of molecular weights and MWD is already widely used in industry, it makes this technique an attractive alternative to other more complicated and time consuming methods.

10 CONCLUSIONS

The purpose of this study was to apply the principals of green chemistry to the production of CMC in order to reduce its environmental impact by utilising water as an alternative solvent and microwave energy as an alternative heating source.

The optimisation of the previously discarded historical “dry” aqueous process for the production of CMC was carried out by focusing on elements of the two key stages, namely mercerisation and etherification, in order to improve the reaction efficiency and product quality of the process to bring it in line with the currently used organic solvent (“wet”) process.

For the *mercerisation stage* it was found that both NaOH concentration and swelling temperature have an impact on the degree of swelling of the alkali cellulose. It was found a NaOH concentration of 37% in a temperature range of 0 to 20°C provided the most robust swelling conditions for an industrial dry/aqueous process. The use of a nitrogen blanket to exclude oxygen was also found to result in improved swelling of the alkali cellulose. This was thought to be the indirect result of better cooling of the reaction when a nitrogen blanket was used. The nitrogen blanket also resulted in a different conformation of the CMC with a desirable more uniform distribution of substitution.

For the *etherification stage* a comparison of the etherification reagents MCA and its sodium salt, SMCA resulted in a similar reaction efficiency, although MCA was preferable because this allowed for the implementation of the optimised swelling conditions i.e. a NaOH concentration of 37% in a temperature range of 0 to 20°C. Differences in the conformation in solution of the two reaction products was indicative of differences in the distribution of substitution, where the SMCA product appeared to be less uniformly distributed than the MCA product. The optimum reaction efficiencies during MCA addition were achieved for temperatures in the range of 25 to 30°C.

Overall it was found that temperature changes during the swelling period in the etherification stage influenced the distribution of substitution and product characteristics but had no impact on the reaction efficiency. Temperature changes during the adsorption period, on the other hand, influenced the reaction efficiency but had no impact on the distribution of substitution and the product characteristics

On comparison of the optimised dry/aqueous process to the historical process it was found that the overall carboxymethylation reaction efficiency had been improved, most significantly for the low DS products. The overall product quality had also been improved with a significant reduction in the undesirable insoluble content of the final product. The quality of the CMC's produced via the optimised dry/aqueous process were found to have comparable product quality to the solvent slurry ("wet") CMC product over the DS range 0.7 to 0.85,. The reaction efficiency for the optimised dry/aqueous process in the low DS region was 74.8% which is tolerably close to the 76.8% achieved for the solvent slurry process. However, as the DS increased the reaction efficiency decreased, preventing further improvements.

Therefore the overall reaction efficiency for the optimised dry/aqueous process approached but could not completely match that of the solvent slurry process in all aspects. However, it has been shown that the use of water as an alternative solvent for the industrial production of technical grade CMC is a commercially viable option.

The investigation of using microwave radiation as an alternative heating mechanism found that microwave heating significantly reduced the reaction time and also improved the reaction efficiency to some extent. The best results were obtained at 85 W and a reaction time of 20 minutes. This is a key area of further study, because if additional improvements in reaction efficiency could be achieved in conjunction with significant savings in energy and time, this would close the gap between the dry/aqueous and solvent slurry processes. The only concern around a microwave based-process is the availability of suitable industrial scale reactors.

As part of this study a simplified analysis for the determination of distribution of substitution along the polymer chain was developed. It was found that there was a strong correlation between the slopes of the conformational plots, as determined by SEC-MALS, and the degree of thixotropy of the polymer solutions. As the slope of the conformational plot increased the degree of thixotropy of the solution decreased and this was, in turn, indicative of a more uniform distribution of substituents. This technique is an attractive alternative to the other more complex methods currently available.

11 FUTURE WORK

One of the key issues which emerged from this investigation was the need to find a suitable reactor to perform the microwave reactions for the dry/aqueous production of CMC. Such a reactor would require the ability to supply adequate mixing as well as the ability to maintain the moisture levels within the reactor.

The microwave investigations should be repeated in a suitable dedicated microwave reactor in order to obtain more accurate power and time variables for the reaction.

It is felt that there would be a great deal of benefit in conducting an EHS and LCA study for the solvent slurry and optimised dry/aqueous process to more fully understand the environmental impacts of each process and, to be better able to compare these processes and all the factors associated with each.

12 REFERENCES

- Adden, A., 2009. *Substitution Patterns In and Over Polymer Chains - New Approaches for Carboxymethyl Cellulose*, Braunschweig: Technischen Universität Carolo-Wilhelmina.
- Agilent Technologies, 2012. *A Guide of Multi-Detector Gel Permeation Chromatography*, UK: Agilent Technologies, Inc..
- Agilent Technologies, 2015. *An Introduction to Gel Permeation Chromatography and Size Exclusion Chromatography*, USA: Agilent Technologies, Inc..
- Agilent Technologies, 2015b. *Polymer Molecular Weight Distribution and Definitions of MW Averages*, USA: Agilent Technologies, Inc..
- Alban Reyes, D. C., Gorzsas, A., Stridh, K. & de Wit, P., 2017. Alkalization of Dissolving Cellulose Pulp with Highly Concentrated Caustic at low NaOH Stoichiometric Excess. *Carbohydrate Polymers*, Volume 165, pp. 213-220.
- Alban Reyes, D. C. et al., 2016. The Influence of Different Parameters on the Mercerisation of Cellulose for Viscose Production. *Cellulose*, Volume 23, pp. 1061-1072.
- Almlof, H., 2010. *Extended Mercerization Prior to Carboxymethyl Cellulose Preparation*, Karlstad: Karlstad University Studies.
- Ambjornsson, H. A., Schenzel, K. & Germgard, U., 2013. Carboxymethyl Cellulose Produced at Different Mercerization Conditions and Characterised by NIR FT Raman Spectroscopy in Combination with Multivariate Analytical Methods. *Bioresources*, 8(2), pp. 1918-1932.
- Ametek Brookfield, 2017. *More Solutions to Sticky Problems*, s.l.: Ametek Brookfield.
- Anastas., P. & Warner, J., 1998. *Green Chemistry: Theory and Practice*. New York: Oxford University Press.
- Atalla, R. H. & Van der Hart, D. L., 1984. Native Cellulose: A Composite of Two Distinct Crystalline Forms. *Science*, Volume 223, pp. 283-285.

- Baar, A., Kulicke, W.-M., Szablikowski, K. & Kiesewetter, R., 1994. Nuclear Magnetic Resonance Spectroscopic Characterisation of Carboxymethylcellulose. *Macromol. Chem. Phys.*, Volume 195, pp. 1483-1492.
- Balat, M. & Balat, H., 2009. Recent Trends in Global Production and Utilisation of Bio-Ethanol Fuel. *Applied Energy*, Volume 86, pp. 2273-2282.
- Barnes, H. A., 1997. Thixotropy - a Review. *Journal of Non-Newtonian Fluid Mechanics*, Volume 70, pp. 1-33.
- Benchabane, A. & Bekkour, K., 2008. Rheological Properties of Carboxymethyl Cellulose (CMC) Solutions. *Colloid Polymer Science*, Volume 286, pp. 1173-1180.
- Benoit, R., Louis, C. & Frechette, M., 1991. Solution and Ionization of Some Carboxylic Acids in Water and Dimethyl Sulfoxide. *Thermochimica Acta*, Volume 176, pp. 221-232.
- Bergh, M., 2011. *Absorbent cellulose based fibers. Investigation of carboxymethylation and sulfonation of cellulose*, Goteborg, Sweden: Chalmers University of Technology.
- Billmeyer, F. W., 1971. *Textbook of Polymer Science*. 2nd ed. New York: Wiley-Interscience.
- Biswas, A., Kim, S., Selling, G. W. & Cheng, H., 2014. Conversion of Agricultural Residues to Carboxymethylcellulose and Carboxymethylcellulose Acetate. *Industrial Crops and Products*, Volume 60, pp. 259-265.
- Branan, W. M., 1953. *Manufacture of Cellulose Ethers*. United States of America, Patent No. 2,636,879.
- Branan, W. M., 1954. *Manufacture of Cellulose Ether*. United States of America, Patent No. 2,667,480.
- Budtova, T. & Navard, P., 2016. Cellulose in NaOH-water based solvents: a review. *Cellulose*, Volume 23, pp. 5-55.

- Byrne, F. P. et al., 2016. Tools and Techniques for Solvent Selection: Green Solvent Selection Guides. *Sustainable Chemical Process*, 4(7).
- Capello, C., Fischer, U. & Hungerbuhler, K., 2007. What is a Green Solvent? A Comprehensive Framework for the Environmental Assessment of Solvents. *Green Chemistry*, Volume 9, pp. 927-934.
- Cheng, F. et al., 1998. The Uniformity of Distribution of Substituents Along the Chain of Carboxymethyl Cellulose Synthesized in Two-Phase Medium. *Chinese Journal of Polymer Science*, 16(2), pp. 117-125.
- Cheprasova, M. Y., Markin, V., Bazarnova, N. & Kotalevskii, I., 2012. Carboxymethylation of Wood in Different Solvents by the Action of Microwave Radiation. *Russian Journal of Bioorganic Chemistry*, 38(7), pp. 726-729.
- Cheprasova, M. Y., Markin, V. I., Bazarnova, N. & Kotalevskii, I. V., 2012. Carboxymethylation of Wood in Different Solvents by the Action of Microwave Radiation. *Russian Journal of Bioorganic Chemistry*, Volume 38, pp. 726-729.
- Clasen, C. & Kulicke, W.-M., 2001. Determination of Viscoelastic and Rheo-optical Material Functions of Water Soluble Cellulose Derivatives. *Progress in Polymer Science*, Volume 26, pp. 1839-1919.
- Connelly, A., 2015. *Going Green - Solvents*. [Online]
Available at: <https://andyjconnelly.wordpress.com/2016/11/22/going-green-solvents/>
[Accessed 8 November 2017].
- Cordrey, J. M., Druckenmiller, S. T. & Lufkin, J. E., 1963. *Process for Making Alkali Metal Salt of Carboxymethylcellulose*. United States of America, Patent No. 3,088,943.
- Cuissinat, C. & Navard, P., 2006. Swelling and Dissolution of Cellulose Part 1: Free Floating Cotton and Wood fibres in NMMO-Water Mixtures. *Macromolecules Symposium*, Volume 244, pp. 1-18.
- Dallinger, D. & Kappe, C. O., 2007. Microwave-Assisted Synthesis in Water as Solvent. *Chemical Review*, Volume 107, pp. 2563-2591.

Davidson, R. L., 1980. *Handbook of Water Soluble Gums and Resins*. Gael: McGraw-Hill.

deButts, E., Hudy, J. & Elliott, J., 1957. Rheology of Sodium Carboxymethylcellulose Solutions. *Industrial and Engineering Chemistry*, 49(1), pp. 94-98.

dos Santos, D. M. et al., 2015. Microwave-Assited Carboxymethylation of Cellulose Extracted From Brewer's Spent Yeast. *Carbohydrate Polymers*, Volume 131, pp. 125-133.

Edali, M., Esmail, M. N. & Vatistas, G. H., 2001. Rheological Properties of High Concentrations of Carboxymethyl Cellulose Solutions. *Journal of Applied Polymer Science*, Volume 79, pp. 1787-1801.

Egal, M. M., 2006. *Structure and properties of cellulose/NaOH aqueous solutions, gels and regenerated objects*. Ecole Doctorale, Paris, Frans: Sciences Fondamentales et Appliquees.

Elliot, J. H. & Ganz, A. J., 1974. Some Rheological Properties of Sodium Carboxymethylcellulose Solutions and Gels. *Rheol. Acta*, Volume 13, pp. 670-674.

Enebro, J., Momcilovic, D., Siika-aho, M. & Karlsson, S., 2007. A New Approach for Studying Correlations between Chemical Structure and the Rheological Properties in Carboxymethyl Cellulose. *Biomacromolecules*, Volume 8, pp. 3253-3257.

Esveld, E., Chemat, F. & van Haveren, J., 2000. Pilot Scale Continuous Microwave Dry-Media Reactor - Part 1:Design and Modeling. *Chem. Eng. Technol.*, Volume 23, pp. 279-283.

Farran, A. et al., 2015. Green Solvents in Carbohydrate Chemistry: From Raw Materials to Fine Chemicals. *Chemical Reviews*, Volume 115, pp. 6811-6853.

Feddersen, R. L. & Thorp, S. N., 1993. Sodium Carboxymethylcellulose. In: J. N. Whistler & R. Lester, eds. *Industrial Gums: Polysaccharides and Their Derivatives*. San Diego: Academic Press, pp. 537-578.

- Fidale, L. c., Ruiz, N., Heize, T. & El Seoud, O. A., 2008. Cellulose swelling by aprotic and protic solvents: what are the similarities and differences?. *Macromol. Chem. Phys.*, Volume 209, pp. 1240-1254.
- Fink, H.-P., Dautzenberg, H., Kunze, J. & Philipp, B., 1986. The Composition of Alkali Cellulose: A New Concept. *Polymer*, Volume 27, pp. 944-948.
- Fischer, S. et al., 2002. Evaluation of Molten Inorganic Salt Hydrates as Reaction Medium for the Derivatization of Cellulose. *Cellulose*, Volume 9, pp. 293-300.
- Ford, N., Havard, T. & Wallace, P., 1998. Analysis of Macromolecules Using Low- and Right- Angle Laser Light Scattering and Photo Correlation Spectroscopy. In: T. Provder, ed. *Partice Size Distribution III*. s.l.:American Chemical Society, pp. 39-51.
- Francis, P. S., 1961. Solution prproperties of Water-Soluble Polymers. I. Control of Aggregation of Sodium Carboxymethylcellulose (CMC) by Choice of Solvent and/or Electrolyte. *Journal of Applied Polymer Science*, V(15), pp. 261-270.
- Gaborieau, M. & Castignolles, P., 2011. Size-Exclusion Chromomatography (SEC) of Branched Polymers and Polysaccharides. *Anal Bioanal Chem*, Volume 399, pp. 1413-1423.
- Gardner, K. & Blackwell, J., 1974. The Hydrogen Bonding in Native Cellulose. *Biochimica et Biophysica Acta*, Volume 343, pp. 232-237.
- Gericke, M., Fardim, P. & Heinze, T., 2012. Ionic Liquids - Promising but Challenging Solvents for Homogeneous Derivatization of Cellulose. *Molecules*, Volume 17, pp. 7458-7502.
- Ghannam, M. T. & Esmail, M. N., 1997. Rheological Properties of Carboxymethyl Cellulose. *Journal of Applied Polymer Science*, Volume 64, pp. 289-301.
- Grassie, V. R. & Wallis, C. R., 1954. *Alkali Cellulose Preparation*. United States of America, Patent No. 2,680,737.
- Green, H., 1949. *Industrial Rheology and Rheoloical Structures*. New York: Wiley.

Haney, M. A., 1985. The Differential Viscometer II. On-Line Viscosity Detector for Size Exclusion Chromatography. *Journal of Applied Polymer Science*, Volume 30, pp. 3037-3049.

Hearle, J., 1958. A Fringed Fibril Theory of Structure in Crystalline Polymers. *Journal of Polymer Science*, Volume 28, pp. 432-435.

Hearle, J. W. S., 1963. The Fine Structure of Fibres and Crystalline Polymers I. Fringed Fibril Structure. *Journal of Applied Polymer Science*, Volume 7, pp. 1175-1192.

Hedlund, A. & Germgard, U., 2007. Some Aspects on the Kinetics of Etherification in the Preparation of CMC. *Cellulose*, Volume 14, pp. 161-169.

Heinze, T., 2005. Carboxymethyl Ethers of Cellulose and Starch - A Review. *Macromol. Symp.*, Volume 233, pp. 13-29.

Heinze, T., Liebert, T., Klufers, P. & Meister, F., 1999. Carboxymethylation of Cellulose in Unconventional Media. *Cellulose*, Volume 6, pp. 153-165.

Heydarzadeh, H., Najafpour, G. & Nazari-Moghaddam, A., 2009. Catalyst-Free Conversion of Alkali Cellulose to Fine Carboxymethyl Cellulose at Mild Conditions. *World Applied Sciences Journal*, Volume 6, pp. 564-569.

Hivechi, A., Hajir Bahrami, S., Arami, M. & Karimi, A., 2015. Ultrasonic Mediated Production of Carboxymethyl Cellulose: Optimisation of Conditions Using Response Surface Methodology. *Carbohydrate Polymers*, Volume 134, pp. 278-284.

Hodge, A., Gordon, J., Drewitt, N. & Downing, J., 1953. *Manufacture of Carboxymethyl Cellulose*. United States of America, Patent No. 2,639,281.

Hong Chen, M. & Wyatt, P. J., 1999. The Measurement of Mass and Size Distributions, Conformation, and Branching of Important Food Polymers by MALS Following Sample Fractionation. *Macromol. Symp.*, Volume 140, pp. 155-163.

Howsmon, J. A. & Sisson, W. A., 1963. Structures and Properties of Cellulose Fibres B. Submicroscopic Structure. In: E. Ott, H. M. Spurlin & M. W. Grafflin,

eds. *High Polymers, Volume V, Cellulose and Cellulose Derivatives*. New York: Interscience, pp. 231-346.

Kamide, K., Saito, M. & Miyazaki, Y., 1993. Molecular Weight Determination. In: B. Hunt & M. James, eds. *Polymer Characterisation*. Dordrecht: Springer, pp. 115-144.

Klemm, D., Heublein, B., Fink, H.-P. & Bohn, A., 2005. Cellulose: Fascinating Biopolymer and Sustainable Raw Material. *Angew. Chem. Int. Ed.*, Volume 44, pp. 3358-3393.

Klemm, D. et al., 2001a. *Comprehensive Cellulose Chemistry. Fundamentals and Analytical Methods*. Weinheim: Wiley-VCH Verlag GmbH.

Klemm, D. et al., 2001b. *Comprehensive Cellulose Chemistry. Functionalisation of Cellulose*. Weinheim: Wiley-VCH Verlag GmbH.

Klug, E. D. & Tinsley, J. S., 1950. *Preparation of Carboxyalkyl Ethers of Cellulose*. United States of America, Patent No. 2,517,577.

Kok, C. M. & Rudin, A., 1981. Relationship Between the Hydrodynamic Radius and the Radius of Gyration of a Polymer in Solution. *Makromol. Chem., Rapid Commun.*, Volume 2, pp. 655-659.

Kolpak, F. J. & Blackwell, J., 1976. Determination of the Structure of Cellulose II. *Macromolecules*, 9(2), pp. 273-278.

Kolpak, F. J., Weih, M. & Blackwell, J., 1978. Mercerization of Cellulose: 1. Determination of the Structure of Mercerized Cotton. *Polymer*, Volume 19, pp. 123-131.

Koroskenyi, B. & McCarthy, S. P., 2002. Microwave-Assisted Solvent-Free or Aqueous-Based Synthesis of Biodegradable Polymers. *Journal of Polymers and the Environment*, 10(3), pp. 93-104.

Kroon-Batenburg, L., Kroon, J. & Nordholt, M., 1986. *Polym. Commun*, Volume 27, pp. 290-292.

Kulicke, W.-M., Kull, A. H., Kull, W. & Thielking, H., 1996. Characterization of Aqueous Carboxymethylcellulose Solutions in Terms of Their Molecular Structure and its Influence on Rheological Behaviour. *Polymer*, Volume 13, pp. 2723-2731.

Kuo, Y.-N. & Hong, J., 2005. Investigation of Solubility of Microcrystalline Cellulose. *Polymers for Advanced Technologies*, Volume 16, pp. 425-428.

Leonelli, C. & Veronesi, P., 2015. Microwave Reactors for Chemical Synthesis and Biofuels Preparation. In: Z. Fang, R. J. Smith & X. Qi, eds. *Production of Biofuels and Chemicals with Microwave*. Dordrecht: Springer Science+Business Media, pp. 17-40.

Li, B. et al., 2010. Effects of Dispersed Medium Systems on Substitution Pattern and Solution Performance of Carboxymethyl Cellulose. *Front. Mater. Sci. China*, 4(3), pp. 306-313.

Liebert, T. F. & Heinze, T. J., 2001. Exploitation of Reactivity and Selectivity in Cellulose Functionalization Using Unconventional Media for the Design of Products Showing New Superstructures. *Biomacromolecules*, Volume 2, pp. 1124-1132.

Malvern Instruments Limited, 2015. *Principles of Triple Detection GPC/SEC*, UK: Malvern Instruments Limited.

MarketsandMarkets, 2015. Carboxymethyl Cellulose Market Worth \$1.46 Billion by 2020. *Manufacturing Close-up*.

Markin, V., Cheprasova, M. Y. & Bazarnova, N., 2015. General Areas of the Use of a Microwave Radiation for Processing of Plant Raw Materials (Review). *Russian Journal of Bioorganic Chemistry*, 41(7), pp. 686-699.

Markin, V., Cheprasova, M. Y., Bazarnova, N. & Frolova, E., 2014. Pine Wood Carboxymethylation Under Microwave Radiation. *Russian Journal of Bioorganic Chemistry*, 40(7), pp. 733-736.

McBurney, L., 1954. Degradation of Cellulose. In: E. Ott, H. M. Spurlin & M. W. Grafflin, eds. *High Polymers, Volume V, Cellulose and Cellulose Derivatives*. New York: Interscience Publishers, INC, pp. 99-196.

- Miura, K. & Nakano, T., 2015. Analysis of Mercerisation Process Based on the Intensity Change of Deconvoluted Resonances of ^{13}C CP/MAS NMR: Cellulose Mercerized Under Cooling and Non-cooling Conditions. *Materials Science and Engineering C*, Volume 53, pp. 189-195.
- Nakano, T., Tanimoto, T. & Hashimoto, T., 2013. Morphological Change Induced with NaOH-Water Solution for Ramie Fiber: Change Mechanism and Effects of Concentration and Temperature. *J Mater Sci*, Volume 48, pp. 7510-7517.
- Nicholson, M. D., 1976. *Reactions of Cellulose in the Dimethyl Sulfoxide/ Paraformaldehyde (DMSO/PF) Solvent - Doctor's Dissertation*, Appleton, Wisconsin: The Institute of Paper Chemistry.
- Nigam, P. S. & Singh, A., 2011. Production of Liquid Biofuels from Renewable Resources. *Progress in Energy and COmbustion Science*, Volume 37, pp. 52-68.
- NIIR Board, 2003. *Modern Technology of Industrial Chemicals*. s.l.:Asia Pacific Business Press Inc..
- Nishimura, H. & Sarko, A., 1987. Mercerization of Cellulose IV. Mechanism of Mecerization and Crystallite Sizes. *Journal of Applied Polymer Science*, Volume 33, pp. 867-874.
- Nomanbhay, S. & Ong, M. Y., 2017. A Review of Microwave-Assisted Reactions for Biodiesel Production. *Bioengineering*, 4(57).
- Okano, T. & Sarko, A., 1984. Mercerization of Cellulose. I. X-ray Diffraction Evidence for Intermediate Structures. *Journal of Applied Polymer Science*, Volume 29, pp. 4175-4182.
- Okano, T. & Sarko, A., 1985. Mercerisation of Cellulose II, Alkali-Cellulose Intermediates and a Possible Mercerasation Mechanism. *Joournal of Applied Polymer Science*, Volume 30, pp. 325-332.
- Olaru, N., Olaru, L., Stoleriu, A. & Timpu, D., 1998. Carboxymethylcellulose Synthesis in Organic Media Containing Ethanol and/or Acetone. *Journal of Applied Polymer Science*, Volume 67, pp. 481-486.

- Olaru, N. & Olaru, O., 1992. Mathematical Models for the Synthesis of Carboxymethylation in the Isopropyl Alcohol System. *Cellulose Chemistry and Technology*, Volume 26, pp. 685-690.
- Omiya, T., 1984. *Process for Producing an Alkali Salt of A Carboxymethylcellulose Ether*. United States of America, Patent No. 4,426,518.
- O'Sullivan, A. C., 1997. Cellulose: The Structure Slowly Unravels. *Cellulose*, Volume 4, pp. 173-207.
- Paddison, O. H. & Sommers, R. W., 1961. *Process for the Manufacture of Carboxymethyl Cellulose Involving 3-Component, 2-Phase Liquid Reaction*. United States of America, Patent No. 2,976,278.
- Perez, S. & Mazeau, K., 2005. *Conformations, structures, and morphologies of cellulose*, s.l.: Marcel Dekker.
- Podzimek, S., 2011. *Light Scattering, Size Exclusion Chromatography and Asymmetric Flow Field Flow Fractionation*. Hoboken, New Jersey: John Wiley & Sons, Inc.
- Polshettiwar, V. & Varma, R. S., 2010. Fundamentals of Aqueous Microwave Chemistry. In: V. Polshettiwar & R. S. Varma, eds. *Aqueous Microwave Assisted Chemistry: Synthesis and Catalysis*. s.l.:Royal Society of Chemistry, pp. 1-9.
- Porro, F., Bedue, O., Chanzy, H. & Heux, L., 2007. Solid-State ¹³C NMR Study of Na-Cellulose Complexes. *Biomacromolecules*, Volume 8, pp. 2586-2593.
- Prusov, A., Prusova, S. & Zakharov, A., 2014. Interaction of Cellulose and Ligocellulosic Polymers with Water and Aqueous Systems. *Russian Chemical Bulletin*, 63(9), pp. 1926-1945.
- Prusova, S., Ryabinina, I. & Prusov, A., 2002. Rheological Properties and Structure of Aqueous Solutions of Polysaccharides. Solutions of Sodium Carboxymethylcellulose Fractions of Different Molar Mass. *Fibre Chemistry*, 34(3), pp. 177-180.
- Purves, C. B., 1963. Chemical Nature of Cellulose and Its Derivatives A. Historical Survey B. Chain Structure. In: E. Ott, H. M. Spurlin & M. W. Grafflin,

eds. *High Polymers, Volume V, Cellulose and Cellulose Derivatives*. New York: Interscience, pp. 29-98.

Ramos, L., Frollini, E. & Heinze, T., 2005. Carboxymethylation of Cellulose in the New Solvent Dimethyl Sulfoxide/Tetrabutylammonium Fluoride. *Carbohydrate Polymers*, Volume 60, pp. 259-267.

Rathi, A. K., Gawande, M. B., Zboril, R. & Varma, R. S., 2015. Microwave-Assisted Synthesis - Catalytic Applications in Aqueous Media. *Coordination Chemistry Reviews*, Volume 291, pp. 68-94.

Reed, W. F., 1995. Data Evaluation for Unified Multi-Detector Size Exclusion Chromatography - Molar Mass, Viscosity and Radius of Gyration Distributions. *Macromol. Chem. Phys.*, Volume 196, pp. 1539-1575.

Richardson, S. & Gorton, L., 2003. Characterisation of the Substituent Distribution in Starch and Cellulose Derivatives - Review. *Analytica Chimica Acta*, Volume 497, pp. 27-65.

Richardson, S. et al., 2002. Initial Characterization of Ethyl(hydroxyethyl) Cellulose Using Enzymatic Degradation and Chromatographic Methods. *Biomacromolecules*, Volume 3, pp. 1359-1363.

Rinaudo, M., Danhelka, J. & Milas, M., 1993. A New Approach to Characterising Carboxymethylcellulose by Size Exclusion Chromatography. *Carbohydrate Polymers*, Volume 21, pp. 1-5.

Roberts, B. A. & Strauss, C. R., 2005. Toward Rapid "Green" Predictable Microwave-Assisted Synthesis. *Acc. Chem. Res.*, Volume 38, pp. 653-661.

Roy, C., Budtova, T., Navard, P. & Bedue, O., 2001. Structure of Cellulose-Soda Solutions at Low Temperatures. *Biomacromolecules*, Volume 2, pp. 687-693.

Salmi, T., Damlin, P., Mikkola, J.-P. & Kangas, M., 2011. Modelling and Experimental Verification of Cellulose Substitution Kinetics. *Chemical Engineering Science*, Volume 66, pp. 171-182.

Salmi, T. et al., 1994. Kinetic Study of the Carboxymethylation of Cellulose. *Ind. Eng. Chem. Res.*, Volume 33, pp. 1454-1459.

- Sameii, N., Mortazavi, S., Rashidi, A. & Sheikhzadah-Najar, S., 2008. An investigation on the Effect of Hot Mercerization on Cotton Fabrics Made up of Open-End Yarns. *Journal of Applied Sciences*, Volume 8, pp. 4204-4209.
- Serkov, A., 2000. Fabrication of alkali cellulose. *Fibre Chemistry*, 32(2), pp. 95-99.
- Sjostrom, E., 1993. Chapter 9 Cellulose Derivatives. In: *Wood Chemistry Fundamentals and Applications (Second Edition)*. San Diego: Academic Press, pp. 204-224.
- Smith, L. J., Fiebig, K. M., Schwalbe, H. & Dobson, C. M., 1996. The Concept of a Random Coil, Residual Structure in Peptides and Denatured Proteins. *Folding & Design*, Volume 1, pp. R95-R106.
- Stigsson, V., Kloow, G. & Germgard, U., 2001. Historical Overview of CMC Production on an Industrial Scale. *Paper Asia*, Issue 10, pp. 16-21.
- Stigsson, V., Kloow, G. & Germgard, U., 2006. The Influence of the Solvent System Used During Manufacturing of CMC. *Cellulose*, Volume 13, pp. 705-712.
- Stigsson, V., Kloow, G., Germgard, U. & Andersson, N., 2005. The Influence of Cobalt (II) in Carboxymethyl Cellulose Processing. *Cellulose*, Volume 12, pp. 395-401.
- Stigsson, V., Wilson, D. I. & Germgard, U., 2004. Production Variance in Purified Carboxymethyl Cellulose (CMC) Manufacture. *Dev. Chem. Eng. Mineral Process.*, Volume 12, pp. 217-231.
- Striegel, A. M., 2016. Viscometric Detection in Size-Exclusion Chromatography: Principles and Select Applications. *Chromatographia*, Volume 79, pp. 945-960.
- Strunk, P., Lindgren, A., Eliasson, B. & Agnemo, R., 2012. Chemical Changes of Cellulose Pulps in the Processing to Viscose Dope. *Cellulose Chemistry and Technology*, Volume 46, pp. 559-569.
- Su, W.-F., 2013. *Principles of Polymer Design and Synthesis*. Berlin Heidelberg: Springer-Verlag.

Swinehart, R. W., 1950. *Method of Making Carboxymethyl Cellulose*. United States of America, Patent No. 2,524.024.

Thielking, H. & Schimdt, M., 2012. Cellulose Ethers. In: *Ullmann's Encyclopedia of Industrial Chemistry, Vol. 7*. Weinheim: Wiley-VCH Verlag GmbH & Co. KGaA, pp. 381-397.

Triantafillopoulos, D. N., 1988. *Measurement of Fluid Rheology and Interpretation of Rheograms, Second Edition*, Michigan: Kaltec Scientific, Inc.

Triggs, W. W., 1949. *Manufacture of Carboxymethylcellulose*. United Kingdom, Patent No. 670094.

Unlu, C. H., 2013. Carboxymethylcellulose from Recycled Newspaper in Aqueous Medium. *Carbohydrate Polymers*, Volume 97, pp. 159-164.

van Grinkel, C. G. & Gayton, S., 1996. The Biodegradability and Nontoxicity of Carboxymethyl Cellulose (DS 0.7) and Intermediates. *Environmental Toxicology and Chemistry*, 15(3), pp. 270-274.

Vlassopoulos, D., Fytas, G., Pakula, T. & Roovers, J., 2001. Multiarm Star Polymers Dynamics. *Journal of Physics: Condensed Matter*, Volume 13, pp. R855-R876.

von Blottnitz, H. & Curran, M. A., 2007. A Review of Assessments Conducted on Bio-Ethanol as a Transportation Fuel from a Net Energy, Greenhouse gas, and Environmental Life Cycle Perspective. *Journal of Cleaner Production*, Volume 15, pp. 607-619.

Wang, Y., 2008. *Cellulose Fiber Dissolution in Sodium Hydroxide Solution at Low Temperature: Dissolution Kinetics and Solubility Improvement*, s.l.: Georgia Institute of Technology.

Weiner, B. B., 2010. *What is Particle Size*, Holtsville: Brookhaven Intruments.

White, R. D., 1999. Application of Gel Permeation Chromatography with Multi-Angle Light Scattering to the Characterisation of Polysaccharides. In: *Polysaccharide Applications*. s.l.:American Chemical Society, pp. 299-316.

- Wu, N., Hubbe, M. A., Rojas, O. J. & Park, S., 2009. Permeation of Polyelectrolytes and Other Solutes into the Pore Spaces of Water-Swollen Cellulose: A Review. *Bioresources*, 4(3), pp. 1222-1262.
- Wyatt Technology, 2010. *The Ultimate Guide to Buying a Light Scattering Instrument for Absolute Macromolecular Characterisation*, Santa Barbara: Wyatt Technology Corporation.
- Wyatt, P. J., 1997. Multiangle Light Scattering: The Basic Tool for Macromolecular Characterization. *Instrument Science & Technology*, Volume 25, pp. 1-18.
- Wyatt, P. J., 2013. *American Laboratory*. [Online] Available at: <https://www.americanlaboratory.com/913-Technical-Articles/147482-The-Story-of-MALS/> [Accessed 23 January 2018].
- Xiquan, L., Tingzhu, Q. & Shaoqui, Q., 1990. Kinetics of the Carboxymethylation of Cellulose in the Isopropyl Alcohol System. *Acta Polymerica*, 41(4), pp. 220-222.
- Yamashiki, T. et al., 1988. Studies on the Swelling of Cotton Fibers in Alkali Metal Hydroxides. III. Structure-property Relations in Fibers Swollen at 0°C. *Polymer Journal*, Volume 20, pp. 447-457.
- Yau, W., Kirkland, J. & Bly, D., 1980. *Modern Size-Exclusion Liquid Chromatography: Practice of Gel Permeation and Gel Filtration Chromatography*. New York: Wiley-Interscience.
- Zhang, G., Zhang, L., Deng, H. & Sun, P., 2011. Preparation and Characterisation of Sodium Carboxymethyl Cellulose from Cotton Stalk Using Microwave Heating. *J Chem Technol Biotechnol*, Volume 86, pp. 584-589.
- Zugenmaier, P., 2001. Conformation and Packing of Various Crystalline Cellulose Fibers. *Progress in Polymer Science*, Volume 26, pp. 1341-1417.
- Zugenmaier, P., 2008. *Crystalline Cellulose and Cellulose Derivatives*. Berlin: Springer.

APPENDIX A

Below is a schematic representation of the 185 L pilot plant set-up which was used during this investigation.

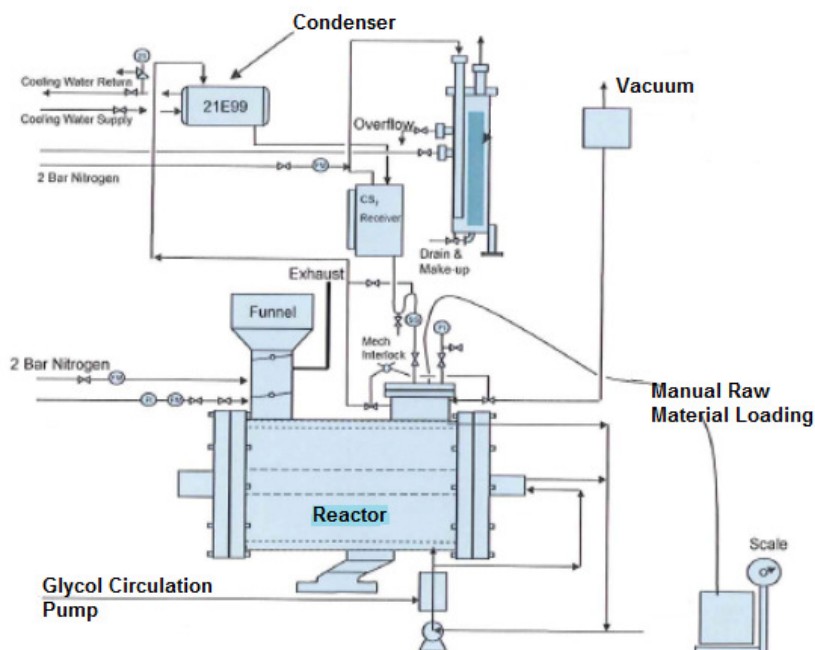


Figure A-1 Schematic representation of the pilot plant set-up used for the carboxymethylation reactions

The 2 L lab scale reactor had the same reaction set-up but was controlled manually, with heating and cooling supplied by a recirculating bath and nitrogen from a lab cylinder.

The results that follow are for the carboxymethylation reactions performed for the investigation relating to Chapter 4 (the nitrogen investigation) and Chapter 5 (the investigation into the esterification reagent).

Information such as temperatures were collected manually and the data manipulated in excel to produce the temperature profiles for the batches. Each reaction condition was run in triplicate and the average temperature profile for the 3 reactions was taken to prepare the reaction temperature profile for the condition.

Table A-1 Batch temperatures for the MCA powder reactions with nitrogen

		MCA Powder With Nitrogen			
	Temperature	Batch 35	Batch 36	Batch 37	Average
Temperature Profile Caustic Addition	0	0.4	0.1	0.1	0.2
	5	0.1	-0.5	0.5	0.0
	10	1.1	0.4	0.6	0.7
	15	3.4	2.1	1.5	2.3
	20	7.5	4.7	3.1	5.1
	25	10.5	7.4	5.4	7.8
	30	11.3	9.8	8.9	10.0
	35	10.5	10.4	10.5	10.5
	40	9.2	9.7	10.0	9.6
	45	9.2	8.9	9.2	9.1
	50	10.7	7.9	8.3	9.0
	55	15.9	7.9	8.3	10.7
	60	18.8	7.6	7.9	11.4
Temperature Profile MCA/SMCA Addition	65	18.2	8.3	8.6	11.7
	70	16.4	9.5	10.3	12.1
	75	14.5	11.4	12.3	12.7
	80	12.8	12.9	14.4	13.4
	85	11.5	13.7	15.1	13.4
	90	10.3	13.6	14.8	12.9
	95	9.5	13.1	14.0	12.2
	100	8.9	12.3	13.1	11.4
	105	8.3	11.4	11.9	10.5
	110		10.7	10.9	10.8
115		9.8	10.1	10.0	
Temperature Profile (Heating and Reaction)	10	9.3	9.2	11.5	10.0
	20	19.1	13.7	20.8	17.9
	30	33.2	25.3	33.9	30.8
	40	48.7	39.2	48.8	45.6
	50	66.0	55.2	65.8	62.3
	60	67.7	67.4	67.9	67.7
	70	65.4	66.4	65.8	65.9
	80	64.8	64.9	64.7	64.8
	90	64.5	64.3	64.4	64.4
	100	64.6	64.3	64.5	64.5
	110	64.5	64.5	64.7	64.6
	120	64.6	64.7	64.9	64.7
	130	64.6	64.7	65.0	64.8
	140	64.8	65.0	65.0	64.9
	150	65.0	65.1	65.2	65.1
160	65.2	65.1	65.1	65.1	
170	65.2	65.1	65.1	65.1	
180	65.2	65.1	65.2	65.2	

Table A-2 Batch temperatures for the SMCA powder reactions with nitrogen

		SMCA Powder With Nitrogen			
	Temperature	Batch 38	Batch 39	Batch 40	Average
Temperature Profile Caustic Addition	0	0.1	0.1	0.5	0.2
	5	0.5	0.5	0.5	0.5
	10	0.8	1.1	1.9	1.3
	15	2.3	3.2	3.7	3.1
	20	3.8	4.6	5.1	4.5
	25	4.2	4.9	5.4	4.8
	30	4.0	4.7	5.4	4.7
	35	3.6	4.4	5.1	4.4
	40	3.3	4.0	4.7	4.0
	45	3.3	4.0	4.7	4.0
	50	3.0	3.6	4.3	3.6
	55	2.9	3.4	4.1	3.5
Temperature Profile MCA/SMCA Addition	60	3.0	3.3	4.1	3.5
	65	2.9	3.2	3.9	3.3
	70	2.9	3.0	3.8	3.2
	75	2.8	2.9	3.7	3.1
	80	2.6	2.8	3.6	3.0
	85	2.5	2.6	3.4	2.8
	90	2.4	2.6	3.4	2.8
	95	2.3	2.6	3.4	2.8
Temperature Profile (Heating and Reaction)	100	2.2	2.4	3.4	2.7
	105	2.2	2.4	3.4	2.7
	10	3.2	3.0	4.2	3.5
	20	10.5	8.8	10.8	10.0
	30	22.0	19.4	21.7	21.0
	40	34.2	31.9	33.8	33.3
	50	46.4	44.4	46.1	45.6
	60	58.8	58.6	58.7	58.7
	70	66.6	65.8	66.1	66.2
	80	66.8	65.6	65.7	66.0
	90	66.3	64.8	65.1	65.4
	100	66.1	65.3	65.1	65.5
	110	65.5	65.3	64.9	65.2
	120	65.1	64.7	65.0	64.9
	130	65.1	64.5	65.0	64.9
	140	65.2	64.7	64.9	64.9
150	65.2	64.8	64.8	64.9	
160	65.1	65.0	64.8	65.0	
170	65.1	65.1	64.8	65.0	
180	65.0	65.1	64.8	65.0	

Table A-3 Batch temperatures for the MCA powder reactions without nitrogen blanket

		MCA Powder Without Nitrogen			
	Temperature	Batch 50	Batch 51	Batch 52	Average
Temperature Profile Caustic Addition	0	-0.3	0.4	0.4	0.2
	5	0.5	0.8	0.5	0.6
	10	1.6	2.1	1.2	1.6
	15	3.4	3.8	2.2	3.1
	20	5.1	5.8	3.8	4.9
	25	6.6	9.1	6.4	7.4
	30	9.1	12.4	11.7	11.1
	35	11.9	13.3	13.7	13.0
	40	12.1	12.7	13.7	12.8
	45	11.5	11.8	13.3	12.2
	50	10.8	11.0	12.7	11.5
	55	10.3	10.4	12.2	11.0
Temperature Profile MCA/SMCA Addition	60	9.9	9.9	11.5	10.4
	65	9.9	9.9	11.5	10.4
	70	10.0	9.8	12.1	10.6
	75	11.2	11.2	13.9	12.1
	80	13.6	13.6	16.8	14.7
	85	17.8	18.9	22.1	19.6
	90	22.8	22.8	23.4	23.0
	95	21.9	21.3	21.5	21.6
	100	19.9	18.8	19.6	19.4
	105	18.5	16.8	17.9	17.7
	110	16.8	15.4	16.7	16.3
	115	15.7	14.2	15.7	15.2
Temperature Profile (heating and Reaction)	120	14.8	13.1	15.0	14.3
	125	14.1	12.5	14.2	13.6
	10	13.3	12.5	15.4	13.7
	20	17.0	19.4	23.6	20.0
	30	26.6	30.8	35.1	30.8
	40	39.0	44.9	48.0	44.0
	50	49.3	61.8	63.7	58.3
	60	60.7	70.8	68.6	66.7
	70	66.1	69.2	67.4	67.6
	80	65.7	67.3	66.1	66.4
	90	65.2	66.0	65.3	65.5
	100	64.9	65.2	64.6	64.9
	110	64.9	65.0	64.6	64.8
	120	65.2	64.9	64.6	64.9
	130	65.2	64.8	65.0	65.0
140	65.4	65.0	65.2	65.2	
150	65.5	65.0	65.4	65.3	
160	65.6	65.1	65.4	65.4	
170	65.7	65.0	65.5	65.4	
180	65.7	65.0	65.6	65.4	

Although the data for the entire reaction was collected, the area of greatest interest was the swelling and adsorption periods of the reaction and so temperature profiles mostly focused on these periods.

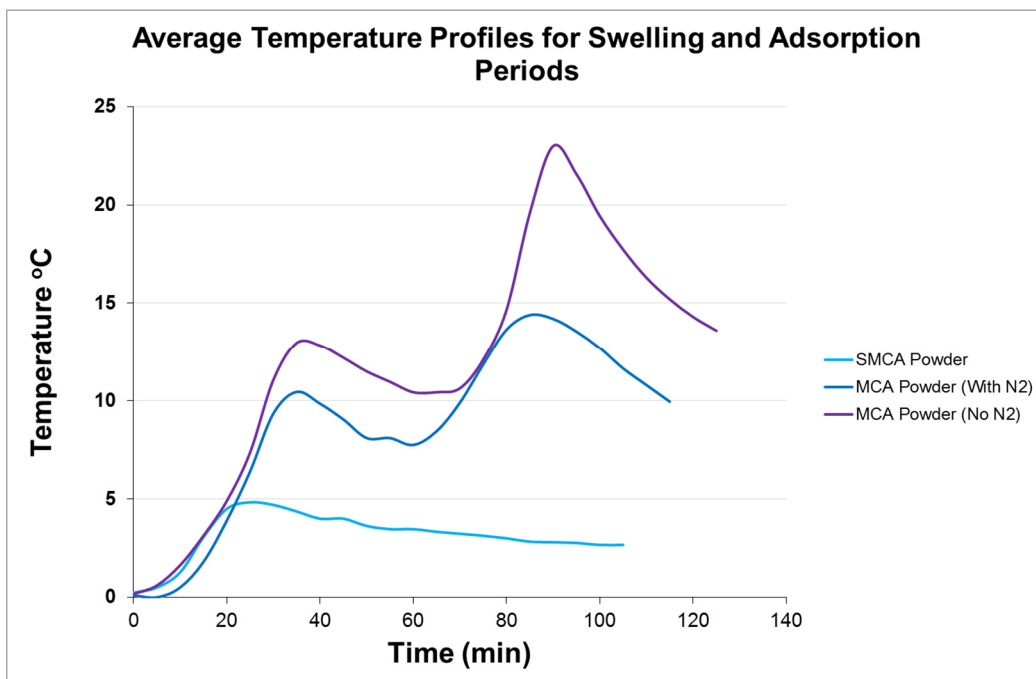


Figure A-2 Average temperature profiles for the swelling and adsorption periods

The final products from each of the batches was then analysed and the average of the results used. Two types of analysis were performed, the table below shows how the results of the chemical analysis which were collected and averaged for use in the report.

Table A-4 Results of the analytical characterisation for the MCA, SMCA and MCA without nitrogen blanket

	MCA Only			SMCA Only			MCA Only No Nitrogen		
	35	36	37	38	39	40	50	51	52
Moisture	7.39	6.22	5.97	5.34	6.97	7.28	5.22	4.1	5.8
% Purity as is	64.08	65.45	64.45	64.32	63.30	62.35	64.39	66	66.65
% Purity dry	69.19	69.79	68.54	67.95	67.61	67.23	67.94	68.82	70.75
DS	0.72	0.75	0.74	0.75	0.71	0.75	0.74	0.75	0.76
pH	9.35	10.22	9.67	9.94	9.62	9.65	8.66	7.98	10.26
Viscosity 2h	223	289	265	81	143	129	92	78	72
Clarity NTU	7.32			32.6			56.1		
Insol's	0.12	0.1	0.73	1.35	0.68	0.76	0.1	0.35	1.17
Average Results									
Moisture	6.53			6.53			5.04		
% Purity as is	64.66			63.32			65.68		
% Purity dry	69.17			67.60			69.17		
DS	0.74			0.74			0.75		
pH	9.75			9.74			9.46		
Viscosity	259			118			81		
Clarity NTU	7.32			32.60			56.10		
Insol's	0.43			0.93			0.76		

The second type of analysis was the molecular characterisation, which was performed on a composite sample of the three batches, the raw results for this characterisation are shown below.

Summary results table and overlays for C6 and C8 samples.

General		Peak 1										
Sample name	Sample description	Mn (kDa)	Mp (kDa)	Mw (kDa)	Polydispersity (Mw/Mn)	rn (nm)	rw (nm)	rz (nm)	rh(v)n (nm)	rh(v)w (nm)	rh(v)z (nm)	[η]w (mL/g)
C6 (MCA Powder with N2)	Batch 35.36.37	41.9	74.7	324	7.727	62.3	56.6	108.9	9	24.3	85.2	540.031
C8 (MCA Powder with no N2)	Batch 50.51.52	33.3	60.9	254.4	7.63	56.7	48.9	85.9	7.4	20.4	81.3	419.233

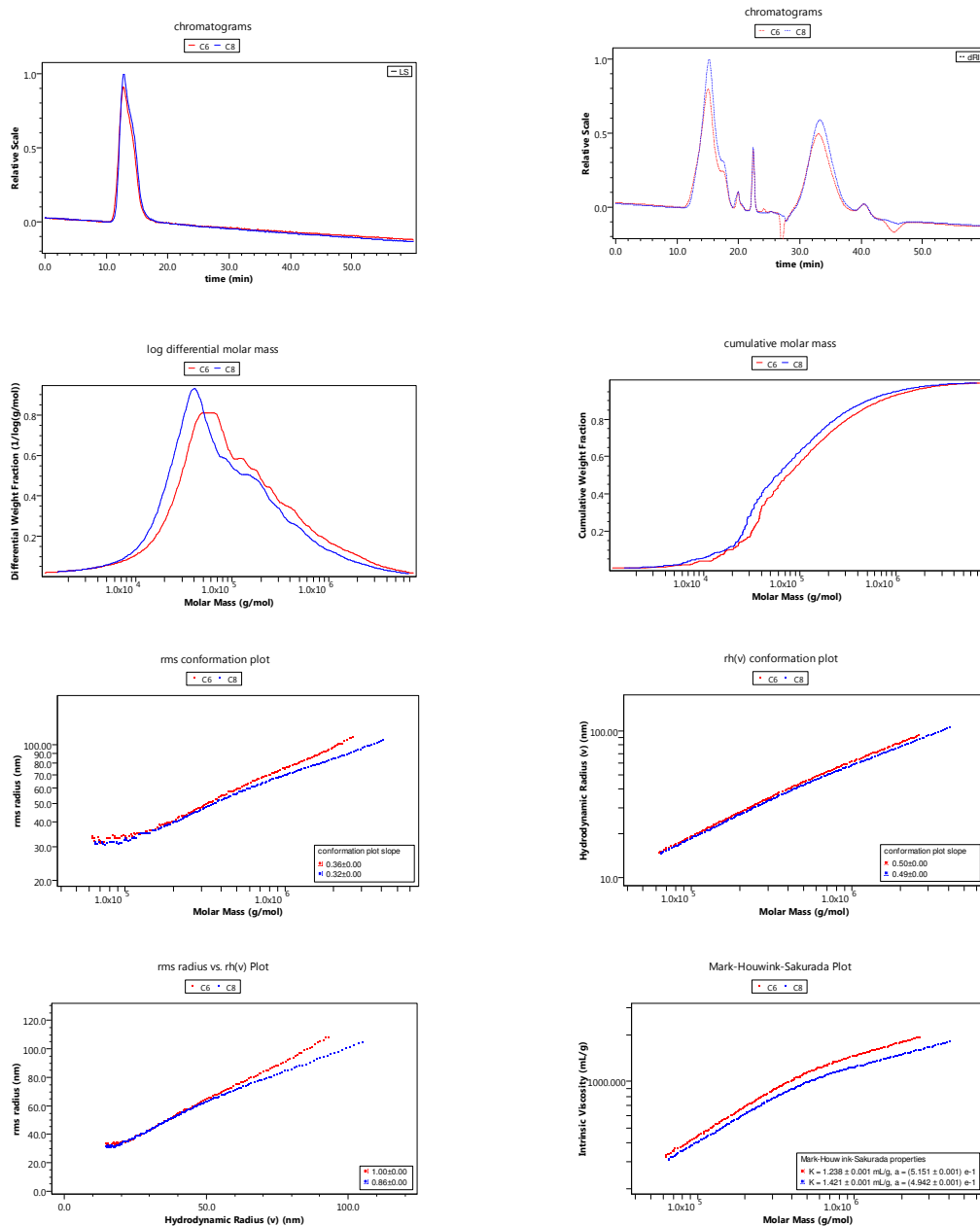


Figure A-3 Raw SEC-MALS results for the MCA reactions with and without nitrogen blanket

Summary results table and Overlays for C5 nd C6 samples

General		Peak 1										
Sample name	Sample description	Mn (kDa)	Mp (kDa)	Mw (kDa)	Polydispersity (Mw/Mn)	rn (nm)	rw (nm)	rz (nm)	rh(v)n (nm)	rh(v)w (nm)	rh(v)z (nm)	$[\eta]$ w (mL/g)
C5 (SMCA Powder)	Batch no.38:39:40	33	59.3	195.5	5.931	30.9	44.3	75	7.9	18.6	72.1	406.241
C6 (MCA Powder)	Batch no.35:36:37	41.4	74.5	323.3	7.818	62.3	56.7	109.6	8.9	24.2	85.5	537.612

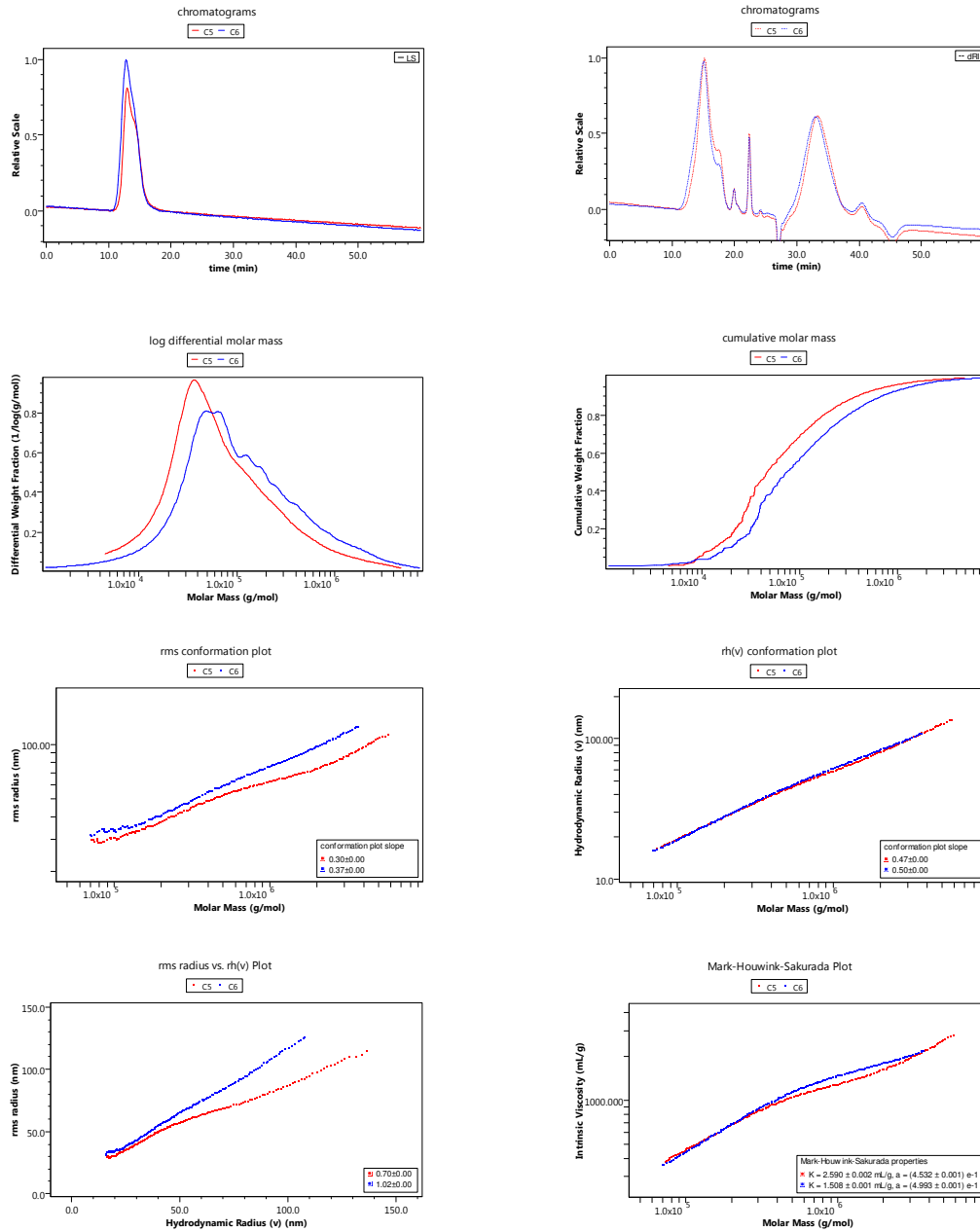


Figure A-4 Raw SEC-MALS results for the MCA and SMCA reactions

For Chapter 6 the temperature profiles of the reactions were collected and processed in the same way as demonstrated for Chapter 4 and 5's results. The table below is a summary of those average figures.

Table A-5 Average temperatures for the reactions which were part of study investigating the impact of temperature during the MCA addition and adsorption periods

	Time	17°C	20°C	25°C	28°C	32°C	39°C	45°C
NaOH addition	0	8	8	8	8	8	8	8
	5	9	9	9	11	9	9	9
	10	10	10	11	12	10	11	11
	15	13	12	13	13	13	12	12
	20	14	14	15	14	14	14	14
	25	15	15	16	16	15	15	16
	30	16	16	18	17	16	16	17
	35	16	16	17	17	16	16	17
	40	15	15	16	16	15	15	16
	45	14	15	15	15	14	14	14
	50	13	13	14	14	13	13	13
	55	12	13	14	13	12	12	13
SMCA addition	60	11	13	13	13	12	12	12
	65	11	13	14	14	14	13	15
	70	11	13	16	17	17	18	20
	75	13	15	19	20	22	23	27
	80	15	17	22	23	26	29	33
	85	16	19	23	25	29	33	38
	90	17	19	24	27	31	36	42
	95	17	20	25	28	32	38	44
	100	15	19	25	27	32	39	45
	105	14	17	23	26	31	38	45
	110	12	16	22	25	30	38	45
	115	10	15	21	24	29	38	45
120	10	14	20	24	29	37	45	

The chemical and molecular characterisation results were also processed in the same way and the tables below show a summary of the averaged chemical characterisation data for all the reactions, as well as the GPC analysis results for the batch composites.

Table A-6 Analytical results for the reactions which were part of study investigating the impact of temperature during the MCA addition and adsorption periods

Reaction	CMC 17	CMC 20	CMC 22	CMC 25	CMC 28	CMC 32	CMC 39	CMC 45
Moisture	4.16	4.61	5.07	6.14	5.97	4.88	5.43	4.55
% Purity as is	64.64	64.97	65.47	64.19	63.69	65.32	64.85	65.71
% Purity dry	67.44	68.10	68.97	68.26	67.72	68.69	68.57	68.84
DS	0.69	0.73	0.71	0.76	0.77	0.74	0.74	0.72
pH	7.04	7.09	7.38	8.48	9.21	9.80	10.02	8.49
2% Viscosity (As is)	164	170	164	164	127	123	120	130
Clarity NTU	11.7	22.7	14.6	12.6	17.2	17.0	16.1	17.3
Insol's	0.41	0.47	0.17	0.30	0.41	0.51	0.37	0.48
% NaCl (dry)	19.55	20.29	19.68	19.59	19.90	19.56	18.91	19.65
% NaGly (dry)	7.89	8.09	7.64	7.54	7.82	7.46	6.66	7.25

Summary Results table and overlays for batch 372, 374, 378, 379, 381, 384 and 386 samples.

General		Peak 1										
Sample name	Sample description	Mn (kDa)	Mp (kDa)	Mw (kDa)	Polydispersity (Mw/Mn)	rn (nm)	rw (nm)	rz (nm)	rh(v)n (nm)	rh(v)w (nm)	rh(v)z (nm)	[η]w (mL/g)
Batch 374	CMC17	68.3	99.5	436.2	6.388	56.6	64.5	146	10.4	25.5	81	474.845
Batch 372	CMC20	68.3	99.5	436.2	6.388	56.6	64.5	146	10.4	25.5	81	474.845
Batch 378	CMC25	68.3	99.5	436.2	6.388	56.6	64.5	146	10.4	25.5	81	474.845
Batch 379	CMC28	67.8	97.5	373.7	5.511	54.6	61.3	134.2	10.9	24.7	76.3	490.851
Batch 381	CMC32	68.05	98.5	404.95	5.9495	55.6	62.9	140.1	10.65	25.1	78.65	482.848
Batch 384	CMC39	67.925	98	389.325	5.73025	55.1	62.1	137.15	10.775	24.9	77.475	486.8495
Batch 386	CMC45	66.5	97.1	381.1	5.733	53.1	62.1	138.5	11	25.3	80	519.019

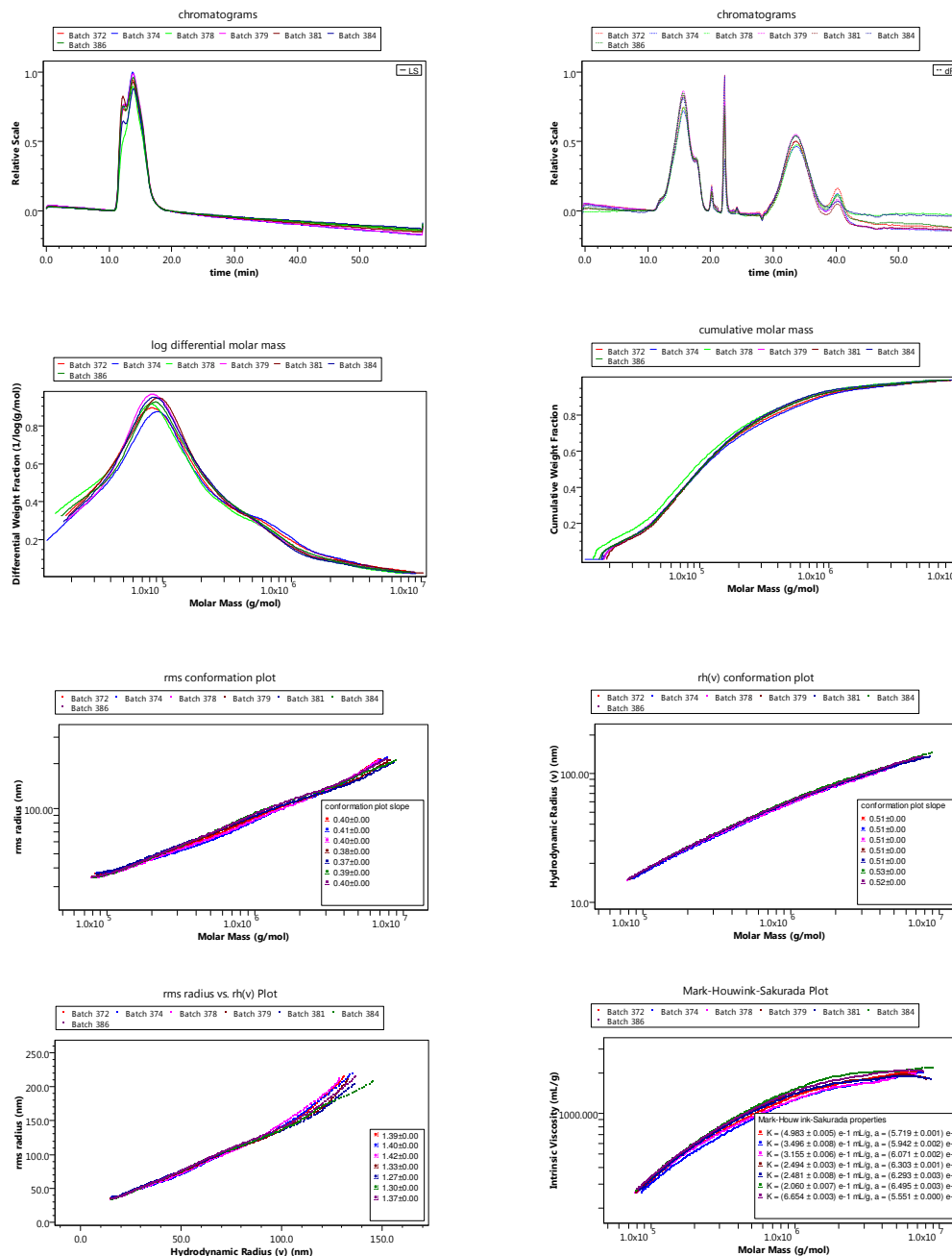


Figure A-5 Raw SEC-MALS results for the for the reactions which were part of study investigating the impact of temperature during the MCA addition and adsorption periods

For the microwave reactions performed in Chapter 7 the reactions were only carried out a single time. The complete characterisation of those products in the following tables.

Table A-7 Characterisation results for the microwave reactions performed at 85 W

	CMC MW 04	CMC MW 05	CMC MW 06	CMC MW 07
Watts	85	85	85	85
Reaction Time (minutes)	5	10	15	20
% moisture	4.72	5.63	3.88	3.69
% Purity as is	57.94	57.41	58.43	58.52
% Purity dry	60.81	60.84	60.79	60.76
DS	0.67	0.67	0.69	0.71
% NaCl	20.92	21.63	21.70	21.63

Table A-8 Characterisation results for the microwave reactions performed at 255 W

	MP 255 T2 (MW 08)	MP 255 T4 (MW 09)	MP 255 T6 (MW 10)	MP 255 T8 (MW 11)
Watts	255	255	255	255
Reaction Time (minutes)	2	4	6	8
% moisture	1.70	1.58	1.56	1.38
% Purity as is	63.40	63.53	63.60	63.75
% Purity dry	64.49	64.54	64.61	64.64
DS	0.56	0.55	0.56	0.56
% NaCl	20.56	20.26	20.86	20.56

Table A-9 Characterisation results for the microwave reactions performed at 425 W

	MP 425 T0.5 (MW 12)	MP 425 T1 (MW 13)	MP 425 T2 (MW 14)	MP 425 T3.5 (MW 15)
Watts	425	425	425	425
Reaction Time (minutes)	0.5	1	2	3
% moisture	1.91	2.14	2.03	1.24
% Purity as is	62.20	63.35	63.25	63.01
% Purity dry	63.41	64.74	64.56	63.80
DS	0.58	0.60	0.61	0.63
% NaCl	20.92	20.54	20.33	20.42

Table A-10 Characterisation results for the microwave reactions performed at 595 W

	MP 595 T3 (MW 16)	MP 595 T1 (MW 17)	MP 595 T1.5 (MW 18)
Watts	595	595	595
Reaction Time (minutes)	0.5	1	2
% moisture	2.02	1.74	1.59
% Purity as is	63.49	63.62	63.49
% Purity dry	64.80	64.74	64.52
DS	0.58	0.57	0.55
% NaCl	21.24	21.02	20.89

For the hysteresis loop study conducted in Chapter 9 the results from the Brookfield RST-CC Rheometer were exported as an excel spreadsheet where the data was then used to draw up hysteresis loop curves.

The tables below show the raw data for the analysis for the CMC_{Aqu2} product at 1%, 2% and 3%.

Table A-11 Raw hysteresis loop results for CMC_{Aqu2} at 1% solution concentration

CMCAqu2 1%

Result: 208.6509
[Pa/s]

Number	Time (s)	Shear Stress (Pa)	Shear Rate (1/s)	Viscosity (Pa·s)	Temp (°C)
1	2	0.6	10	0.06	21.7
2	4	1.567	27	0.0585	21.7
3	6	2.501	44	0.0574	21.7
4	8	3.424	60	0.0567	21.7
5	10	4.227	77	0.0548	21.7
6	12	5.007	94	0.0533	21.7
7	14	5.715	111	0.0516	21.7
8	16	6.387	127	0.0501	21.7
9	18	7.109	144	0.0493	21.7
10	20	7.77	161	0.0483	21.7
11	22	8.406	178	0.0473	21.7
12	24	9.042	195	0.0465	21.7
13	26	9.706	211	0.0459	21.7
14	28	10.326	228	0.0453	21.7
15	30	10.929	245	0.0446	21.7
16	32	11.562	262	0.0442	21.7
17	34	12.172	278	0.0437	21.7
18	36	12.836	295	0.0435	21.7
19	38	13.453	312	0.0431	21.7
20	40	14.014	329	0.0426	21.7
21	42	14.651	346	0.0424	21.7
22	44	15.252	362	0.0421	21.7
23	46	15.853	379	0.0418	21.7
24	48	16.452	396	0.0416	21.7
25	50	16.98	413	0.0411	21.7
26	52	17.488	429	0.0407	21.7
27	54	18.005	446	0.0403	21.7
28	56	18.564	463	0.0401	21.7
29	58	19.114	480	0.0398	21.7
30	60	19.689	497	0.0396	21.7
31	62	20.232	513	0.0394	21.7
32	64	20.762	530	0.0392	21.7
33	66	21.388	547	0.0391	21.7
34	68	21.895	564	0.0388	21.7
35	70	22.471	581	0.0387	21.7
36	72	22.985	597	0.0385	21.7
37	74	23.561	614	0.0384	21.7

CMCAqu2 1%

Number	Time (s)	Shear Stress (Pa)	Shear Rate (1/s)	Viscosity (Pa·s)	Temp (°C)
38	76	24.108	631	0.0382	21.7
39	78	24.616	648	0.038	21.7
40	80	25.168	664	0.0379	21.7
41	82	25.684	681	0.0377	21.7
42	84	26.256	698	0.0376	21.7
43	86	26.781	715	0.0375	21.7
44	88	27.323	732	0.0374	21.7
45	90	27.837	748	0.0372	21.7
46	92	28.382	765	0.0371	21.7
47	94	28.913	782	0.037	21.7
48	96	29.39	799	0.0368	21.7
49	98	29.903	815	0.0367	21.7
50	100	30.375	832	0.0365	21.7
51	102	30.845	849	0.0363	21.7
52	104	31.344	866	0.0362	21.7
53	106	31.827	883	0.0361	21.7
54	108	32.536	899	0.0362	21.7
55	110	33.021	916	0.036	21.7
56	112	33.536	933	0.0359	21.7
57	114	34.047	950	0.0359	21.7
58	116	34.534	966	0.0357	21.7
59	118	35.055	983	0.0357	21.7
60	120	35.568	1000	0.0356	21.7
1	122	35.559	1000	0.0356	21.7
2	124	35.064	983	0.0357	21.7
3	126	34.516	966	0.0357	21.7
4	128	34.049	950	0.0359	21.7
5	130	33.514	933	0.0359	21.7
6	132	33	916	0.036	21.7
7	134	32.491	899	0.0361	21.7
8	136	31.985	883	0.0362	21.7
9	138	31.458	866	0.0363	21.7
10	140	30.977	849	0.0365	21.7
11	142	30.49	832	0.0366	21.7
12	144	29.997	815	0.0368	21.7
13	146	29.537	799	0.037	21.7
14	148	28.972	782	0.0371	21.7
15	150	28.248	765	0.0369	21.7
16	152	27.753	748	0.0371	21.7
17	154	27.178	732	0.0372	21.7

CMCAqu2 1%

Number	Time (s)	Shear Stress (Pa)	Shear Rate (1/s)	Viscosity (Pa·s)	Temp (°C)
18	156	26.643	715	0.0373	21.7
19	158	26.102	698	0.0374	21.7
20	160	25.572	681	0.0375	21.7
21	162	25.034	664	0.0377	21.7
22	164	24.466	648	0.0378	21.7
23	166	23.937	631	0.0379	21.7
24	168	23.365	614	0.038	21.7
25	170	22.834	597	0.0382	21.7
26	172	22.293	581	0.0384	21.7
27	174	21.686	564	0.0385	21.7
28	176	21.134	547	0.0386	21.7
29	178	20.544	530	0.0387	21.7
30	180	20.013	513	0.039	21.7
31	182	19.426	497	0.0391	21.7
32	184	18.869	480	0.0393	21.7
33	186	18.296	463	0.0395	21.7
34	188	17.76	446	0.0398	21.7
35	190	17.219	429	0.0401	21.7
36	192	16.69	413	0.0404	21.7
37	194	16.124	396	0.0407	21.7
38	196	15.562	379	0.041	21.7
39	198	14.936	362	0.0412	21.7
40	200	14.345	346	0.0415	21.7
41	202	13.783	329	0.0419	21.7
42	204	13.095	312	0.042	21.7
43	206	12.467	295	0.0422	21.7
44	208	11.837	278	0.0425	21.7
45	210	11.167	262	0.0427	21.7
46	212	10.533	245	0.043	21.7
47	214	9.949	228	0.0436	21.7
48	216	9.307	211	0.044	21.7
49	218	8.634	195	0.0444	21.7
50	220	7.972	178	0.0448	21.7
51	222	7.309	161	0.0454	21.7
52	224	6.617	144	0.0459	21.7
53	226	5.975	127	0.0469	21.7
54	228	5.253	111	0.0475	21.7
55	230	4.53	94	0.0482	21.7
56	232	3.791	77	0.0492	21.7
57	234	3.055	60	0.0506	21.7

CMCAqu2 1%

Number	Time (s)	Shear Stress (Pa)	Shear Rate (1/s)	Viscosity (Pa·s)	Temp (°C)
58	236	2.169	44	0.0498	21.7
59	238	1.312	27	0.049	21.7
60	240	0	10	0	21.7

Table A-12 Raw hysteresis loop results for CMC_{Aqu2} at 2% solution concentration

CMCAqu2 2%

Result: 2184.4463
[Pa/s]

Number	Time (s)	Shear Stress (Pa)	Shear Rate (1/s)	Viscosity (Pa·s)	Temp (°C)
1	2	5.358	10	0.5363	21.6
2	4	11.711	27	0.4372	21.6
3	6	16.85	44	0.3868	21.6
4	8	21.218	60	0.3516	21.6
5	10	24.926	77	0.3232	21.6
6	12	28.349	94	0.3019	21.6
7	14	31.417	111	0.2838	21.6
8	16	34.242	127	0.2686	21.6
9	18	36.879	144	0.2557	21.6
10	20	39.367	161	0.2445	21.6
11	22	41.755	178	0.2348	21.6
12	24	44.072	195	0.2265	21.6
13	26	46.349	211	0.2193	21.6
14	28	48.52	228	0.2127	21.6
15	30	50.66	245	0.2068	21.6
16	32	52.737	262	0.2015	21.5
17	34	54.84	278	0.1969	21.5
18	36	56.901	295	0.1927	21.5
19	38	58.852	312	0.1886	21.5
20	40	60.781	329	0.1849	21.5
21	42	62.684	346	0.1814	21.5
22	44	64.534	362	0.1781	21.5
23	46	66.437	379	0.1752	21.5
24	48	68.175	396	0.1722	21.5
25	50	69.897	413	0.1694	21.5
26	52	71.546	429	0.1666	21.5
27	54	73.225	446	0.1641	21.5

CMCAqu2 2%

Number	Time (s)	Shear Stress (Pa)	Shear Rate (1/s)	Viscosity (Pa·s)	Temp (°C)
28	56	74.85	463	0.1616	21.5
29	58	76.46	480	0.1593	21.5
30	60	78.073	497	0.1572	21.5
31	62	79.648	513	0.1551	21.5
32	64	81.233	530	0.1532	21.5
33	66	82.727	547	0.1513	21.5
34	68	84.246	564	0.1494	21.5
35	70	85.811	581	0.1478	21.5
36	72	87.246	597	0.1461	21.5
37	74	88.725	614	0.1445	21.5
38	76	90.142	631	0.1429	21.5
39	78	91.568	648	0.1414	21.5
40	80	93.01	664	0.14	21.5
41	82	94.435	681	0.1386	21.5
42	84	95.84	698	0.1373	21.5
43	86	97.194	715	0.136	21.5
44	88	98.604	732	0.1348	21.4
45	90	99.921	748	0.1335	21.4
46	92	101.262	765	0.1324	21.4
47	94	102.799	782	0.1315	21.4
48	96	104.143	799	0.1304	21.4
49	98	105.406	815	0.1293	21.4
50	100	106.687	832	0.1282	21.4
51	102	107.928	849	0.1271	21.4
52	104	109.21	866	0.1261	21.4
53	106	110.47	883	0.1252	21.4
54	108	111.737	899	0.1242	21.4
55	110	112.971	916	0.1233	21.4
56	112	114.218	933	0.1224	21.4
57	114	115.471	950	0.1216	21.4
58	116	116.701	966	0.1208	21.4
59	118	117.925	983	0.1199	21.4
60	120	119.141	1000	0.1191	21.4
1	122	119.058	1000	0.1191	21.4
2	124	117.693	983	0.1197	21.4
3	126	116.374	966	0.1204	21.4
4	128	115.006	950	0.1211	21.4
5	130	113.652	933	0.1218	21.4
6	132	112.296	916	0.1226	21.4
7	134	110.937	899	0.1234	21.4

CMCAqu2 2%

Number	Time (s)	Shear Stress (Pa)	Shear Rate (1/s)	Viscosity (Pa·s)	Temp (°C)
8	136	109.61	883	0.1242	21.4
9	138	108.232	866	0.125	21.4
10	140	106.862	849	0.1259	21.4
11	142	105.536	832	0.1268	21.4
12	144	104.167	815	0.1277	21.4
13	146	102.842	799	0.1288	21.4
14	148	101.463	782	0.1298	21.4
15	150	100.043	765	0.1308	21.4
16	152	98.609	748	0.1318	21.4
17	154	97.187	732	0.1329	21.4
18	156	95.723	715	0.1339	21.4
19	158	94.288	698	0.1351	21.4
20	160	92.836	681	0.1363	21.4
21	162	91.108	664	0.1371	21.4
22	164	89.642	648	0.1384	21.4
23	166	88.146	631	0.1397	21.4
24	168	86.642	614	0.1411	21.4
25	170	85.175	597	0.1426	21.4
26	172	83.572	581	0.144	21.4
27	174	82.016	564	0.1455	21.4
28	176	80.417	547	0.147	21.4
29	178	78.826	530	0.1487	21.4
30	180	77.251	513	0.1505	21.4
31	182	75.588	497	0.1522	21.4
32	184	73.955	480	0.1541	21.4
33	186	72.288	463	0.1561	21.4
34	188	70.597	446	0.1582	21.4
35	190	68.914	429	0.1605	21.4
36	192	67.207	413	0.1628	21.4
37	194	65.483	396	0.1654	21.4
38	196	63.713	379	0.168	21.4
39	198	61.795	362	0.1705	21.4
40	200	59.936	346	0.1734	21.4
41	202	57.977	329	0.1763	21.4
42	204	56	312	0.1795	21.4
43	206	54.018	295	0.183	21.4
44	208	51.915	278	0.1864	21.4
45	210	49.818	262	0.1904	21.4
46	212	47.686	245	0.1947	21.4
47	214	45.43	228	0.1991	21.4

CMCAqu2 2%

Number	Time (s)	Shear Stress (Pa)	Shear Rate (1/s)	Viscosity (Pa·s)	Temp (°C)
48	216	43.148	211	0.2041	21.4
49	218	40.792	195	0.2096	21.4
50	220	38.411	178	0.2161	21.4
51	222	35.883	161	0.2229	21.4
52	224	33.195	144	0.2301	21.4
53	226	30.454	127	0.2389	21.4
54	228	27.52	111	0.2486	21.4
55	230	24.468	94	0.2606	21.4
56	232	21.193	77	0.2748	21.4
57	234	17.607	60	0.2918	21.4
58	236	13.72	44	0.315	21.4
59	238	9.24	27	0.3451	21.4
60	240	4.093	10	0.4094	21.4

Table A-13 Raw hysteresis loop results for CMC_{Aqu2} at 3% solution concentration

CMCAqu2 3%

Result: 11282.2978
[Pa/s]

Number	Time (s)	Shear Stress (Pa)	Shear Rate (1/s)	Viscosity (Pa·s)	Temp (°C)
1	2	30.809	10.055	3.064	21.3
2	4	51.831	26.755	1.9372	21.3
3	6	67.748	43.571	1.5549	21.3
4	8	80.013	60.391	1.3249	21.3
5	10	89.987	77.178	1.166	21.3
6	12	98.553	93.954	1.0489	21.3
7	14	106.179	110.722	0.959	21.3
8	16	113.155	127.497	0.8875	21.3
9	18	119.689	144.282	0.8296	21.3
10	20	125.863	161.048	0.7815	21.3
11	22	131.738	177.833	0.7408	21.3
12	24	137.39	194.607	0.706	21.3
13	26	142.777	211.38	0.6755	21.3
14	28	147.982	228.167	0.6486	21.3
15	30	153.026	244.937	0.6248	21.3
16	32	157.936	261.712	0.6035	21.3
17	34	162.685	278.501	0.5841	21.3
18	36	167.288	295.278	0.5665	21.3
19	38	171.689	312.059	0.5502	21.3

CMCAqu2 3%

Number	Time (s)	Shear Stress (Pa)	Shear Rate (1/s)	Viscosity (Pa·s)	Temp (°C)
20	40	176.012	328.834	0.5353	21.3
21	42	180.293	345.609	0.5217	21.3
22	44	184.314	362.386	0.5086	21.3
23	46	188.274	379.169	0.4965	21.3
24	48	192.155	395.951	0.4853	21.3
25	50	195.849	412.73	0.4745	21.3
26	52	199.497	429.508	0.4645	21.3
27	54	203.048	446.287	0.455	21.3
28	56	206.538	463.068	0.446	21.3
29	58	209.926	479.845	0.4375	21.3
30	60	213.326	496.629	0.4295	21.3
31	62	216.546	513.41	0.4218	21.3
32	64	219.781	530.183	0.4145	21.3
33	66	222.906	546.966	0.4075	21.3
34	68	226.103	563.745	0.4011	21.3
35	70	229.167	580.519	0.3948	21.3
36	72	232.072	597.299	0.3885	21.3
37	74	234.971	614.083	0.3826	21.3
38	76	237.83	630.866	0.377	21.3
39	78	240.611	647.637	0.3715	21.3
40	80	243.425	664.421	0.3664	21.3
41	82	246.102	681.199	0.3613	21.3
42	84	248.799	697.985	0.3565	21.3
43	86	251.339	714.76	0.3516	21.3
44	88	253.899	731.542	0.3471	21.3
45	90	256.427	748.311	0.3427	21.3
46	92	258.848	765.102	0.3383	21.3
47	94	261.311	781.876	0.3342	21.3
48	96	263.664	798.661	0.3301	21.3
49	98	266	815.437	0.3262	21.3
50	100	268.336	832.217	0.3224	21.3
51	102	270.559	848.999	0.3187	21.3
52	104	272.79	865.774	0.3151	21.3
53	106	275.072	882.555	0.3117	21.3
54	108	277.231	899.335	0.3083	21.3
55	110	279.468	916.117	0.3051	21.3
56	112	281.667	932.897	0.3019	21.3
57	114	283.802	949.667	0.2988	21.3
58	116	285.912	966.456	0.2958	21.3
59	118	288.049	983.231	0.293	21.3

CMCAqu2 3%

Number	Time (s)	Shear Stress (Pa)	Shear Rate (1/s)	Viscosity (Pa·s)	Temp (°C)
60	120	290.157	1000.012	0.2902	21.3
1	122	289.776	1000.009	0.2898	21.3
2	124	286.989	983.228	0.2919	21.3
3	126	284.264	966.445	0.2941	21.3
4	128	281.534	949.664	0.2965	21.3
5	130	278.794	932.885	0.2989	21.3
6	132	276.032	916.104	0.3013	21.3
7	134	273.291	899.329	0.3039	21.3
8	136	270.62	882.547	0.3066	21.3
9	138	267.819	865.766	0.3093	21.3
10	140	265.111	848.981	0.3123	21.3
11	142	262.353	832.208	0.3152	21.3
12	144	259.619	815.425	0.3184	21.3
13	146	256.851	798.643	0.3216	21.3
14	148	254.023	781.861	0.3249	21.3
15	150	251.201	765.084	0.3283	21.3
16	152	248.298	748.307	0.3318	21.3
17	154	245.405	731.524	0.3355	21.3
18	156	242.461	714.741	0.3392	21.3
19	158	239.534	697.958	0.3432	21.3
20	160	236.528	681.187	0.3472	21.3
21	162	233.503	664.404	0.3514	21.3
22	164	230.435	647.629	0.3558	21.3
23	166	227.335	630.844	0.3604	21.3
24	168	224.236	614.061	0.3652	21.3
25	170	221.046	597.288	0.3701	21.3
26	172	217.809	580.508	0.3752	21.3
27	174	214.584	563.721	0.3807	21.3
28	176	211.335	546.952	0.3864	21.3
29	178	207.913	530.165	0.3922	21.3
30	180	204.522	513.383	0.3984	21.3
31	182	201.029	496.603	0.4048	21.3
32	184	197.304	479.829	0.4112	21.3
33	186	193.695	463.045	0.4183	21.3
34	188	190.009	446.267	0.4258	21.3
35	190	186.29	429.484	0.4338	21.3
36	192	182.472	412.713	0.4421	21.3
37	194	178.561	395.925	0.451	21.3
38	196	174.547	379.15	0.4604	21.3
39	198	170.318	362.362	0.47	21.3

CMCAqu2 3%

Number	Time (s)	Shear Stress (Pa)	Shear Rate (1/s)	Viscosity (Pa·s)	Temp (°C)
40	200	166.016	345.584	0.4804	21.3
41	202	161.65	328.809	0.4916	21.3
42	204	157.171	312.03	0.5037	21.3
43	206	152.528	295.248	0.5166	21.3
44	208	147.82	278.462	0.5308	21.3
45	210	142.835	261.687	0.5458	21.3
46	212	137.772	244.909	0.5625	21.3
47	214	132.481	228.127	0.5807	21.3
48	216	127.038	211.353	0.6011	21.3
49	218	121.347	194.569	0.6237	21.3
50	220	115.353	177.784	0.6488	21.3
51	222	109.048	161.012	0.6773	21.3
52	224	102.46	144.228	0.7104	21.3
53	226	95.404	127.451	0.7486	21.3
54	228	87.915	110.67	0.7944	21.3
55	230	79.714	93.893	0.849	21.3
56	232	70.718	77.118	0.917	21.3
57	234	60.777	60.337	1.0073	21.3
58	236	49.426	43.558	1.1347	21.3
59	238	35.803	26.788	1.3365	21.3
60	240	18.69	10.036	1.8623	21.3